

4-2-2012

Contribution of the Mnr2 Protein to Magnesium Homeostasis in *Saccharomyces cerevisiae*

Nilambari Prafulla Pisat

University of Missouri-St. Louis, nilambarip@hotmail.com

Follow this and additional works at: <https://irl.umsl.edu/dissertation>



Part of the [Biology Commons](#)

Recommended Citation

Pisat, Nilambari Prafulla, "Contribution of the Mnr2 Protein to Magnesium Homeostasis in *Saccharomyces cerevisiae*" (2012).
Dissertations. 379.

<https://irl.umsl.edu/dissertation/379>

This Dissertation is brought to you for free and open access by the UMSL Graduate Works at IRL @ UMSL. It has been accepted for inclusion in Dissertations by an authorized administrator of IRL @ UMSL. For more information, please contact marvinh@umsl.edu.

**Contribution of the Mnr2 Protein to Magnesium Homeostasis
in *Saccharomyces cerevisiae***

by

Nilambari P. Pisat

M.L.S., University of Mumbai, 1999

B.Sc., Microbiology and Biotechnology, University of Mumbai, 1997

Submitted to the Graduate School at

The University of Missouri-St. Louis

In Partial Fulfillment of the Requirements for the Degree

DOCTOR OF PHILOSOPHY

In

BIOLOGY

With an emphasis in Cellular and Molecular Biology

August 2009

Dissertation Committee

Colin MacDiarmid, Ph.D. (Advisor)

Teresa Thiel, Ph.D.

Wendy Olivas, Ph.D.

Bethany Zolman, Ph.D.

Contribution of the Mnr2 Protein to Magnesium Homeostasis in *Saccharomyces cerevisiae*

Nilambari P. Pisat

ABSTRACT

Magnesium (Mg^{2+}) is an essential divalent cation involved in many important cellular functions. All cells regulate their intracellular Mg^{2+} concentration to maintain key biological processes, despite the importance of this process, relatively little is known about the regulation of Mg^{2+} homeostasis in eukaryotes. The goal of this work was to characterize a homolog of the bacterial CorA protein from the yeast *Saccharomyces cerevisiae* that was suspected to be involved in mineral nutrient homeostasis.

Mnr2 is a close homolog of the Alr1 and Alr2 proteins, which are known to mediate Mg^{2+} influx across the plasma membrane in yeast. Mnr2 inactivation was associated with increased sensitivity of yeast to divalent cations such as Mn^{2+} , Ca^{2+} , and Zn^{2+} . I also observed an increase in the Mg^{2+} content of an *mnr2* mutant strain suggesting that Mnr2 plays a role in Mg^{2+} homeostasis. The effect of *mnr2* mutation on Mg^{2+} content was most pronounced under Mg^{2+} -deficient conditions (1 μ M), and was associated with a growth defect. The higher Mg^{2+} content of the *mnr2* mutant strain was not due to an increase in the rate of Mg^{2+} uptake, but occurred as a consequence of an inability to deplete intracellular Mg^{2+} content to support growth in deficient conditions. These results suggested that Mnr2 was a Mg^{2+} transporter responsible for regulating access to Mg^{2+} stored within an intracellular compartment. Supporting this hypothesis, I used two independent techniques to determine that the majority of Mnr2 was associated with the vacuolar membrane. In addition, combining *mnr2* with the *tfp1* mutation (which inactivates the vacuolar H^+ -ATPase) suppressed the high Mg^{2+} content phenotype associated with the *mnr2* mutation, providing genetic evidence for a role of Mnr2 in vacuole function.

My results also demonstrate that the function of Mnr2 to release Mg^{2+} from the

vacuole is dependent on the activity of the Alr1 and Alr2 proteins, which are required to supply excess Mg^{2+} to the cytosol, enabling vacuolar storage of this cation. Furthermore, I observed that when overexpressed, Mnr2 was mislocalized to the plasma membrane. This Mnr2 overexpression suppressed the growth defect of an *alr1 alr2* strain in low Mg^{2+} conditions, suggesting that Mnr2 was capable of mediating Mg^{2+} uptake when present at the plasma membrane. Although the overexpression of Mnr2 did not restore the Mg^{2+} content of the *alr1 alr2* to normal levels, it did allow yeast to maintain a basal level of Mg^{2+} content while dramatically stimulating growth, consistent with supplying the minimal Mg^{2+} required for growth. These results also indicate that Mnr2 can function independently of the Alr proteins to mediate Mg^{2+} transport. Overall, these data support a role for Mnr2 in directly mediating Mg^{2+} transport over the vacuole membrane.

I also investigated the effect of the *mnr2* mutation and Mg^{2+} deficiency on the regulation of the plasma membrane Mg^{2+} transport system, Alr1. The *mnr2* mutation caused an increase in the steady-state level of Alr1 protein accumulation, but had no effect on *ALR1* promoter activity. I also identified an effect of the *mnr2* mutation on the gel mobility of the Alr1 protein, suggesting that this mutation affects the post-translational modification of Alr1. This modification was dependent on Mg^{2+} supply, consistent with the *mnr2* mutation limiting access to intracellular Mg^{2+} stores.

In conclusion, this work is the first description of a transporter or ion channel that regulates Mg^{2+} homeostasis by controlling access to an intracellular Mg^{2+} store. The results of this research provide a revised model for Mg^{2+} homeostasis in yeast and suggest that Mg^{2+} storage may play a role in Mg^{2+} homeostasis in higher eukaryotes.

DEDICATION

I dedicate this dissertation to my mother, Rashmi Pisat, for inspiring me and supporting my career choice, and my friend and husband, Harish Shinde, for supporting me throughout this endeavor. Thank You!

ACKNOWLEDGEMENTS

This dissertation would not be complete without the support of the following people and organizations.

My supervisor, Dr. Colin MacDiarmid for his advice and patience during the experimental work and invaluable help during the writing of this dissertation.

My committee members, Dr. Teresa Thiel, Dr. Wendy Olivas and Dr. Bethany Zolman for their time, and continued guidance throughout my time at UMSL.

Maryann Hempen, who is essential to every Biology department graduate, was kind, helpful and always had answers for my questions.

The past and present MacDiarmid lab members for their help and support. I would like to extend my gratitude to Andrew Franklin and Charles Jackson for their friendship and support, and Phaik Har Lim and Abhinav Pandey for helping me with my experimental work.

The endless list of friends here at UMSL, in the United States of America and back at home in India for providing me with the most needed encouragement and their time to express my concerns regarding this work.

My husband, Harish for his help and encouragement with the dissertation writing and endless support in taking care of our daughter, Anika.

My father and brother for letting me travel miles away from home to pursue the career of my choice. In addition, my family members back in Mumbai (India) who have provided me with encouragement and lifted my spirits during my lowest moments.

Finally, the University of Missouri-St Louis for funding this research.

TABLE OF CONTENTS

<i>ABSTRACT</i>	<i>ii</i>
<i>DEDICATION</i>	<i>iv</i>
<i>ACKNOWLEDGEMENTS</i>	<i>v</i>
<i>TABLE OF CONTENTS</i>	<i>vi</i>
<i>LIST OF FIGURES</i>	<i>x</i>
<i>LIST OF TABLES</i>	<i>xi</i>
Chapter 1 Introduction	1
1.1 Mg²⁺ in biology _____	1
1.2 Chemistry and biochemistry of Mg²⁺ _____	2
1.3 Mg²⁺ in human health _____	3
1.4 Mg²⁺ in agriculture _____	5
1.5 Yeast as a eukaryotic model system for Mg²⁺ homeostasis _____	6
1.6 Regulation of cytosolic Mg²⁺ _____	7
1.7 Bacterial Mg²⁺ transporters _____	9
1.7.1 CorA	9
1.7.1.1 Structural Features of CorA	10
1.7.2 MgtA, B and C	11
1.7.3 MgtE	13
1.8 The CorA superfamily of Mg²⁺ channels in eukaryotes _____	14
1.8.1 CorA family members in yeast and fungi	14
1.8.1.1 Alr1 and Alr2	14
1.8.1.2 Mrs2 and Lpe10	15
1.8.2 CorA family members in eukaryotic microbes	16
1.8.3 CorA family members in plants	17
1.8.4 CorA proteins in mammals	18
1.9 Novel mammalian Mg²⁺ channels _____	19
1.9.1 TRPM6 and TRPM7	19

1.9.2	Mg ²⁺ -regulated transporters	20
1.10	Regulation of Mg²⁺ transporter expression in eukaryotes _____	23
1.11	Objectives of this research _____	24
Chapter 2 Materials and Methods		26
2.1	Buffers, solutions and enzymes _____	26
2.2	Bacterial growth media and antibiotics _____	26
2.3	Bacterial and yeast plasmid vectors _____	26
2.4	Oligonucleotides _____	27
2.5	Polymerase chain reaction (PCR) _____	28
2.6	Plasmid constructs _____	28
2.7	Bacterial transformation _____	31
2.7.1	Preparation of electrocompetent cells.....	31
2.7.2	Electroporation of competent cells	32
2.8	DNA isolation and purification _____	32
2.8.1	Routine plasmid purification from <i>E. coli</i> (Method 1).....	32
2.8.2	Plasmid purification for DNA sequencing (Method 2)	33
2.9	Restriction endonuclease digestion _____	33
2.10	Yeast growth media _____	33
2.10.1	Complex yeast media.....	33
2.10.2	Synthetic media.....	34
2.10.2.1	Synthetic minimal media.....	34
2.10.2.2	Low Magnesium Medium (LMM)	34
2.10.2.3	Low sulfate medium	35
2.11	Yeast strains used in this study _____	35
2.11.1	Construction of yeast mutant strains	38
2.12	Yeast transformation _____	39
2.13	Genomic and plasmid DNA isolation from yeast _____	39
2.14	Sporulation and spore isolation _____	40
2.15	β-Galactosidase activity assay _____	41

2.16	Measurement of Mg²⁺ content by Atomic Absorption Spectroscopy (AAS)	42
2.17	Measurement of yeast elemental content using ICP-MS	43
2.18	Sucrose gradient fractionation of yeast organelles	43
2.19	Protein extraction and immunological detection	44
2.19.1	Protein extraction using TCA	44
2.19.2	SDS-Polyacrylamide Gel Electrophoresis (PAGE)	45
2.19.3	Electroblotting and immunodetection	46
2.19.4	Indirect immunofluorescence	47
Chapter 3 Role of Mnr2 in ion homeostasis		49
3.1	Introduction	49
3.2	Effect of the <i>mnr2</i> mutation on tolerance to biologically important metal ions	49
3.3	Effect of <i>mnr2</i> mutation on growth and Mg²⁺ content	51
3.4	Effect of the <i>mnr2</i> mutation on Mg²⁺ uptake	52
3.5	Models for Mnr2 function	53
3.6	Determination of Mnr2 subcellular location	55
3.7	Determination of Mnr2 location using cell fractionation	58
3.8	Determination of Mnr2 location using epifluorescence microscopy	59
3.9	Genetic evidence for a role of Mnr2 in vacuole function	60
3.10	Interaction of the <i>ALR</i> and <i>MNR2</i> genes	62
3.11	Direct assays of cation transport by Mnr2	65
3.12	Effect of the <i>mnr2</i> mutation on ER function	69
3.13	Summary and discussion	72
3.13.1	The vacuole as a site for storage of excess Mg ²⁺	72
3.13.2	Vacuolar stores of Mg ²⁺ can be utilized to offset cytosolic Mg ²⁺ deficiency	73
3.13.3	Mnr2 is required for the release of vacuolar Mg ²⁺ stores	74
3.13.4	Mnr2 is directly responsible for Mg ²⁺ transport	74
3.13.5	Cation transport by <i>mnr2</i> mutants	75
3.13.6	Mg ²⁺ storage is not restored by the overexpression of Mnr2	77
3.13.7	Role of Alr2 in Mg ²⁺ homeostasis	78
3.13.8	Mnr2 may be required for the maintenance of ER function in Mg ²⁺ -deficient	

LIST OF FIGURES

Figure 1.1	Structure of CorA from <i>Thermotoga maritima</i>	10
Figure 1.2	Yeast CorA proteins	14
Figure 3.1	Divalent cation sensitivity of <i>mnr2</i> mutant strains	50
Figure 3.2	Effect of the <i>mnr2</i> mutation on content of biologically important elements	51
Figure 3.3	Mnr2 plays a role in Mg ²⁺ homeostasis	52
Figure 3.4	Intracellular Mg ²⁺ content supports growth in Mg ²⁺ -deficient conditions	54
Figure 3.5	Modification of the N-terminus did not affect Mnr2 function	56
Figure 3.6	myc-Mnr2 co-fractionated with the vacuolar membrane	58
Figure 3.7	cit-Mnr2 was located in the vacuolar membrane	60
Figure 3.8	Genetic analysis of Mg ²⁺ homeostasis	61
Figure 3.9	<i>ALR1</i> and <i>ALR2</i> are epistatic to <i>MNR2</i>	64
Figure 3.10	Suppression of <i>alr1 alr2</i> phenotypes by Mnr2 overexpression	67
Figure 3.11	The <i>mnr2</i> mutation induced the unfolded protein response	70
Figure 3.12	Model for Mnr2 function in yeast	73
Figure 4.1	Effect of the <i>mnr2</i> mutation on Alr1 accumulation	82
Figure 4.2	Analysis of <i>ALR1</i> gene expression with a <i>lacZ</i> fusion construct	84
Figure 4.3	Alr1 stability was unaffected by Mg ²⁺ repletion	86
Figure 4.4	Effect of cycloheximide and Mg ²⁺ treatment on Alr1 stability	87
Figure 4.5	Growth and Mg ²⁺ content of Mg ²⁺ -loaded and unloaded cells during incubation in Mg ²⁺ -free medium	89
Figure 4.6	Effect of intracellular Mg ²⁺ supply on Alr1 modification during Mg ²⁺ -depletion	90
Figure 4.7	Growth and Mg ²⁺ content of yeast strains during incubation in Mg ²⁺ -replete conditions	91
Figure 4.8	Alr1 modification under Mg ²⁺ -replete conditions	92

LIST OF TABLES

Table 2.1	Oligonucleotides used in this study	27
Table 2.2	Plasmids used in this study	30
Table 2.3	Yeast strains	35

Chapter 1 Introduction

1.1 Mg²⁺ in biology

Magnesium (Mg²⁺) is essential for all life, ranging from unicellular bacteria to complex multi-cellular plants and animals. Mg²⁺ is required for a variety of functions in the cell, serving as a cofactor for many different enzymes, and providing structural stability to ribosomes, proteins and nucleic acids. All living organisms must regulate the concentration of various ions and nutrients to maintain normal cellular functions, and Mg²⁺ is no exception. Since Mg²⁺ is required for so many different biological processes, imbalance of Mg²⁺ could have severe physiological consequences. For this reason, cells are required to maintain an appropriate Mg²⁺ concentration in the cytosol and organelles. Key components of this homeostatic regulation are the transporters and channels that have evolved to move charged Mg²⁺ ions across hydrophobic membranes. Mg²⁺ accumulation by cells is regulated primarily by control of influx, sequestration in organelles and efflux from the organelle and/or the cell. Since these processes require specific channels and transporters, much research has been directed towards identifying novel proteins that can mediate Mg²⁺ transport. For this reason, in the past decade many novel Mg²⁺ transporters have been identified and characterized. However, in many cases, the details of how cells utilize these transporters to respond to environmental challenges remain unclear.

The research presented in this dissertation involves the application of a combination of genetic, biochemical and molecular techniques to characterize a potential Mg²⁺ transporter (Mnr2) from *Saccharomyces cerevisiae* (Baker's yeast). My work suggests that the Mnr2 protein functions to buffer against cytosolic Mg²⁺ deficiency by releasing Mg²⁺ from an intracellular storage compartment. The organization of this document is as follows: **Chapter 1** provides a general introduction to Mg²⁺ as an element and its importance in health and agriculture, followed by a synopsis of the current knowledge of Mg²⁺ transporter proteins across the kingdoms of life. **Chapter 2** describes the general experimental methodology used to conduct this research. **Chapter 3** focuses on determining the role of Mnr2 protein in Mg²⁺ homeostasis and its characterization. **Chapter 4** analyzes the effect of *mnr2* mutation on the expression and modification of

the Alr1 protein, a related Mg^{2+} channel. Lastly, **Chapter 5** provides a summary of my findings and describes the significance of this work, as well as describing possible avenues for future research in this area.

1.2 Chemistry and biochemistry of Mg^{2+}

After potassium, Mg^{2+} ion is the second most abundant intracellular divalent cation [reviewed in (Maguire, 2006)]. Its small ionic size, high charge density, octahedral geometry and strong ionic interaction with water and other ligands makes the Mg^{2+} ion unique within the biologically important cations (Maguire & Cowan, 2002). Mg^{2+} forms ionic bonds with negatively charged molecules such as phosphate and carboxylate ions (Cowan, 2002; Maguire & Cowan, 2002), and can form semi-covalent bonds with nitrogen atoms of porphyrin rings (for example, in chlorophyll) [reviewed in (Maguire, 2006)]. Furthermore, in aqueous solution, Mg^{2+} binds strongly to waters of hydration, which can interact in turn with other ligands or ions [reviewed in (Maguire & Cowan, 2002) and (Maguire, 2006)]. As a consequence, the majority of intracellular Mg^{2+} in cells is bound to biological ligands, and less than 1% exists as free ionized ($[Mg^{2+}]_i$) in the cytoplasm (Millart et al, 1995).

The difference between the ionic and hydrated radii of the Mg^{2+} atom is 400 fold, by far the largest amongst all the cations. While both Mg^{2+} and Ca^{2+} are hexacordinate cations with octahedron geometry, the coordination sphere of Ca^{2+} is relatively flexible compared to that of Mg^{2+} . This difference has been suggested to have influenced the biological roles played by these individual cations. Within cells, Ca^{2+} primarily serves as a second messenger for signal transduction pathways, and its concentration is normally maintained at a very low level in the cytosol. Ca^{2+} mediates its effect on physiology by binding to a variety of ligands, in order to trigger conformational changes within signaling factors. In contrast, the intracellular concentration of Mg^{2+} is normally high, and the Mg^{2+} atom tends to function as an essential cofactor, binding and holding water other molecules in a specific position within the active sites of enzymes, e.g. ATP, or as a stabilizing factor cross-linking the subunits of protein and RNA complexes. Mg^{2+} is a ubiquitous cofactor for more than 300 enzymatic reactions (Sreedhara & Cowan, 2002). For example, Mg^{2+} is required for the enzymes that catalyze phosphate ester hydrolysis,

phosphoryl transfer reactions (Wolf & Cittadini, 2003), nucleic acid metabolism, and cell signaling (Cowan, 2002; Sreedhara & Cowan, 2002). Mg^{2+} also plays an important role in ensuring the structural stability of ribosomes (Cowan, 1995), chlorophyll (Maguire, 2006) and nucleoprotein complexes (Gregan et al, 2001b). Additionally, Mg^{2+} has an indirect effect on the cell physiology of other ions by modulating the activity of ion channels and transporters (Benz & Kohlhardt, 1991; Petit-Jacques et al, 1999; Tang et al, 2000; Wei et al, 2002).

1.3 Mg^{2+} in human health

Mg^{2+} has been implicated in a variety of processes related to vertebrate health. Mg^{2+} is required for active immunological responses such as granulocyte oxidative burst, lymphocyte proliferation, and endotoxin binding to monocytes [reviewed in (Johnson et al, 1980; Tong & Rude, 2005)]. Additionally, several studies have demonstrated that Mg^{2+} deficiency is correlated with an increase in interleukin-1, tumor necrosis factor- α , interferon- γ and substance P, some of the factors involved in key processes such as immune defense, inflammation, regulation of immune cell biology, and apoptosis (Weglicki et al, 1994; Weglicki & Phillips, 1992; Weglicki et al, 1992). Furthermore, Mg^{2+} homeostasis also influences smooth muscle tone, and is thus implicated in critical illnesses such as acute myocardial infarction, acute cerebral ischemia and asthma (Laurant & Touyz, 2000).

The normal Mg^{2+} content of an adult human body is 25 g [reviewed in (Elin, 1987; Tong & Rude, 2005; Wallach, 1988)]. About 53% of total Mg^{2+} is stored in bone, 27% in muscle, 19% in soft tissues, 0.5% in erythrocytes and only 0.3% in the serum (Elin, 1987). Small bowel, kidney, and bone are responsible for Mg^{2+} homeostasis in humans (Rude, 1993). About 90% of intestinal absorption of Mg^{2+} occurs along the jejunum and ileum by a passive paracellular mechanism (Brannan et al, 1976; Kerstan, 2002). Due to its role in reclaiming Mg^{2+} from the urine, the kidney forms the primary organ of homeostasis (Sutton & Domrongkitchaiporn, 1993). The three distinct locations of Mg^{2+} reabsorption in the kidney are the proximal tubule, the thick ascending loop (TAL) of Henle, and the distal tubule. Most reabsorption of Mg^{2+} (65% to 75%) occurs in the TAL (Cole & Quamme, 2000; Quamme & de Rouffignac, 2000). When whole

body Mg^{2+} stores are depleted, the systems responsible for Mg^{2+} reabsorption are induced, increasing the efficiency of reclamation from the urine (Dai et al, 2001).

Mg^{2+} deficiency and defective Mg^{2+} homeostasis are commonly associated with human disease. Surveys conducted in intensive care units have reported that 20-65% of patients are Mg^{2+} -deficient (Deheinzeln et al, 2000; Reinhart & Desbiens, 1985; Ryzen et al, 1985) and that such patients have mortality rates 2 to 3 times higher than those who are not Mg^{2+} deficient (Fiaccadori et al, 1988). Vomiting, acute and chronic diarrhea, and malabsorption syndromes due to mucosal damage from radiation therapy or pancreatitis are some of the leading causes of Mg^{2+} deficiency resulting from gastrointestinal disorders [reviewed in (Tong & Rude, 2005)]. Renal Mg^{2+} loss can also occur due to osmotic diuresis, hypercalcemia, alcohol consumption, and following administration of drugs such as diuretics, antibiotics, and those used in cancer therapy. Additionally, metabolic acidosis due to starvation, diabetes, and chronic alcoholism, along with some rare renal diseases, contribute to Mg^{2+} deficiency [reviewed in (Tong & Rude, 2005)].

Low intake of Mg^{2+} is associated with the development of risk factors for fatal cardiovascular diseases, stroke, type II diabetes mellitus and hypertension [reviewed in (Seelig & Rosanoff, 2003)]. There is an increasing concern that citizens of developed countries do not routinely obtain the recommended daily allowance (RDA) of dietary Mg^{2+} . Many processed foods are depleted of Mg^{2+} during manufacturing, and most are not fortified with Mg^{2+} as they are for some other essential nutrients and vitamins. In addition, many modern crop varieties are relatively nutrient poor. Due to their bulky nature, even one-a-day vitamin and mineral supplement do not provide the RDA of Mg^{2+} (Seelig & Rosanoff, 2003). Dietary supplementation with large amounts of inorganic Mg^{2+} sources can have unpleasant side effect making such supplementation more difficult to achieve than for other nutrients.

Severe Mg^{2+} deficiency often occurs as a consequence of a disease condition, and maybe exacerbated by the drugs administered for the condition [reviewed in (Tong & Rude, 2005)]. Some of the clinical manifestations of moderate to severe Mg^{2+} deficiency include electrolyte abnormalities (hypokalemia, hypocalcemia), neuromuscular (tetany, seizures) and cardiovascular symptoms (dysrhythmias, hypertension), asthma (smooth muscle constriction, increased mucous production and plugging) and preeclampsia

(hypertension, proteinuria, edema and multi-organ failure). Patients suffering from moderate to severe Mg^{2+} deficiency can be administered intravenous Mg^{2+} to correct the deficiency [reviewed in (Rude et al, 1978; Ryzan et al, 1985; Tong & Rude, 2005)]. However, diagnosing Mg^{2+} deficiency is not simple, as serum Mg^{2+} content does not provide an accurate indication of Mg^{2+} status [reviewed in (Tong & Rude, 2005)], and more sophisticated assays have yet to be developed.

1.4 Mg^{2+} in agriculture

As a consequence of its position as the central atom in the chlorophyll porphyrin ring, Mg^{2+} is critical to plant life. Insertion of Mg^{2+} in chlorophyll allows this molecule to absorb a much broader range of light wavelengths, consequently capturing more energy for photosynthesis. Plants grown under Mg^{2+} deficient conditions exhibit severe interveinal chlorosis (leaf yellowing) on fully expanded leaves (Deng et al, 2006; Hermans & Verbruggen, 2005). Mg^{2+} deficiency affects crop productivity and is a common agricultural problem (Bennett, 1997). The major strategy for the correction of Mg^{2+} deficiency in soil is the addition of lime, although this intervention may not be economically feasible in underdeveloped countries.

Many studies have suggested that Mg^{2+} deficiency may also exacerbate Aluminium (Al^{3+}) toxicity in plants (Matsumoto, 2000; Silva et al, 2001a; Silva et al, 2001b; Silva et al, 2001c). Al^{3+} toxicity is a major factor limiting crop productivity in acidic soils (pH < 5.0), which constitute about 40% of the world's arable land (Delhaize & Ryan, 1995). The high concentration of Al^{3+} in acidic soils inhibits root growth, thus negatively impacting crop yield. Mg^{2+} was hypothesized to compete with Al^{3+} for binding to root cells (Grauer UE, 1992; Kinraide & Parker, 1987). Work in yeast suggested that Al^{3+} inhibited Mg^{2+} uptake over the plasma membrane, possibly by competitive inhibition of the Mg^{2+} transport system (MacDiarmid & Gardner, 1996). Subsequent work identified two membrane proteins (Alr1 and Alr2) that could confer Al^{3+} tolerance to yeast when overexpressed (MacDiarmid, 1997; MacDiarmid & Gardner, 1998). The Alr proteins are related to the CorA family of Mg^{2+} transporters from bacteria, and genetic studies indicated that they perform the same function in yeast. Alr1 protein overexpression was suggested to overcome Al^{3+} toxicity by increasing the capacity for

Mg²⁺ uptake in the presence of this inhibitor. CorA homologs also exist in plants, and several of them have been shown to mediate Mg²⁺ transport (Drummond et al, 2006; Gardner, 2003; Li et al, 2001b). Although the role that Mg²⁺ transport plays in the phenomenon of Al³⁺ toxicity in plants is not yet fully understood (Yang et al, 2007), increased expression of plant Mg²⁺ transporters has been shown to successfully alleviate Al³⁺ toxicity (Deng et al, 2006), suggesting that at least in some plant species, the mechanism of Al³⁺ toxicity is similar to that proposed for yeast.

1.5 Yeast as a eukaryotic model system for Mg²⁺ homeostasis

Saccharomyces cerevisiae (Budding yeast or Bakers' yeast) is a versatile eukaryotic model organism for biochemical and genetic studies. Due to its ability to propagate as both haploid and diploid strains, yeast provides an opportunity to determine the phenotypes of recessive alleles and also to study allelic interactions. Additionally, the ability to perform efficient homologous recombination permits easy manipulation of genes, either by introducing point mutations or by the complete elimination of a particular gene. Mating or transformation processes allow rapid generation of strains carrying a genotype of interest. Transformation with independently replicating plasmids is another easy method of introducing genes into yeast strains. By employing different plasmid replication origins to vary plasmid copy number, and employing differentially regulated promoters, we can specifically modify gene expression in yeast.

Another advantage of the yeast model system is that with the yeast genome completely sequenced, it is possible to identify homologs of genes from higher eukaryotes based on conservation and then conduct reverse genetic studies to determine their function. Additionally, homologs of yeast genes from higher eukaryotes can be cloned and expressed in mutant yeast strains to determine if any functional overlap exists. For example, the *AtMRS2-1* gene in *Arabidopsis thaliana* was identified based on its homology to the yeast *MRS2* gene, which encodes a protein responsible for Mg²⁺ transport into mitochondria. Overexpressing *AtMRS2-1* in a yeast *mrs2* deletion strain showed that this protein complemented the yeast mutation (Schock et al, 2000). A quicker route to the identification of yeast genes homologs in higher eukaryotes is by functional complementation, which was used to independently isolate the *AtMGT10* gene

via complementation of a yeast *alr1 alr2* mutant strain (Li et al, 2001b).

Yeast is an excellent model system to conduct biochemical analysis of transporters and other enzymes. For example, the role of putative ion transporter genes can be studied by measuring changes in the metal content of strains in which these genes are overexpressed or deleted, and by screening for metal-ion associated tolerance or sensitivity phenotypes. The rapid development of simple genetic screens for transport and regulatory mutants is one reason why transporters and regulatory factors involved in eukaryotic zinc (Zn^{2+}), iron (Fe^{3+}), copper (Cu^{2+}), and phosphate (P) metabolism were first identified in this organism (Eide, 1998; Persson et al, 2003). For the same reasons, yeast is the organism in which eukaryotic Mg^{2+} homeostasis is best understood (Gardner, 2003), and why it was chosen as the model system used to perform the work described in this dissertation.

1.6 Regulation of cytosolic Mg^{2+}

As previously discussed, the diverse roles played by Mg^{2+} make it critical for a cell to regulate cytosolic Mg^{2+} concentration correctly. The cytosolic $[Mg^{2+}]_i$ has been estimated to range from 0.5-1.0 mM in various cell types (Grubbs, 2002). Perhaps as a reflection of the relative abundance of Mg^{2+} in the cytosol, Mg^{2+} ions interact relatively weakly with their binding sites in proteins ($K_a < 10^5 M^{-1}$) (Cowan, 2002). For this reason, small variations in $[Mg^{2+}]_i$ can have large effects on physiology, and maintaining a consistent $[Mg^{2+}]_i$ is important for cell function. This regulation is achieved by the action of specific Mg^{2+} transporters that mediate the influx or efflux of Mg^{2+} from the cell, or sequester Mg^{2+} within organelles (Nelson, 1999).

Cation transport mechanisms can be classified as either active or passive. Influx of Mg^{2+} via specific channels is a passive process driven by the electrochemical gradient (Dai & Quamme, 1991). Efflux of protons (in bacteria, plants, and fungi) or Na^+ (in animal cells) by ATP-driven pumps in the plasma membrane generates a negative charge of the cytosol. In animal cells, Mg^{2+} efflux is one of the most important processes regulating cytosolic Mg^{2+} concentration. The efflux of Mg^{2+} requires energy to overcome the electrical potential gradient driving Mg^{2+} influx. In mammalian cells, Mg^{2+} efflux is coupled to Na^+ influx via the action of a Na^+/Mg^{2+} exchanger (Romani & Scarpa, 1992;

Romani & Scarpa, 2000). This system was first characterized in erythrocytes (Ferreira et al, 2004; Flatman & Smith, 1990; Flatman & Smith, 1996). In several cell types, removal of extracellular Na^+ resulted in a significant increase in $[\text{Mg}^{2+}]_i$, indicating that $\text{Mg}^{2+}/\text{Na}^+$ exchange plays a general role in vertebrate Mg^{2+} homeostasis (Handy et al, 1996; Tashiro & Konishi, 1997).

The accumulation of excess Mg^{2+} in organelles also is likely to contribute to cytosolic Mg^{2+} homeostasis. In yeast, for example, the average concentration of Mg^{2+} within organelles is 14-fold higher than in the cytosol (Okorokov et al, 1978; Okorokov et al, 1980). Increasing the medium Mg^{2+} concentration from 50 μM to 50 mM increased the Mg^{2+} content of yeast cells four-fold, but had little effect on growth rate (Beeler et al, 1997) suggesting that the cytosolic Mg^{2+} levels are tightly regulated. The ability of yeast to accumulate much more Mg^{2+} than the minimum required implies the existence of an intracellular storage compartment. Recent studies indicate that the yeast vacuole (the equivalent of the mammalian lysosome) is a site for Mg^{2+} sequestration. Accumulation of vacuolar polyphosphate, a linear polymer of inorganic phosphate, is required for substantial Mg^{2+} accumulation by yeast (Beeler et al, 1997; Nishimura et al, 1999). Polyphosphate has been shown to bind Mg^{2+} with high affinity (Beeler et al, 1997), and could act as a sink for Mg^{2+} ions in the vacuole (Beeler et al, 1997; Nishimura et al, 1999; Okorokov et al, 1975). More direct evidence comes from recent studies using X-ray microanalysis, which have identified the vacuole as a site of Mg^{2+} accumulation in yeast cells (Simm et al, 2007). In these studies, Mg^{2+} and P were found associated with the vacuole, and P and Mg^{2+} content were strongly correlated, suggesting that regulation of P and Mg^{2+} content is interrelated. Using the same technique, vacuolar accumulation of Mg^{2+} was also observed in eukaryotic microbes such as *Leishmania* (LeFurgey et al, 1990; Scott et al, 1997). Changes in cytosolic Mg^{2+} in response to hormonal stimuli suggest that intracellular sequestration of Mg^{2+} also may occur in mammalian cells (Romani et al, 1993; Zhang & Melvin, 1992; Zhang & Melvin, 1994; Zhang & Melvin, 1996; Zhang & Melvin, 1997), although it is not yet clear which organelle is responsible.

In addition to a role in removal of excess cytosolic Mg^{2+} , intracellular compartments potentially provide a reservoir of Mg^{2+} that could be used to buffer the cytosolic Mg^{2+} concentration. In yeast, the intracellular Mg^{2+} store accumulated during

growth in replete conditions was sufficient to support a 3.5-fold increase in cell number in the absence of external Mg^{2+} (Beeler et al, 1997). The yeast vacuole can store and release other essential metal ions to offset deficiency (MacDiarmid et al, 2000; MacDiarmid et al, 2003). In mammalian cells, the release of Mg^{2+} from an intracellular compartment was stimulated by exposure to muscarine (which mimics the action of the neurotransmitter acetylcholine) (Zhang & Melvin, 1996). The regulated release of Mg^{2+} stores could potentially play a role in modulating signal transduction pathways, or may buffer against changes in extracellular Mg^{2+} supply, such as might occur under conditions of dietary Mg^{2+} deficiency.

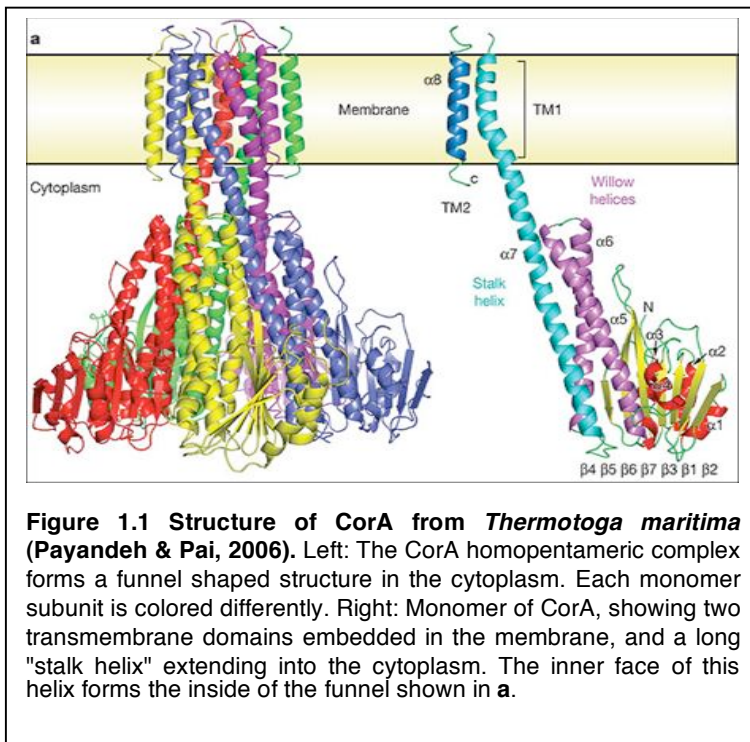
1.7 Bacterial Mg^{2+} transporters

1.7.1 CorA

Mg^{2+} transport activity in *E. coli* was first reported in 1969 (Silver, 1969), and it was noted that Mg^{2+} and Co^{2+} could be accumulated by the same system. To isolate mutants that lacked activity of this transport system, researchers took advantage of the lack of specificity of the transporter by selecting for strains that were unable to accumulate Co^{2+} ions (Park et al, 1976; Silver, 1969). By 1985, the gene encoding the Co^{2+} transport system (*corA* for Cobalt Resistant) was cloned from the enteric bacteria *Salmonella typhimurium* (Hmiel et al, 1986). The *corA* gene is constitutively expressed in *S. typhimurium*, and its promoter does not respond to changes in Mg^{2+} availability. Additionally, *corA* gene expression is also independent of growth phase and/or type of growth media (Smith & Maguire, 1998; Tao et al, 1998). CorA thus represents a "housekeeping" system for the routine acquisition of Mg^{2+} by bacteria. The influx of Mg^{2+} via CorA is dependent on membrane potential, and this system resembles a Mg^{2+} -selective ion channel (Froschauer et al, 2004; Maguire, 2006). The CorA protein has a high affinity for Mg^{2+} (15 μ M), but it can also transport other divalent cations such as Co^{2+} and Ni^{2+} with lower affinity (Hmiel et al, 1986; Payandeh & Pai, 2006; Snavely et al, 1989a). Although CorA can transport divalent cations other than Mg^{2+} , there is no evidence that it is required for the homeostasis of other cations (Maguire & Cowan, 2002).

1.7.1.1 Structural Features of CorA

Structurally CorA protein can be divided into two general regions: a long, weakly conserved hydrophilic amino (N) terminal end located in the cytosol, and a short, well-conserved, hydrophobic carboxy (C) terminal domain embedded in the membrane (**Figure 1.1**). Although substantial variation exists at the level of primary amino acid sequence, CorA proteins of any origin can be identified by two distinct features. First, CorA proteins always have two transmembrane domains (TMD) close to the C terminal end. The relatively low number of these domains suggests that coordination of several monomers is required to form a Mg^{2+} transporting structure, a prediction confirmed by recent crystallographic studies (Eshaghi et al, 2006; Lunin et al, 2006; Payandeh & Pai, 2006). Second, CorA proteins have a single characteristic glycine-methionine-asparagine (GMN) motif at the C terminal end of the penultimate TMD. The GMN motif is critical for Mg^{2+} transport, as mutation of any of the residues in this sequence eliminated Mg^{2+} transport (Knoop et al, 2005; Worlock & Smith, 2002). A small number of CorA proteins show some variation in the sequence of the GMN motif. This change may alter ion specificity, since at least one of these variants was shown to transport divalent cations other than Mg^{2+} [e.g., Zn^{2+} , (Knoop et al, 2005; Worlock & Smith, 2002)].



Several different groups recently determined the X-ray structure of the CorA protein using a homolog from the thermophilic Gram-negative bacteria *Thermotoga maritima* (Eshaghi et al, 2006; Lunin et al, 2006; Payandeh & Pai, 2006). As seen in the resulting structure (**Figure 1.1**), CorA forms a funnel-shaped homo-pentamer with two

membrane-embedded domains per monomer. In the homo-pentamer, the first TMD of each CorA monomer combines to form part of the metal ion translocation channel. The second TMD lies perpendicular to the membrane and is present on the periphery of the first TMD. The large N terminal end extends from the bottom of the first TMD into the cytoplasm as a long α -helix called the stalk helix, which forms the inner face of the funnel-like N-terminal domain.

The crystal structure also revealed the presence of an apparent Mg^{2+} -binding site between the aspartate residues present at the bottom of the stalk helix, and the α -helix domain of the adjacent monomer. The intracellular location of the Mg^{2+} binding sites suggests a model for the regulation of Mg^{2+} transport by the cytoplasmic Mg^{2+} concentration. The model predicts that the intracellular availability of Mg^{2+} ions determines the mobility of the long stalk helix of each monomer with respect to its adjacent monomer. The mobility of the stalk helix in turn determines the opening or closing of the ion translocation pore at the membrane, thus regulating the influx of Mg^{2+} ions (Payandeh & Pai, 2006). Thus, CorA proteins form Mg^{2+} -gated channels, the activity of which is regulated by feedback inhibition. Subsequent studies have provided further genetic and physiological evidence supporting this general model (Payandeh et al, 2008; Schindl et al, 2007).

1.7.2 MgtA, B and C

During the early investigations of Mg^{2+} transport by *E. coli* and *S. typhimurium*, it was recognized that as *corA* mutants of *E. coli* still exhibited robust Mg^{2+} uptake activity, bacteria expressed alternative systems for Mg^{2+} acquisition from the environment (Hmiel et al, 1989; Park et al, 1976). Further genetic studies revealed the presence of another system in *E. coli* (the *mgt* gene) (Park et al, 1976), and two more systems in *S. typhimurium* (encoded by the *mgtA* and *mgtB* genes) (Hmiel et al, 1989). Loss of all three systems in *S. typhimurium* rendered the cells unable to grow except in the presence of a much higher Mg^{2+} concentration than was normally present in growth medium. Tracer uptake studies showed that each system had a distinct cation specificity and kinetic characteristics (Snively et al, 1989a). Both MgtA and MgtB can transport Ni^{2+} , but are inhibited by Co^{2+} . However, the two proteins show differences in their ability to transport

Zn²⁺, Ca²⁺ and Mn²⁺, and in their temperature dependence [reviewed in (Maguire, 2006)].

The *mgtA* and *mgtB* genes were cloned from *S. typhimurium* by complementation of the Mg²⁺ deficient growth phenotype of a *corA mgtA mgtB* mutant, which required supplementation with 10-100 mM Mg²⁺ for growth [reviewed in (Maguire, 2006; Snavely et al, 1989b)]. The MgtA/B proteins were found to be members of the P-type ATPase superfamily. Generally, P-type ATPases function to move cations from the cytoplasm to the extracellular environment or into organelles against an electrochemical gradient. The discovery that the MgtA and MgtB proteins were P-type ATPases was a surprise, as Mg²⁺ influx is driven by the electrochemical gradient, and was not believed to require additional energy input [reviewed in (Maguire, 2006)].

While CorA is constitutively expressed, the *mgt* genes are repressible, and these proteins are only expressed in Mg²⁺-deficient cells (Snavely et al, 1989a). The expression of both Mgt proteins is regulated by a two-component signal transduction system (PhoP-PhoQ) (Garcia Vescovi et al, 1996). PhoQ is a membrane sensor-kinase, while PhoP is a transcription factor (Miller et al, 1989). In the presence of 100 μM or greater Mg²⁺, PhoQ binds Mg²⁺ and changes its conformation, leading to the dephosphorylation of its cytosolic domain. Conversely, when external Mg²⁺ is low, PhoQ is activated and auto-phosphorylates its cytosolic domain, which activates the associated PhoP protein. PhoP then binds to the promoters of regulated genes (including *mgtA* and *mgtB*) to induce their expression (Tao et al, 1998; Tao et al, 1995).

Interestingly, well before the realization of their role in Mg²⁺ homeostasis, the *phoPQ* genes were known to be required for virulence and the regulation of pathogenicity-related genes in *S. typhimurium* and other pathogenic bacteria (Gunn & Miller, 1996). For this reason, it was somewhat surprising to learn that Mg²⁺ was the environmental signal that regulated the activity of the PhoP/PhoQ pathway (Garcia Vescovi et al, 1996; Groisman, 2001; Vescovi et al, 1997). In accordance with this model however, it was found that the *mgt* genes were induced upon entry of *S. typhimurium* into macrophages and epithelial cells (Miller, 1991; Miller & Mekalanos, 1990) and also during infection of mice (Heithoff et al, 1999; Mahan et al, 1993). Currently it is believed that the intracellular environment of the macrophage is Mg²⁺-deficient, providing a convenient signal for the induction of pathogenicity-related genes.

Analysis of the *mgtB* operon in *S. typhimurium* revealed a second gene, *mgtC*, which is required for intra-macrophage survival of *S. typhimurium* and pathogenicity in mice (Blanc-Potard & Groisman, 1997; Lawley et al, 2006). Similar to *mgtB*, *mgtC* is regulated by the PhoPQ two-component system, and is required for growth in low Mg^{2+} environments (Blanc-Potard & Groisman, 1997; Blanc-Potard & Lafay, 2003; Buchmeier et al, 2000). Initially, MgtC was suggested to represent a fourth Mg^{2+} transporter in *S. typhimurium*, but a later study showed that expression of MgtC in a *corA mgtA mgtB* mutant had only a minor effect on growth of the mutant strain, and did not promote any detectable increase in Mg^{2+} uptake (Moncrief & Maguire, 1998). Additionally, expression of MgtC in *Xenopus laevis* oocytes failed to promote Mg^{2+} uptake suggesting that MgtC does not directly transport Mg^{2+} (Gunzel et al, 2006). Currently, the role of MgtC in pathogenicity and Mg^{2+} homeostasis remains unclear.

1.7.3 MgtE

The first member of the MgtE family of transporters was unexpectedly cloned from *Bacillus firmus* OF4 (Smith et al, 1995) and *Providencia stuartii* (Townsend et al, 1995) by complementation of a triple mutant *corA mgtA mgtB* strain with genomic libraries constructed from these species. Homologs of MgtE are found both in Eubacteria and Archaea, but eubacterial species carry both CorA and MgtE genes, whereas Archaea primarily use MgtE alone. In general, much less is known about the physiological role of the bacterial members of this family than for the bacterial CorA and the Mgt proteins. However, the recognition of higher eukaryotic homologs of MgtE has generated some recent interest in this family of proteins (Goytain & Quamme, 2005b). Recently Hattori and coworkers (2007) determined the crystal structure of MgtE from *Thermus thermophilus*. The MgtE transporter forms a homodimer with the five TMDs contributed by the C terminus of each subunit forming a pore in the membrane. Four putative Mg^{2+} ions were found bound at the interface between the connecting helices between the cystathionine- β -synthase (CBS) domains and the TMDs, while a fifth Mg^{2+} ion was bound to a conserved residue within the pore. The model suggested that MgtE activity was regulated by its cytosolic sensor domain: the authors proposed that binding of Mg^{2+} to the interface of the connecting helices in the cytosolic domain generated a movement

in the connecting helices that triggered the reorganization of the TMDs to close or open the pore, thus regulating channel activity. Thus, the structures of MgtE and CorA reveal some interesting similarities in the mechanism by which these transporters respond to changes in cytosolic Mg^{2+} concentration.

1.8 The CorA superfamily of Mg^{2+} channels in eukaryotes

1.8.1 CorA family members in yeast and fungi

1.8.1.1 Alr1 and Alr2

The first eukaryotic Mg^{2+} transporter proteins to be identified were the Alr1 and Alr2 proteins from *S. cerevisiae* (MacDiarmid & Gardner, 1998) (**Figure 1.2**). The *ALR*

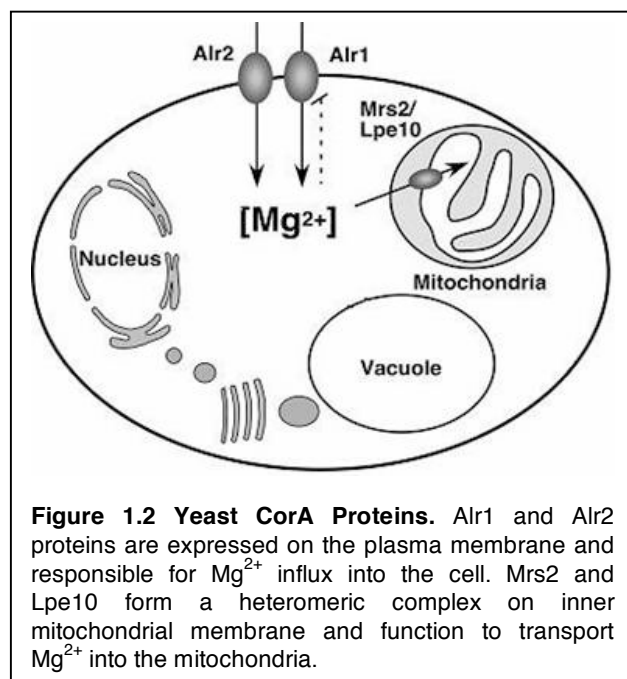


Figure 1.2 Yeast CorA Proteins. Alr1 and Alr2 proteins are expressed on the plasma membrane and responsible for Mg^{2+} influx into the cell. Mrs2 and Lpe10 form a heteromeric complex on inner mitochondrial membrane and function to transport Mg^{2+} into the mitochondria.

genes (ALuminum Resistance) were identified as a consequence of their ability to confer increased tolerance to Al^{3+} when overexpressed. Al^{3+} toxicity to yeast was maximal under conditions of reduced Mg^{2+} supply (MacDiarmid & Gardner, 1996), suggesting that Al^{3+} inhibits a system required for Mg^{2+} uptake. The Alr proteins were suggested to represent this system. Both Alr1 and Alr2 are plasma membrane proteins (Graschopf et al, 2001), consistent with a role in

Mg^{2+} uptake. Genetic studies showed that *alr1* mutants had a growth defect that was suppressed by adding excess Mg^{2+} to the medium (MacDiarmid & Gardner, 1998). In contrast, deletion of the *ALR2* gene had no effect on growth, indicating that this gene made only a minor contribution to homeostasis under normal conditions. When overexpressed however, Alr2 suppressed the Mg^{2+} requirement phenotype of an *alr1* strain, suggesting that Alr1 and Alr2 are redundant in function (MacDiarmid & Gardner, 1998). Subsequent studies have indicated that the relatively minor contribution of *ALR2*

in these studies may have been due to a combination of low expression in the yeast strains used (MacDiarmid, 1997), combined with a mutation that reduces its activity relative to Alr1 (Graschopf et al, 2001).

Relatively little is known about the specificity and activity of the Alr proteins. The overexpression of Alr1 in yeast allowed the detection of Mg^{2+} -dependent inward currents by patch clamping, and the large magnitude of these currents was consistent with Alr1 functioning as a cation channel (Liu et al, 2002). Indirect evidence suggests that Alr1 has broad substrate specificity, even in comparison with the bacterial CorA proteins. Overexpression of Alr1 or Alr2 dramatically increased the sensitivity of yeast to a variety of divalent cations including Co^{2+} , Zn^{2+} , Ni^{2+} , Mn^{2+} and Ca^{2+} (MacDiarmid & Gardner, 1998). Alr1 overexpression also increased the rate of accumulation of $^{57}Co^{2+}$ isotope. Preliminary kinetic studies demonstrated that Alr1 could mediate Co^{2+} uptake with a K_m of 100 μM , suggesting that Alr1 has a relatively low affinity for substrates other than Mg^{2+} (MacDiarmid, 1997). Several studies have provided evidence for the existence of low affinity divalent cation transport systems in yeast with K_m values within this general range, including those for Mn^{2+} (Fuhrmann & Rothstein, 1968; Gadd & Laurence, 1996), Ni^{2+} (Joho et al, 1991) and Co^{2+} (Joho et al, 1991). Many of these reports indicate that transport is inhibited by Mg^{2+} ions (Fuhrmann & Rothstein, 1968; Gadd & Laurence, 1996; Joho et al, 1991; Ross, 1995), consistent with a role for a CorA-like system in this process.

1.8.1.2 *Mrs2 and Lpe10*

Two more CorA-related proteins from yeast, Mrs2 and Lpe10, have been shown to play a role in Mg^{2+} homeostasis within the mitochondria (**Figure 1.2**). The Mrs2 protein is encoded by a nuclear gene and accumulates on the inner mitochondrial membrane. *MRS2* is essential for the splicing of mitochondrial group II introns (Wiesenberger et al, 1992), and the yeast *mrs2* mutant shows a "petite" phenotype (an inability to use non-fermentable carbon sources), along with a mitochondrial cytochrome deficiency. These phenotypes of the *mrs2* yeast strain may be due to a defect in mitochondrial Mg^{2+} homeostasis. Consistent with this model, these phenotypes were partially suppressed by the overexpression of the bacterial CorA protein in yeast (Wiesenberger et al, 1992).

The Lpe10 protein is an ortholog of Mrs2 that is also found in the inner mitochondrial membrane. An *lpe10* mutant showed similar phenotypes as the *mrs2* mutant, including lower mitochondrial Mg^{2+} content (Gregan et al, 2001a). However, the two proteins cannot substitute for each other, suggesting that Lpe10 cooperates with Mrs2 to transport Mg^{2+} into the mitochondria, possibly through the formation of a heteromeric complex (Gregan et al, 2001a). Consistent with this mode, the Mrs2/Lpe10 complex formed a high capacity ion channel in the inner mitochondrial membrane (Kolisek et al, 2003).

A fifth CorA family protein (Ykl064w), which is closely related to the Alr proteins, was also identified in yeast (MacDiarmid, 1997). Inactivation of the *YKL064w* gene conferred sensitivity to Mn^{2+} ions, leading it to be termed Mnr2 (for Manganese resistance). *mnr2* mutant strains showed no obvious growth defect, but did show altered sensitivity to several divalent cations (including Mn^{2+} , Ca^{2+} and Zn^{2+}). When I began this work, the physiological role of Mnr2 had yet to be determined, and an analysis of its potential role in Mg^{2+} homeostasis is the major focus of this dissertation.

1.8.2 CorA family members in eukaryotic microbes

With an aim to identify proteins important for parasitic virulence, Zhu and coworkers searched the *Leishmania* genome database for potential Mg^{2+} transporters (Zhu et al, 2009). Leishmaniasis is a complex disease caused by the *Leishmania major* parasite, which affects at least 12 million people globally. Survival of *L. major* within macrophages is dependent on their tolerance to Mg^{2+} deficient conditions, which provoked interest in *Leishmania* Mg transporters (Lanza et al, 2004). Two proteins (MGT1 and MGT2) were identified and characterized as the first potential Mg^{2+} transporters in *Leishmania*. The C-terminus of MGT1 and MGT2 shared 42% and 26% identity respectively with CorA from *T. maritima*. Functional complementation assays conducted by overexpressing MGT1 and MGT2 in *E. coli* lacking CorA demonstrated that only MGT1 restored Co^{2+} sensitivity, suggesting that (like bacterial CorA), this protein was capable of mediating Co^{2+} uptake. Both MGT1 and MGT2 were localized to an ER compartment in *Leishmania* parasites. Gene disruption studies showed that single mutants of *mgt1* had no growth defect and were associated with a gain of initial

infectivity compared to the wild type. In contrast, *mgt2* mutation induced much slower growth compared to the wild type and a significant loss of virulence. These results suggested that MGT1 functions as a Mg^{2+} transporter, while MGT2 is important for virulence, and that both MGT1 and MGT2 function as regulators of the life cycle of *Leishmania*.

1.8.3 CorA family members in plants

Schock and coworkers (2000) identified two homologs of the yeast Mrs2 protein in *Arabidopsis thaliana* and named them as AtMRS2-1 and AtMRS2-2. Although similar in sequence, AtMRS2-2 was predicted to contain only one TMD, compared to the two TMDs at the C-terminus of most CorA homologs. Functional characterization of the two gene products demonstrated that only AtMRS2-1 was able to suppress the phenotypes of the *mrs2* mutation. Based on the protein sequences of AtMRS2-1 and AtMRS2-2, eight more homologs of MRS2 were identified in *A. thaliana* (Schock et al, 2000).

Li and colleagues independently reported the identification of the same gene family (10 members) in *A. thaliana*, initially by functional complementation of an *alr1 alr2* yeast strain. They named the family members AtMGT (for *Arabidopsis thaliana* magnesium transporter). The AtMRS2-1 and AtMRS2-2 genes were named AtMGT2 and AtMGT9 respectively (Li et al, 2001b). Expression of AtMGT10 suppressed the growth defect of a yeast *alr1 alr2* mutant, and expression of AtMGT1 suppressed the growth defect of a *S. typhimurium corA mgtA mgtB* mutant, indicating that AtMGT10 and AtMGT1 were functional homologs of the Alr proteins and bacterial CorA respectively. Sub-cellular localization studies of AtMGT1 (Li et al, 2001b) and AtMGT10 (AtMRS2-11) (Drummond et al, 2006) showed that AtMGT1 and AtMGT10 were localized to the plasma membrane and the chloroplast membrane respectively. In addition, the subtle differences in the tissue specificity of AtMGT expression suggested that the different members of this large gene family perform different roles within *Arabidopsis*.

Uptake studies using $^{63}Ni^{2+}$ as a tracer demonstrated that AtMGT1 could mediate Mg^{2+} -sensitive Ni^{2+} uptake when expressed in bacteria (Li et al, 2001b). Mg^{2+} uptake by AtMGT1 was also inhibited by Cobalt (III)-hexamine, which has been demonstrated to be a potent inhibitor of CorA (Kucharski et al, 2000), highlighting functional similarities

between the AtMGT proteins and CorA (Smith et al, 1998). In addition to Co (III)-hexamine, the AtMGT1, AtMGT10 and CorA proteins were inhibited by low concentrations of aluminum ion (Al^{3+}) (Li et al, 2001b), as were the Alr1 and Alr2 proteins (MacDiarmid, 1997). These observations suggest that Al^{3+} ions compete strongly for the Mg^{2+} binding site within the pore of CorA-type channels. They also raise the possibility that Al^{3+} toxicity to plants (a major agricultural problem) may be mediated through its effect on Mg^{2+} channel activity, and that the overexpression of plant Mg^{2+} transporters may alleviate toxicity, as is the case in yeast (MacDiarmid, 1997; MacDiarmid & Gardner, 1996; MacDiarmid & Gardner, 1998).

Another study investigating the *in vivo* function of Mg^{2+} transporters in *A. thaliana* reported that AtMGT5 is important for male gametophyte vitality (Li, 2008). AtMGT5 is a Mg^{2+} transporter localized in the mitochondrial membrane. In a *S. typhimurium corA mgtA mgtB* mutant, AtMGT5 mediated Mg^{2+} influx under low external Mg^{2+} availability, but mediated Mg^{2+} efflux in the presence of Mg^{2+} concentrations above $100\mu M$. Supporting this model, a higher rate of Ni^{2+} efflux was observed for a AtMGT5-expressing strain, compared to those expressing AtMGT1 or AtMGT10. A previous study had suggested that *AtMGT5* transcripts were only expressed in flowers (Li et al, 2001b). Detailed studies confirmed that *AtMGT5* transcripts accumulated in the early stages of flower development, and were exclusively expressed in anthers. Consistent with this anther-specific pattern, homozygous T-DNA insertional mutants of *AtMGT5* had inviable pollen, indicating an essential role of AtMGT5 in male gametophyte development.

1.8.4 CorA proteins in mammals

The only mammalian member of the CorA family (hsaMrs2L) and the first vertebrate Mg^{2+} channel to be identified is most closely related in sequence to yeast Mrs2. The expression of hsaMrs2L in an *mrs2* mutant could partially reverse the respiratory defect of this strain, and hsaMrs2L was localized to the mitochondrial inner membrane in human cells (Zsurka et al, 2001). A genetic investigation of the role of hMrs2L in mitochondria was recently reported (Piskacek et al, 2008). An *hsaMrs2L* conditional knock-out strain generated by expression of shRNA in HEK293 cells showed lower levels of mitochondrial free Mg^{2+} and slower mitochondrial Mg^{2+} uptake,

indicating that *hsaMrs2* is an essential mitochondrial Mg^{2+} transport system in vertebrates. Consistent with this idea, constitutive expression of shRNA directed to *hsaMRS2L* resulted in loss of respiratory complex I, decreased mitochondrial membrane potential, and eventual cell death. These results clearly establish an important role of *hsaMRS2L* in mitochondrial function.

1.9 Novel mammalian Mg^{2+} channels

1.9.1 TRPM6 and TRPM7

TRPM6 and 7 (Nadler et al, 2001) are members of the transient receptor potential melastatin (TRPM) ion channel family [reviewed in (Schlingmann et al, 2007)]. Members of this family mediate divalent cation influx and monovalent cation efflux from the cell (Kozak & Cahalan, 2003; Nadler et al, 2001). A unique feature of TRPM6 and 7 is the presence of an unusual α -kinase domain at the C-terminal end, leading them to be termed "Chanzymes" (Montell, 2003; Riazanova et al, 2001; Runnels et al, 2001).

TRPM6 was first identified by positional cloning of a mutant gene responsible for the rare genetic disease primary hypomagnesemia with secondary hypocalcemia (HSH) (Schlingmann et al, 2002; Walder et al, 2002). HSH patients show severe hypomagnesemia, or Mg^{2+} deficiency, often manifested as cerebral convulsions in early infancy. The trait is associated with a defect in the intestinal absorption of Mg^{2+} (Lombeck et al, 1975; Milla et al, 1979), combined with an excess loss of Mg^{2+} in urine, a consequence of impaired Mg^{2+} reabsorption in the distal convoluted tubule (DCT) (Walder et al, 2002). TRPM6 has subsequently been shown to be essential for renal and intestinal Mg^{2+} absorption (Voets et al, 2004). Consistent with its proposed function, TRPM6 is expressed in the small intestine, colon, kidney, lung and testis (Chubanov et al, 2004; Groenestege et al, 2006) where it could participate in transepithelial reabsorption of Mg^{2+} . Although closely related in sequence to TRPM6, TRPM7 may perform a more general role in Mg^{2+} uptake (Chubanov et al, 2004; Schmitz et al, 2005). Deletion of TRPM7 in a DT40 chicken derived cell-line resulted in depletion of cytosolic Mg^{2+} and subsequent growth arrest unless the cells were supplemented with high levels of Mg^{2+} . This finding provided strong evidence that TRPM7 was critical for Mg^{2+} influx (Schmitz et al, 2003). Unlike the restricted expression of TRPM6, TRPM7 is ubiquitously

expressed suggesting a more general role in Mg^{2+} homeostasis. As suggested by this distribution, TRPM6 and 7 proteins appear to be non-redundant. When TRPM6 was heterologously expressed in a TRPM7 mutant cell line, it was unable to mediate Mg^{2+} transport (Schmitz et al, 2005). For this reason, TRPM6 function was suspected to depend on the presence of TRPM7, and the two proteins were suggested to form a heteromeric complex (Chubanov et al, 2004; Schmitz et al, 2005). The importance of TRPM6 and TRPM7 heteromultimer formation is supported by the observation that when TRPM6 alone was expressed in cells lines, it was unable to reach the cell surface (Chubanov et al, 2004; Schmitz et al, 2005). In addition, loss-of-function mutations in TRPM6 in HSH patients prevented the formation of heteromultimers (Chubanov et al, 2004). Unlike TRPM6, TRPM7 can function independently, and forms functional homomultimeric complexes (Li et al, 2006).

Influx of cations through TRPM6 and TRPM7 is regulated by the ratio between cytosolic free Mg^{2+} and Mg-ATP (Schlingmann et al, 2002). In the presence of high intracellular Mg^{2+} , TRPM7 activity is negatively regulated by a feedback mechanism (Schmitz et al, 2003). Mg^{2+} driven currents in TRPM6 were also sensitive to intracellular Mg^{2+} concentration in the physiological range (0.5 mM). Research efforts have also focused on the role of the kinase domain and its potential regulatory functions. Since phosphotransferase activity of the kinase domain is required for TRPM7 to regulate intracellular Mg^{2+} , TRPM7 was speculated to serve a dual role as both a Mg^{2+} channel and a Mg^{2+} sensor (Schmitz et al, 2004; Schmitz et al, 2003; Takezawa et al, 2004). However, truncation of TRPM7 or TRPM6 before the kinase domain either inactivates the channel (for TRPM7) or suppresses ion channel activation (for TRPM6), and therefore the role of the kinase domain is still unclear (Schlingmann et al, 2002; Schmitz et al, 2003).

1.9.2 Mg^{2+} -regulated transporters

Since differential gene expression has been shown to be a major contributor in the conservation of Mg^{2+} in epithelial cells, one group has followed a strategy of identifying novel genes that show Mg^{2+} -dependent expression (Goytain et al, 2007; Goytain & Quamme, 2005b; Goytain & Quamme, 2005c; Goytain & Quamme, 2005d). This

approach has identified several potential transporter genes, including MagT1 (Goytain & Quamme, 2005d), NIPA1 and NIPA2 (Goytain et al, 2007), MMgT1 and MMgT2 (Goytain & Quamme, 2008), and ACDP2 (Goytain & Quamme, 2005a).

Electrophysiological characterization of cell lines or oocytes heterologously expressing these proteins provided evidence for a role in Mg^{2+} transport. Although several promising candidate genes have been identified and characterized, in general, their role in Mg^{2+} homeostasis remains unclear. Some details on these proteins are listed below.

The first of these proteins identified (MagT1) showed both Mg^{2+} -regulated mRNA and protein expression (Goytain & Quamme, 2005d). The MagT1 protein is homologous to the yeast Ost3 and Ost6 proteins, which encode regulatory subunits of the endoplasmic reticulum oligosaccharyltransferase complex (Knauer & Lehle, 1999). *Xenopus laevis* oocytes expressing MagT1 protein exhibited a voltage dependent, highly selective Mg^{2+} transport activity. The subcellular location of the protein was not determined, and its function remains unclear (Goytain & Quamme, 2005d).

The NIPA1 and NIPA2 proteins were also identified as potential transporters via their Mg^{2+} regulated expression (Goytain et al, 2007; Goytain et al, 2008). Four members of the NIPA family (NIPA1-NIPA4) are present in mouse and human genomes. Previously, NIPA1 and NIPA2 were implicated in Prader-Willi syndrome, a complex developmental disorder that affects newborns (Butler, 1990; Chai et al, 2003). Functional characterization of NIPA1 by expression of mouse cRNA in *Xenopus* oocytes, and measurement of Mg^{2+} -evoked currents revealed that Mg^{2+} influx was concentration-dependent, saturable and reversible (Goytain et al, 2007). Both NIPA1 and NIPA2 are principally localized to the early endosome and the cell surface, suggesting that the proteins can translocate between these two locations. As yet, the link between the genetic disorders associated with *NIPA* gene mutations and Mg^{2+} homeostasis is unclear.

Another apparent Mg^{2+} transporter, MMgT1, mediated Mg^{2+} transport when expressed in *X. laevis* oocytes (Goytain & Quamme, 2008). Two MMgT homologs are found in mouse, but only one in humans. An increase in the expression of both *MMgT* genes was observed in Mg^{2+} deficient conditions (Goytain & Quamme, 2008). When expressed in *Xenopus* oocytes, both MMgTs proteins drove saturable Mg^{2+} transport. The MMgT proteins are the first mammalian Mg^{2+} transporters to be localized to the Golgi

complex (Goytain & Quamme, 2008), but again, little is known of their physiological role.

Mouse *ACDP2* transcript was detected in kidney, brain, and heart, and its expression was found to upregulated under Mg^{2+} deficient conditions (Goytain & Quamme, 2005a). The ACDP proteins have homology to the CorC protein of *S. typhimurium* that functions as a Mg^{2+} efflux protein (Gibson et al, 1991). When ACDP2 was expressed in *X. laevis* oocytes, it generated a rheogenic, voltage-dependent and saturable Mg^{2+} uptake activity.

The SLC (Solute carriers) proteins are the most recent to be identified as potential Mg^{2+} transporters, and may represent the best candidate transporters thus far identified. Three members of the SLC41 family include two domains that share 40% sequence homology with the integral membrane protein of the prokaryotic MgtE Mg^{2+} transporters (Wabakken et al, 2003). The *SLC41A1* transcript was upregulated in the kidney, colon and heart of mice in response to Mg^{2+} deficiency (Goytain & Quamme, 2005b). Heterologous expression of mouse *SLC41A1* cRNA in *Xenopus* oocytes evoked large Mg^{2+} currents (Goytain & Quamme, 2005b). When expressed in *Xenopus* oocytes, SLC41A1 was permeable to several divalent cations, suggesting that it may be a nonselective divalent cation transporter (Goytain & Quamme, 2005b). Although a second group failed to detect any large Mg^{2+} -dependent currents when human SLC41A1 was overexpressed in HEK293 cells, the expression of hSLC41A1 in a *corA mgtA mtgB* mutant of *S. enterica* was found to complement the Mg^{2+} dependent growth-deficient phenotype of this strain, suggesting that hSLC41A1 can mediate Mg^{2+} uptake (Kolisek et al, 2008). Interestingly, these same researchers observed that the incubation of hSLC41A1 overexpressing HEK293 cells in Mg^{2+} free medium led to a significant decrease in the intracellular Mg^{2+} concentration, suggesting that SLC41A1 could mediate Mg^{2+} efflux (Kolisek et al, 2008). This report thus identified SLC41A1 as the first molecular candidate for a Mg^{2+} efflux system in eukaryotes (Kolisek et al, 2008).

The closely related SLC41A2 protein also allowed transport of Mg^{2+} when heterologously expressed in *Xenopus laevis* oocytes (Goytain & Quamme, 2005b). Mg^{2+} uptake by mouse SLC41A2 was a saturable, voltage driven process, suggesting that this protein can function as a Mg^{2+} channel. In contrast to this report however, Mg^{2+} -

dependent inward currents were not detected in a TRPM7 knockout cell line expressing SLC41A2 (Sahni et al, 2007). However, use of the stable $^{26}\text{Mg}^{2+}$ isotope to follow Mg^{2+} uptake revealed that expression of SLC41A2 did allow Mg^{2+} uptake, a conclusion that was supported by complementation of the growth defect exhibited by TRPM7 mutant cells in the absence of supplemental Mg^{2+} (Sahni et al, 2007).

1.10 Regulation of Mg^{2+} transporter expression in eukaryotes

Compared to bacterial Mg^{2+} transporters, much less is known about how Mg^{2+} transporter expression is regulated in eukaryotes. The expression of the yeast Alr1 protein was induced by Mg^{2+} deficiency (Graschopf et al, 2001). Semi-quantitative RT-PCR indicated that the *ALR1* mRNA was strongly expressed in cells grown with 5 μM vs 1 mM Mg^{2+} , suggesting a role for transcriptional regulation in this process. Protein expression was also regulated, as the accumulation of Alr1 increased when yeast were cultured in deficient conditions (5 μM vs 1 mM Mg^{2+}). This regulation was partly post-translational, because transfer of Mg^{2+} -deficient cells to replete conditions (1 or 10 mM Mg^{2+}) decreased the stability of the Alr1 protein. The authors proposed that Mg^{2+} stimulated the ubiquitination of Alr1, which triggered rapid endocytosis and the transfer of Alr1 to the vacuole for degradation. This model was based on four observations: i) in cycloheximide-treated cells, Alr1 protein stability was substantially reduced after exposure to 10 mM Mg^{2+} ; ii) the *end3* mutation, which inhibits endocytosis, (Raths et al, 1993) reduced the rate of degradation; iii) the *rsp5* mutation, which inhibits the activity of an E3 ubiquitin ligase necessary for the addition of ubiquitin (Ub) to membrane proteins (Hein et al, 1995), also inhibited degradation; and iv) the *pep4* mutation, which inactivates vacuolar proteinases (Zubenko et al, 1983), caused Alr1 to accumulate in the vacuole.

In vertebrates, Mg^{2+} deficiency increases the efficiency of Mg^{2+} conservation by the kidney, due to the increased activity of Mg^{2+} transport systems (de Rouffignac & Quamme, 1994). Adaptation to Mg^{2+} deficiency in cultured cells requires transcription, suggesting transporter activity is regulated at the level of gene expression (Dai & Quamme, 1991; Ritchie et al, 2001). As detailed above, the mRNA abundance of many candidate Mg^{2+} transporters and channels is upregulated by Mg^{2+} deficiency, including

SLC41A1 (Goytain & Quamme, 2005b), ACDP2 (Goytain & Quamme, 2005a) and MagT1 (Goytain & Quamme, 2005d), suggesting that these proteins may play a role in regulating the efficiency of Mg^{2+} conservation. At the cellular level, it is also reasonable to assume that the cytosolic concentration of Mg^{2+} ions must be maintained within a certain range. Many different processes depend on Mg^{2+} ions, and either an increase or decrease in Mg^{2+} availability could have a negative effect on these crucial processes. By analogy with other metal ion regulatory systems (and the model suggested for Alr1 regulation), it may be that some transcriptional activator is responsible for sensing Mg^{2+} availability and adjusting the expression of various transporters in order to maintain cytosolic Mg^{2+} concentration. In addition, post-translational regulation of protein accumulation or transporter activity could play a role. As yet however, there is no clear understanding of how gene expression is regulated by Mg^{2+} availability, even in simple eukaryotes like yeast.

1.11 Objectives of this research

As of this report, four yeast homologs of the CorA protein have been characterized in detail (Alr1, Alr2, Mrs2 and Lpe10). All were found to contribute to Mg^{2+} homeostasis via their function in Mg^{2+} transport. The objective of this study is to determine the function of the fifth yeast CorA protein, Ykl064w (Mnr2). Preliminary studies of this protein suggested that it too participated in ion homeostasis, as inactivation of the *MNR2* gene increased sensitivity to several toxic divalent cations, including Mn^{2+} (MacDiarmid, 1997). Although the high degree of homology between the Alr proteins and Mnr2 (34%) strongly suggested that these proteins perform similar functions, the previous study provided no specific evidence to implicate Mnr2 in Mg^{2+} transport (MacDiarmid, 1997). A major goal of my work was to test the hypothesis that Mnr2 is required for Mg^{2+} homeostasis. To do this, I focused on achieving the following goals: *i*) to determine the effect of inactivating the *MNR2* gene on simple measures of Mg^{2+} homeostasis, such as the ability of yeast to tolerate conditions of low Mg^{2+} availability and to maintain cellular Mg^{2+} content; *ii*) to investigate the effect of inactivating various proteins important to Mg^{2+} homeostasis in tandem with Mnr2, to determine the degree to which these proteins overlapped in function; *iii*) to determine the location of Mnr2 in the

cell, and if associated with an organelle, to investigate its role in the function of that organelle; and *iv*) to perform simple biochemical assays to directly investigate the ion transport activity and substrate specificity of the Mnr2 protein. The results of these studies led me to conclude that the Mnr2 protein is a Mg^{2+} transporter or channel located in the vacuolar membrane, where it mediates the release of vacuolar Mg^{2+} stores under Mg^{2+} -deficient conditions. The evidence for this model is described in **Chapter 3**.

I also intended to investigate the biological basis for the metal sensitivity phenotypes previously reported to be associated with the inactivation of *MNR2*. Initially, I believed that these studies might provide information on the substrate specificity of the Mnr2 transporter. However, these studies eventually led me to investigate the effect of the *mnr2* mutation on the expression and activity of another Mg^{2+} transporter, Alr1, and the relationship between these two proteins. The results of these investigations are detailed in **Chapter 4**.

Chapter 2 Materials and Methods

2.1 Buffers, solutions and enzymes

TE buffer	10 mM Tris-Cl (pH 7.5), 1 mM Na-EDTA.
Chloroform/iso-amyl alcohol	Chloroform:iso-amyl alcohol (24:1)
Phenol	Phenol was equilibrated in TE buffer with desired pH by extracting phenol three times with new buffer. The phenol was stored at 4°C protected from light.
Phenol/chloroform	Phenol:chloroform:iso-amyl alcohol (25:24:1)
Zymolyase 20T	Zymolyase 20T (Seikagaku, Tokyo) (110 U/ml) was dissolved in 50 mM potassium phosphate buffer (pH 7.4) with 50% glycerol, and stored at -20°C.

2.2 Bacterial growth media and antibiotics

LB (Luria-Bertani) broth:	1% Bacto Tryptone, 0.5% Bacto yeast extract, 172 mM NaCl, pH 7.0.
LB + Ampicillin:	1% Bacto Tryptone, 0.5% Bacto yeast extract, 172 mM NaCl, pH 7.0, 100 µg/ml Ampicillin.
SOB medium:	2% Bacto Tryptone, 0.5% Bacto yeast extract, 10 mM NaCl, 2.5 mM KCl, 10 mM MgCl ₂ , and 10 mM MgSO ₄ (pH 7.0).

2.3 Bacterial and yeast plasmid vectors

All the plasmids in this study were constructed using homologous recombination in yeast (Hua et al, 1997; Ma et al, 1987). This method provides a reliable, accurate and versatile strategy to insert new DNA fragments in a yeast shuttle vector. Briefly, the target shuttle vector is linearized using a restriction enzyme (sometimes introducing a gap via double digestion), and combined with a PCR product that is amplified using a high fidelity DNA polymerase (EasyA, Stratagene) to reduce the possibility of PCR-induced mutations. The PCR product is generated using primers designed to include at least 30 bases of homology to the region of the target plasmid. A yeast strain is then co-transformed with the vector and PCR product to create conditions suitable for homologous recombination between the plasmid and the PCR product. Recombinant clones generated by gap repair of the plasmid were selected by complementation of auxotrophic marker genes in the yeast strain by the WT gene in the plasmid (commonly the *URA3* gene). To verify correct construction of the plasmid, DNA was extracted from yeast clones and the plasmid was rescued by electroporation-mediated transformation of

E. coli. Plasmids were routinely subjected to restriction digestion and sequencing to verify correct construction.

2.4 Oligonucleotides

Oligonucleotide sequences were selected using the ApE sequence editing software and tested using Amplify 3X software. All oligonucleotides were obtained from Sigma-Genosys.

Table 2.1 Oligonucleotides used in this study

Name	Sequence (5'-3')	Purpose
MNR2-3'-N	GGAACAGCTATGACCATGATTACGCCA AGCTTACAAGATCTCGCCAAGGA	YCpMNR2 construction
MNR2-5'-N	CACGACGTTGTAAAAACGACGGCCAGTG AATTCGCAAAACGAAGATGAAGA	YCpMNR2 construction
3' pFL38 polylinker	ACGACAGGTTTCCCGACT	YCpALR1-HA construction
5' pFL38 polylinker	CGGGCCTCTTCGCTATTA	YCpALR1-HA construction
1267 alr1-his3 ko	AATATCCCAAACCACCACGCGATACTG GAAACCACTTGCCACCTATCA	Construction of palr::his3 in pYES2
633 alr1-his3 ko	TATGAATTATTCAGGGGAGGTGAGCCA ACACTATTGCTTTGCTGTGGG	Construction of palr::his3 in pYES2
cit-Mnr2 3'	TTCATCCTTTTGTGAGTTATCAGTGCT ATGTTTGTACAATTCATCCATAC	Construction of YCpMNR2-cit
cit-Mnr2 5'	ATTTCTGAAGAGGACTTGAATTCAAGG CCTATGTCTAAAGGTGAAGAATT	Construction of YCpcit-MNR2
ALR1-lacZ-1	CCGCCTCTCCCCGCGGTTGGCCGATT CATTCCCGAAAAGGGGAGGATGAAGA GA	Construction of YEpALR1- lacZ
ALR1-lacZ-2	ACGGCGGATCGCAAGCTTGGCTGCAG GTCGACGGATCCATGGTAAAATGCTTT TACG	Construction of YEpALR1- lacZ
5'MNR2 His5 KO	CGACCAGATCGATTCCCTGGGGCATGCT GCATGGCTAGGGATAACAGGGTA	Construction of pmnr2SpHIS5
3'MNR2 His5 KO	CCCGAATCTTCTCTTAGTATACATATA TGCAGTTCGAGCTCGTTTAAACT	Construction of pmnr2SpHIS5
MNR2-3'	GAATTCCTTGGTCAAGCGTAGTCTGGG ACGTCGTATGGGTTTAAAACCCGAATC TTCTCT	Construction of YEpGmyc- MNR2
MNR2-5	ATTTCTGAAGAGGACTTGAATTCAAGG CCTTGTGACATAGCACTGATAACTCA CAAAAAG	Construction of YEpGmyc- MNR2
MNR2-myc tag transfer 1	TGAGAAGTG TAGAGAAGAAAAAGATTA AAAATCGATTTAAAGCTATGGAG	Construction of YCpmyc- MNR2
MNR2-myc tag transfer 2	CTGGATGTGGATTTGGAATT	Construction of YCpmyc- MNR2

MNR2-kan 3'	TGCAGCTGATGCGACTAA	Generation of the <i>mnr2::KAN^R</i> PCR product
MNR2-kan 5'	TGTTTCAGGGCATAAGCAG	Generation of the <i>mnr2::KAN^R</i> PCR product
forward vma1 kan amp	AAATTGGGGACGGCGAAG	Generation of the <i>tfp1::KAN^R</i> PCR product
Reverse vma1 kan amp	ACGCGCTCTCGATCAATG	Generation of the <i>tfp1::KAN^R</i> PCR product
5'-yfpamp (+myc)	CTGAAGAGGACTTGAATTCAAGGCCTT GTCGAGGATCCATGTCTAAAGGT	Amplification of YFP from YEpGcit-Alr1 (construction of YCpCit-Alr1)
Alr1 seq primer reverse	ACCATCGTGTTAGCCAGTGA	Amplification of YFP from YEpGcit-Alr1 (construction of YCpCit-Alr1)

2.5 Polymerase chain reaction (PCR)

PCR performed for routine analytical purposes utilized Taq polymerase prepared in the laboratory (Pluthero, 1993). A 50 μ l PCR reaction contained 20 mM Tris-HCl pH 8.4, 50 mM KCl, 0.5 mM MgCl₂, 0.2 mM of each dNTP, 1 μ M of each primer, 1-2 units of Taq polymerase, and approximately 1 ng of plasmid or 100 ng of genomic DNA template. Reactions were carried out in a MyCycler thermal cycler (Bio-Rad). Reactions were set for a 30 second denaturing step at 95°C, a 30 second annealing step at the appropriate annealing temperature of the primers, and extension at 72°C for 1 min/Kb of the expected product.

PCR products required for cloning were generated using either Easy-A High Fidelity DNA polymerase (Stratagene) or Platinum Taq DNA Polymerase High Fidelity (Invitrogen) according to the manufacturer's instructions. For subsequent cloning procedures, PCR products were purified using a Wizard-SV Gel and PCR Clean up system (Promega) according to manufacturer's instructions, or precipitated using 3 M sodium acetate and isopropanol as described in **Ch. 2.13**.

2.6 Plasmid constructs

Construction of each of the plasmids used in this work is described below.

palr2TRP1: A genomic clone of the *ALR2* gene in pBC KS⁻ (Stratagene) (pA8 Δ 6, (MacDiarmid, 1997) was digested with *Bgl*III to excise part of the *ALR2* coding sequence, and a 0.8 kb *Bgl*III fragment of pFL45-S containing the *TRP1* marker was ligated into the

pBC KS⁻ vector using ligase enzyme. A *KpnI* fragment of the new construct containing the *alr2::TRP1* deletion allele was excised before yeast transformation.

YEpALR1-lacZ: The 5' intergenic region of *ALR1* including the start codon was amplified from genomic DNA with the ALR1-lacZ-1 and ALR1-lacZ-2 primers. The PCR product was inserted directly 5' of the *lacZ* ORF in the shuttle vector YEp353 via gap repair.

palr1HIS3: The *HIS3* gene was amplified from yeast genomic DNA via PCR with the oligonucleotides 1267 alr1-his3 ko and 633 alr1-his3 ko. The *ALR1* ORF in YEpGALR1 was gapped by digestion with *BstXI* and *EcoRI* restriction enzymes, and the amplified *HIS3* PCR product was inserted via gap repair. The palr1HIS3 insert was excised with *BlpI* and *EagI* prior to yeast transformation.

YCpMNR2: A 4.2 kb fragment containing the coding sequence and 5' and 3' flanking regions of the *MNR2* gene was amplified from genomic DNA of DY1457 using the primers MNR2-3'-N and MNR2-5'-N. The PCR product was inserted in the multiple cloning site of the pFL38 shuttle vector by gap repair.

pmnr2SpHIS5: The *SpHIS5* gene was amplified from the pKT211 plasmid using the primers 5'MNR2 His5 KO and 3'MNR2 His5 KO. The YCpMNR2 plasmid was linearized by *BamHI* digestion, and the PCR product was inserted in the *MNR2* ORF via gap repair. To inactivate *MNR2* in yeast, the insert of pmnr2SpHIS5 was excised by digestion with *EcoRI* and *HindIII* prior to yeast transformation.

YEpGmyc-MNR2: This plasmid was based on pMYC-Zap11-880 (Bird et al, 2000). The *MNR2* ORF was amplified from genomic DNA via PCR with the oligonucleotides MNR2-3' and MNR2-5. The PCR product was inserted in pMYC-Zap11-880 via gap repair, replacing the *ZAP1* ORF with *MNR2*. The second codon of the *MNR2* ORF is fused to five repeats of the myc epitope tag, and expression is driven by the UAS of the *GAL1* promoter fused to a minimal *CYCI* promoter.

YCpmyc-MNR2: The *MNR2* ORF including the five myc tags at the 5' end was amplified from YEpGmycMNR2 using the oligonucleotides MNR2-myc tag transfer 1 and MNR2-myc tag transfer 2. YCpMNR2 was digested with *NarI* and *AvrII*, and the PCR product was inserted into the gap via recombination in yeast.

YCpcit-MNR2: A monomeric variant of YFP (yEmCitrine) was amplified from

the pKT211 vector using the oligonucleotides Cit-Mnr2 3' and Cit-Mnr2 5'. The product was inserted between the five myc-epitope tags and the 5' end of *MNR2* ORF in the YCpmyc-MNR2 plasmid via gap repair. The resulting protein retains four myc tags preceding the *YFP* ORF at the N-terminal end.

YCpcit-ALR1: This plasmid was constructed by Frank Donovan and Lauren Stein) The oligonucleotides 5'-yfpamp (+myc) and Alr1 seq primer reverse were used to amplify a PCR product containing a *YFP* gene (citrine variant) fused to a portion of the N-terminal region of *ALR1*. The template for this reaction was a *GALI*-promoter driven version of *ALR1* with an N-terminal Citrine tag (constructed by Abhinav Pandey). The PCR product was inserted at the N-terminal end of the YCp-myc-Alr1 plasmid (constructed by Phaik Har Lim) that had been linearized with *SaII*. Gap repair in yeast reconstituted a plasmid in which five myc tags and the *YFP* gene are inserted between the *ALR1* promoter and the Alr1 CDS.

Table 2.2 Plasmids used in this study

Plasmid	Marker/ Replication origin	Description	Reference
pFL38	<i>URA3/CEN</i>	Low copy shuttle vector	(Bonneaud et al, 1991)
pFL44-S	<i>URA3/2μ</i>	High copy shuttle vector	(Bonneaud et al, 1991)
pKT211	<i>SpHIS5/none</i>	YFP and <i>SpHIS5</i> cassette	(Sheff & Thorn, 2004)
YCpDCP1myc	<i>URA3/CEN</i>	myc-tagged <i>DCP1</i> gene in shuttle vector	(Sean Houshmandi)
YIpALR1-HA	<i>URA3/none</i>	<i>ALR1</i> tagged with triple HA epitope at C-terminus	(Graschopf et al, 2001)
YCpALR1	<i>URA3/CEN</i>	<i>ALR1</i> genomic clone in pFL38	(MacDiarmid & Gardner, 1998)
YEpl353	<i>URA3/2μ</i>	Promoter-less <i>lacZ</i> gene	(Myers et al, 1986)
YCpZRC1HA	<i>URA3/CEN</i>	<i>ZRC1</i> with C-terminal triple HA tag	(MacDiarmid et al, 2002)
pMCZ-Y	<i>URA3/2μ</i>	UPRE- <i>CYC1-lacZ</i> reporter	(Kawahara et al, 1997)
pLGA312	<i>URA3/2μ</i>	<i>CYC1-lacZ</i> reporter	(Guarente et al, 1984)

pHAC1 ¹	<i>LEU2/CEN</i>	Genomic clone of <i>HAC1</i> with intron deleted	(Ellis et al, 2004)
YCpMNR2	<i>URA3/CEN</i>	<i>MNR2</i> genomic clone in pFL38	This study
YCpmyc-MNR2	<i>URA3/CEN</i>	Mnr2-N-terminal 5xmyc fusion in pFL38	This study
YCpcit-MNR2	<i>URA3/CEN</i>	N-terminal fusion of citrine to Mnr2	This study
YEpgmyc-MNR2	<i>URA3/2μ</i>	<i>MNR2</i> tagged with five myc tags at N-terminus	This study
YEpalR1-lacZ	<i>URA3/2μ</i>	<i>ALR1</i> promoter fused to <i>lacZ</i> ORF	This study
palr2TRP1	<i>TRP1</i> /none	<i>TRP1</i> deletion allele of <i>ALR2</i>	This study
palr1HIS3	<i>URA3, HIS3/2μ</i>	<i>HIS3</i> deletion allele of <i>ALR1</i>	This study
YCpcit-ALR1	<i>URA3/CEN</i>	5xmyc-Citrine-Alr1 behind <i>ALR1</i> promoter	(Frank Donovan, Lauren Stein)

2.7 Bacterial transformation

2.7.1 Preparation of electrocompetent cells

The *E. coli* strain DH10βTM [F⁻ *mcrA* Δ (*mrr-hsdRMS-mcrBC*) ϕ 80*lacZ*ΔM15 Δ*lacX74 recA1 endA1 araD139* Δ(*ara, leu*) 7697 *galU galK λ-rpsL nupG*] was transformed by electroporation. To prepare competent cells, 25 ml of Luria-Bertani (LB) broth was inoculated with a single colony of DH10β, and incubated overnight at 37°C with agitation (260 rpm). Ten ml of the overnight culture was added to 1 L of pre-warmed LB media + 2% glucose, and returned to 37°C for incubated with agitation until the culture reached an *A*₆₀₀ value of 0.6 (approximately two hours). The cells were then quickly chilled on an ice water bath and kept chilled for the remainder of the procedure. The cells were collected by centrifugation for 10 min at 5000g in a pre-chilled rotor using a Sorvall RC5B Plus refrigerated centrifuge. The supernatant was discarded and the cell pellet was gently resuspended in 50 ml of chilled sterile Millipore water with further addition of 450 ml chilled Millipore water. Cells were collected as described above. Cells were washed twice with 200 ml sterile Millipore water, twice with 50 ml water, and twice with pre-chilled 10% glycerol. The cell pellet was suspended in 2 ml of 10% glycerol and 100 μl aliquots of cells were distributed into 1.5 ml Eppendorf tubes. The cells were

quick-frozen on a dry ice-ethanol bath and transferred to -80°C freezer for storage.

2.7.2 Electroporation of competent cells

Frozen electrocompetent cells were thawed on ice, and 25 µl of cells were transferred to a chilled 1.5 ml tube. Purified plasmid DNA (10 pg-1 ng), or yeast genomic DNA (10 ng) was added to the cells, and the cells were immediately transferred to a pre-chilled electroporation cuvette (gap width 0.1 cm), which was placed in a Model 2510 Electroporator (Eppendorf). After application of a voltage pulse of 1.8 kV to the cuvette, it was rapidly removed from the electroporator and 1 ml SOC media was added to the cells. The cells were transferred to a 15 ml tube and incubated at 37°C for 1 hour with agitation. Aliquots of the transformed cells were plated on the appropriate selective media and incubated overnight at 37°C.

2.8 DNA isolation and purification

2.8.1 Routine plasmid purification from *E. coli* (Method 1)

For routine preparation of plasmid DNA, I used a modification of a previously described protocol (Sambrook, 1989). LB+Amp (5 ml) was inoculated with a single colony of transformed *E. coli* cells and incubated overnight at 37°C with agitation (260 rpm). The cells were collected by centrifugation (5,000g for 10 min), and the cell pellet was resuspended in 200 µl of Solution I (25 mM Tris-Cl pH 8.0, 10 mM EDTA, 50 mM glucose). To lyse the cells, 400 µl of Solution II was added to the suspension, mixed gently, and incubated at room temperature for exact 5 min until clear suspension was observed. The lysate was neutralized by adding 300 µl of pre-chilled Solution III (3 M potassium acetate, adjusted to pH 4.8 with glacial acetic acid) and mixed until a white precipitate was formed. The tubes were incubated on ice for 20 min, and the white precipitate was separated from the mixture by centrifugation (12,000g for 10 min at 4°C). The supernatant was carefully removed and transferred to a new 1.5 ml Eppendorf tube. The plasmid DNA was precipitated from the supernatant by adding 600 µl of isopropanol, followed by incubation at room temperature for 10 min. The precipitated plasmid DNA was collected by centrifugation (12,000g for 10 min). The supernatant was discarded and pellet was washed with 1 ml of 80% ethanol by inverting the tube several

times. The pellet was dried in a Speed-Vac for 10 min, then redissolved in 300 μ l of TE buffer. To degrade residual RNA, the preparation was treated with 2 μ l of 1mg/ml RNase A and incubated at 65°C for 15 min. The mixture was extracted with 300 μ l of phenol/chloroform, and the aqueous layer containing the plasmid DNA was recovered. Plasmid DNA was precipitated by addition of 1/10th volume of 3 M sodium acetate and one volume of isopropanol. The mixture was incubated at room temperature for 15 min and the plasmid DNA was collected by centrifugation (12,000g for 5 min at room temperature). The pellet was washed with cold 80% ethanol, dried, redissolved in 50 μ l sterile Millipore water, and stored at -20°C. When a higher yield of plasmid DNA was required, the protocol was scaled up appropriately.

2.8.2 Plasmid purification for DNA sequencing (Method 2)

Plasmid DNA intended for inclusion in DNA sequencing reactions was purified using Wizard Plus SV Miniprep or Midiprep kits (Promega), following the manufacturer's instructions.

2.9 Restriction endonuclease digestion

Plasmid DNA was digested with endonuclease enzymes by incubating the DNA with enzyme in the appropriate New England Biolabs buffer in the conditions specified by the manufacturer (usually 5 U of enzyme per μ g DNA for 3 hours at 37°C).

2.10 Yeast growth media

2.10.1 Complex yeast media

YP media was used to grow routine yeast culture. YP contained 1% yeast extract (Fisher), 2% peptone (Fisher) and 2% glucose (YPD) or 3% glycerol (YPGly) as the carbon source. For routine culture of *alr1* mutant strains, 500 mM MgCl₂ was added to YPD. For plates, YPD was gelled by addition of 1.5% agar. For preparation of high Mg²⁺ YPD plates, YPD + agar was prepared at 2X strength, autoclaved, and mixed with an equal volume of sterile 1M MgCl₂ solution

To select for yeast strains expressing the *KAN^R* marker, a sterile stock solution of Geneticin (Invitrogen) was added to YPD media to a final concentration of 150 mg/L.

2.10.2 Synthetic media

2.10.2.1 Synthetic minimal media

Yeast was grown in synthetic dextrose (SD) media in order to select for plasmids or genotype auxotrophic markers. SC media contained 6.7% of "Yeast Nitrogen Base with ammonium sulfate without Amino Acids" (YNB) (Q-Biogene), a carbon source (2% glucose or galactose, or 3% glycerol), 0.01% adenine, 0.01% uracil, 0.01% tryptophan, 0.01% leucine, 0.01% lysine, 0.01% histidine, and 0.01% methionine. Nutrients were omitted as appropriate for marker selection. To grow *alr1* mutant strains, SC medium was supplemented with 500 mM MgCl₂. To select for uracil prototrophic strains, a simplified synthetic medium was routinely used (SC-ura). This medium contained 6.7% YNB, 0.01% Casamino acids (Difco), 0.01% adenine, and 0.01% tryptophan. As a carbon source, the medium contained 2% glucose or 2% galactose, or 3% glycerol.

2.10.2.2 Low Magnesium Medium (LMM)

In experiments requiring low Mg²⁺ concentrations, LMM was routinely used. LMM contained 0.628% "YNB w/o Amino Acids and Divalent Cations" (Q-Biogene), 5 mM CaCl₂, 5 μM CuCl₂, 5 μM FeSO₄, 5 μM MnCl₂ and, 5 μM ZnCl₂. Amino acids, bases, and carbon source were added as required for standard SD. To avoid leaching of Mg²⁺ from glass bottles into LMM, stock solutions and the medium itself were prepared and autoclaved in polycarbonate flasks that were washed using a metal-free acidic detergent (Citronox, Alconox). AAS analysis of LMM media revealed no detectable contamination by Mg²⁺.

An alternative method used for LMM preparation from individual components is described below. Three stock solutions were prepared: 10X major salts without MgCl₂ (400 mM NH₄SO₃, 50 mM KCl, 20 mM NaCl, 1 mM CaCl₂, 1 mM KH₂PO₄), 1000X trace elements (0.2 mM CuSO₄, 2.5 mM MnSO₄, 10 mM H₃BO₃, 0.5 mM KI, 1 mM Na₂MoO₄, 1.5 mM ZnSO₄, 1 mM FeCl₃), and 1000X vitamins (0.0002% Folic Acid, 0.04% Niacin, 0.0002% Biotin, 0.04% Calcium pantothenate, 0.02% Riboflavin, 0.02% p-Aminobenzoic acid, 0.04% Pyridoxine Hydrochloride, 0.04% Thiamine hydrochloride). All solutions were autoclaved except for the 1000X vitamin stock, which was filter sterilized to avoid damage to heat sensitive components, then stored at 4°C.

The final medium was assembled from stock solutions, sterile water, and other nutrients and carbon sources added from sterile stocks as described above. MgCl₂ was added to the LMM to the concentration required for the experiment.

2.10.2.3 Low sulfate medium

In order to prevent precipitation of calcium ions when added in high concentration to synthetic media, a low sulfate medium was used to make high Ca²⁺ plates. The medium contained 1.7% "YNB w/o ammonium sulfate, dextrose, and zinc" (Q-Biogene), 2 µM ZnCl₂, and 75 mM NH₄Cl. Carbon source, amino acids, and nucleotide solutions were added as per the normal requirement.

2.11 Yeast strains used in this study

Saccharomyces cerevisiae strains used or generated for this study are detailed in

Table 2.3.

Table 2.3 Yeast strains

Strain	Relevant genotype	Full genotype	Genetic background	Source/ Reference
DY1456	Wild-type	<i>MATa ade6 can1-100^{oc} his3-11,15 leu2-3,112 trp1-1 ura3-52</i>	W303	(Dix et al, 1994)
DY1457	Wild-type	<i>MATa ade6 can1-100^{oc} his3-11,15 leu2-3,112 trp1-1 ura3-52</i>	W303	(Zhao & Eide, 1997)
DY1514	Wild-type	<i>MATa/a ade2/+ ade6/+ can1-100^{oc}/- his3-11,15/- leu2-3,112/- trp1-1/- ura3-52/-</i>	W303	David Eide
BY4743	Wild-type	<i>MATa/a his3-Δ1/- leu2Δ0/- met15Δ0/+ lys2Δ0/+ ura3Δ0/-</i>	S288C	(Winzeler et al, 1999)
BY4741	Wild-type	<i>MATa his3-Δ leu2Δ0 met15Δ0 lys2Δ0 ura3Δ0</i>	S288C	(Winzeler et al, 1999)
YKL064w	<i>mnr2Δ</i>	<i>MATa/α his3Δ1/- leu2Δ0/- met15Δ0/+ lys2Δ0/+ ura3Δ0/- mnr2::KAN^R/-</i>	S288C	(Winzeler et al, 1999)
<i>tfp1Δ</i>	<i>tfp1Δ</i>	<i>MATa/α his3Δ1/- leu2Δ0/- met15Δ0/+ lys2Δ0/+ ura3Δ0/- tfp1::KAN^R/-</i>	S288C	(Winzeler et al, 1999)
DBY747	Wild-type	<i>MATa his3-Δ1 leu2-3,112 ura3-52 trp1-289</i>	Unknown	(Wiesenberger et al, 1992)
<i>mrs2Δ-2</i>	<i>mrs2Δ</i>	<i>MATa his3-Δ1 leu2-3,112 ura3-52 trp1-289 mrs2::SpHIS5</i>	Unknown	(Bui et al, 1999)

<i>lpe10Δ-1</i>	<i>lpe10Δ</i>	<i>MATa his3-Δ1 leu2-3,112 ura3-52 trp1-289 lpe10::URA3</i>	Unknown	(Gregan et al, 2001a)
NP103	<i>mnr2Δ</i>	<i>MATa his3-Δ1 leu2-3,112 ura3-52 trp1-289 mnr2::KAN^R</i>	Unknown	This study
NP107	<i>mnr2Δ</i> <i>lpe10Δ</i>	<i>MATa his3-Δ1 leu2-3,112 ura3-52 trp1-289 lpe10::URA3 mnr2::KAN^R</i>	Unknown	This Study
NP112	<i>mnr2Δ</i> <i>mrs2Δ</i>	<i>MATa his3-Δ1 leu2-3,112 ura3-52 trp1-289 mrs2::SpHIS5 mnr2::KAN^R</i>	Unknown	This study
NP4	<i>mnr2Δ</i>	<i>MATa ade6 can1-100^{oc} his3-11,15 leu2-3,112 trp1-1 ura3-52 mnr2::KAN^R</i>	W303	This study
NP5	<i>Mnr2Δ</i>	<i>MATa ade6 can1-100^{oc} his3-11,15 leu2-3,112 trp1-1 ura3-52 mnr2::KAN^R</i>	W303	This study
NP10	<i>alr1Δ</i>	<i>MATa ade2 can1-100^{oc} his3-11,15 leu2-3,112 trp1-1 ura3-52 alr1::HIS3</i>	W303	This study
NP26	<i>alr2Δ</i>	<i>MATa can1-100^{oc} his3-11,15 leu2-3,112 trp1-1 ura3-52 alr2::TRP1</i>	W303	This study
NP27	<i>alr2Δ</i>	<i>MATa can1-100^{oc} his3-11,15 leu2-3,112 trp1-1 ura3-52 alr2::TRP1</i>	W303	This study
NP14	<i>alr1Δ</i> <i>alr2Δ</i>	<i>MATa ade6 can1-100^{oc} his3-11,15 leu2-3,112 trp1-1 ura3-52 alr1::HIS3 alr2::TRP1</i>	W303	This study
NP18	<i>alr1Δ</i> <i>mnr2Δ</i>	<i>MATa ade6 can1-100^{oc} his3-11,15 leu2-3,112 trp1-1 ura3-52 alr1::HIS3 mnr2::KAN^R</i>	W303	This study
NP36	<i>alr2Δ</i> <i>mnr2Δ</i>	<i>MATa can1-100^{oc} his3-11,15 leu2-3,112 trp1-1 ura3-52 alr2::TRP1 mnr2::KAN^R</i>	W303	This study
NP20	<i>alr1Δ</i> <i>alr2Δ</i> <i>mnr2Δ</i>	<i>MATa ade2 can1-100^{oc} his3-11,15 leu2-3,112 trp1-1 ura3-52 alr1::HIS3 alr2::TRP1 mnr2::KAN^R</i>	W303	This study
NP174	Wild-type	<i>MATα ade2 can1-100^{oc} his3-11,15 leu2-3,112 trp1-1 ura3-52</i>	W303	This study
NP180	<i>mnr2Δ</i>	<i>MATα ade2 can1-100^{oc} his3-11,15 leu2-3,112 trp1-1 ura3-52 mnr2::SpHIS5</i>	W303	This study
NP193	<i>tfp1Δ</i>	<i>MATα ade2 can1-100^{oc} his3-11,15 leu2-3,112 trp1-1 ura3-52 tfp1::KAN^R</i>	W303	This study

NP201	<i>mnr2Δ</i> <i>tfp1Δ</i>	<i>MATα ade2 can1-100^{oc} his3-11,15</i> <i>leu2-3,112 trp1-1 ura3-52</i> <i>mnr2::SpHIS5 tfp1::KAN^R</i>	W303	This study
CEY4	<i>hac1Δ</i>	<i>MATα ade2 can1-100^{oc} his3-11,15</i> <i>leu2-3,112 trp1-1 ura3-52 hac1::</i> <i>KAN^R</i>	W303	(Ellis et al, 2004)
NP59	Wild-type	<i>MATα ade2 can1-100^{oc} his3-11,15</i> <i>leu2-3,112 trp1-1 ura3-52</i>	W303	This study
NP61	Wild-type	<i>MATα ade2 can1-100^{oc} his3-11,15</i> <i>leu2-3,112 trp1-1 ura3-52</i>	W303	This study
NP63	<i>mnr2Δ</i>	<i>MATα ade2 can1-100^{oc} his3-11,15</i> <i>leu2-3,112 trp1-1 ura3-52</i> <i>mnr2::SpHIS5</i>	W303	This study
NP64	<i>mnr2Δ</i>	<i>MATα ade2 can1-100^{oc} his3-11,15</i> <i>leu2-3,112 trp1-1 ura3-52</i> <i>mnr2::SpHIS5</i>	W303	This study
NP68	<i>hac1Δ</i>	<i>MATα ade2 can1-100^{oc} his3-11,15</i> <i>leu2-3,112 trp1-1 ura3-52</i> <i>hac1::KAN^R</i>	W303	This study
NP69	<i>hac1Δ</i>	<i>MATα ade2 can1-100^{oc} his3-11,15</i> <i>leu2-3,112 trp1-1 ura3-52</i> <i>hac1::KAN^R</i>	W303	This study
NP70	<i>hac1Δ</i> <i>mnr2Δ</i>	<i>MATα ade2 can1-100^{oc} his3-11,15</i> <i>leu2-3,112 trp1-1 ura3-52</i> <i>hac1::KAN^R mnr2::SpHIS5</i>	W303	This study
NP71	<i>hac1Δ</i> <i>mnr2Δ</i>	<i>MATα ade2 can1-100^{oc} his3-11,15</i> <i>leu2-3,112 trp1-1 ura3-52</i> <i>hac1::KAN^R mnr2::SpHIS5</i>	W303	This study
NP88	<i>hac1Δ</i> <i>mnr2Δ</i>	<i>MATα ade2 can1-100^{oc} his3-11,15</i> <i>leu2-3,112 trp1-1 ura3-52</i> <i>hac1::KAN^R mnr2::SpHIS5</i>	W303	This study
NP89	<i>hac1Δ</i> <i>mnr2Δ</i>	<i>MATα ade2 can1-100^{oc} his3-11,15</i> <i>leu2-3,112 trp1-1 ura3-52</i> <i>hac1::KAN^R mnr2::SpHIS5</i>	W303	This study
NP94	<i>mnr2Δ</i>	<i>MATα ade2 can1-100^{oc} his3-11,15</i> <i>leu2-3,112 trp1-1 ura3-52</i> <i>mnr2::SpHIS5</i>	W303	This study
NP97	<i>mnr2Δ</i>	<i>MATα ade2 can1-100^{oc} his3-11,15</i> <i>leu2-3,112 trp1-1 ura3-52</i> <i>mnr2::SpHIS5</i>	W303	This study
NP99	<i>mnr2Δ</i>	<i>MATα ade2 can1-100^{oc} his3-11,15</i> <i>leu2-3,112 trp1-1 ura3-52</i> <i>mnr2::SpHIS5</i>	W303	This study

2.11.1 Construction of yeast mutant strains

To construct NP4, the *mnr2::KAN^R* locus and flanking DNA was amplified from the genome of a diploid *mnr2* mutant strain (*ykl064w*) (Winzeler et al, 1999), using the primers MNR2-kan 3' and MNR2-kan 5'. DY1457 was transformed with the PCR product and geneticin selection applied to isolate a haploid *mnr2Δ* strain. Deletion of the endogenous *MNR2* location was confirmed by PCR. To construct the NP5, NP10, NP27, NP14, NP36, and NP20 strains, a diploid WT strain (DY1514) was sequentially transformed with the *mnr2::KAN^R* PCR product and the inserts of the *palr1HIS3* and *palr2TRP1* plasmids, with selection for the appropriate marker at each stage. Correct deletion of the three genes in the diploid was verified using PCR. The diploid was then transformed with a genomic clone of *ALR1* to complement the *alr1* mutation and allow more efficient sporulation. After sporulation, haploid clones were isolated by the random spore method described in **Ch. 2.13**. To genotype the spores, strains were replica plated to selective medium (SC-histidine, or SC-tryptophan, or YPD+geneticin). Strains carrying the *alr1* mutation were then cured of the *ALR1* plasmid by growth in YPD+500 Mg²⁺ medium (to allow plasmid segregation and loss).

The NP174, NP180, NP193, and NP201 strains were constructed as follows. The insert of *pmnr2SpHis5* was used to transform the diploid WT strain DY1514 and *HIS⁺* strains selected. The *mnr2* deletion was verified by PCR and the resulting strain was then transformed with an *tfp1::KAN^R* PCR product, which was amplified from genomic DNA of YDL185W Open Genetics deletion strain (Winzeler et al, 1999) using the primers 'forward vma1 kan amp' and 'reverse vma1 kan amp'. The double heterozygous mutant strain was sporulated, and clones with all possible combinations of the *tfp1* and *mnr2* mutations were identified by genotyping on selective media.

The NP103, NP107 and NP112 strains were constructed from the DBY747 (WT), *lpe10Δ-1* and *mrs2Δ-2* strains obtained for this study from the laboratory of Rudolf Schweyen. To generate double mutants, these haploid strains were transformed with a *mnr2::KAN^R* PCR product, generated as described above. Deletion of the *mnr2* gene was verified using PCR.

2.12 Yeast transformation

Yeast strains were transformed with plasmids using a modification of a published protocol (Schiestl & Gietz, 1989). A 5 ml culture of a yeast strain in YPD media was incubated overnight at 30°C with agitation (250 rpm). Fresh YPD medium (50 ml) was inoculated with the saturated 5 ml overnight culture and incubated at 30°C in a shaker until the culture reached log phase (A_{600} of 0.5-0.7). The cells were collected by centrifugation (2,000g for 5 min in a Beckman GPR centrifuge) and washed with 50 ml sterile Millipore water. The cells were collected as described above, and the pellet was resuspended in 1 mL of TE/LiOAc buffer (0.1 M LiOAc, 0.01 M Tris-Cl pH 7.5, 1 mM EDTA) and transferred to a 1.5 ml sterile Eppendorf tube. The cells were centrifuged at 13,000 rpm for 1 min in a tabletop centrifuge and the supernatant was discarded. The pellet was resuspended in 1/3rd volume of TE/LiOAc buffer, and 50 μ l aliquots of the cell suspension were distributed into sterile 1.5 ml Eppendorf tubes. Salmon sperm carrier DNA (2 mg/ml) concentration was boiled for 10 min and immediately cooled on ice. Ten μ l of carrier DNA was added to each aliquot of yeast cells and immediately mixed to prevent gelling of the DNA. Plasmid DNA (1-2 μ l) was added to the cells, followed by 300 μ l of PEG/TE/LiOAc buffer (40% Polyethylene glycol, 0.1 M Lithium Acetate, 0.01 M Tris-Cl pH 7.5, 1 mM EDTA). The mixture was incubated at 30°C for 30 min, followed by a heat shock at 42°C for 15 min. The cells were collected by centrifugation at low speed (2,000g for 1 min) and the supernatant was removed. The cells were washed once with 1 ml of Millipore water, resuspended in 0.5 ml of Millipore water, and 200 μ l aliquots plated on selective media. Plates were incubated at 30°C for 3-4 days.

2.13 Genomic and plasmid DNA isolation from yeast

To isolate yeast genomic or plasmid DNA, a 5 ml overnight culture was grown to saturation in synthetic medium (for plasmid isolation, the appropriate selection was applied). Cells were collected by centrifugation at 3,000g for 5 min, washed with 5 ml water, resuspended in 1 ml water, and transferred to a 1.5 ml Eppendorf tube. After centrifugation, the pellet was resuspended in 200 μ l of genomic DNA buffer (2% Triton X-100, 1% SDS, 0.1 M NaCl, 1 mM EDTA, 1 mM Tris, pH 8.0). Phenol/chloroform (200 μ l) and 0.3 g of glass beads (425-600 mesh size, Sigma) were added, and the cells

broken by vortexing for 10 min at 4°C. An aliquot of TE buffer (200 µl) was added, and the mixture centrifuged at 12,000g for 5 min to separate the phases. The aqueous layer was transferred to a new 1.5 ml Eppendorf tube, and the DNA was precipitated by addition of a 1/10th volume of 3 M sodium acetate and one volume isopropanol. The mixture was incubated at room temperature for at least 1 hour, then centrifuged to collect the DNA (12,000g for 10 min). The DNA pellet was washed twice with 1 ml 70% ethanol, dried in a Speed-Vac for 10 min, and redissolved in 200 µl TE buffer. One µg of RNase A was added, and the DNA incubated at 65°C for 15 min to degrade residual RNA. After extraction with an equal volume of phenol/chloroform, the aqueous phase was transferred to a new 1.5 ml Eppendorf tube, and the DNA was precipitated by addition of a 1/10th volume 3 M sodium acetate and 1 V isopropanol. The DNA pellet was washed once with 1 ml of 70% ethanol, dried, and redissolved in 200 µl of sterile Millipore water.

2.14 Sporulation and spore isolation

Strains of the W303 genetic background were sporulated by the following method. YPD medium (5 ml) was inoculated with a single colony of a diploid strain and the culture grown to saturation at 30°C with agitation (260 rpm). Cells were collected by centrifugation (2,000g for 5 min) and washed twice with sterile Millipore water. 5 ml of sporulation medium (1% yeast extract, 10% Potassium acetate, 0.05% glucose, 0.01% adenine, 0.01% uracil, 0.005% arginine, 0.005% histidine, 0.005% tryptophan, 0.005% leucine, 0.005% lysine, 0.005% methionine, 0.005% phenylalanine) was inoculated with 100 µl of the washed culture and the cells incubated at 30°C with agitation (260 rpm) for 3-7 days. Sporulation was verified by examining a sample of the culture with a light microscope.

To sporulate strains of the S288C genetic background, a diploid strain was patched to a fresh YPD plate and the plate incubated for one day at 30°C. The patches were replica plated to a freshly made GNA presporulation plate (5% glucose, 3% Difco nutrient broth, 1% Difco yeast extract, 2% Bacto agar), which was incubated for 1 day at 30°C. The process was repeated once with a fresh GNA presporulation plate. A sample of cells was taken from a patch and used to inoculate 2 ml of supplemented liquid

sporulation medium (1% potassium acetate, 0.005% zinc acetate, 0.002% uracil, 0.004% histidine, 0.004% leucine). The suspension was incubated on a roller wheel for 5-10 days at room temperature, and then for 3-5 days at 30°C. Sporulation was checked with a light microscope.

To isolate purified spores, I used a procedure that took advantage of the hydrophobic nature of the ascospore cell wall to separate spores from unsporulated mother cells and other debris. A sporulated culture was incubated in 200 μ l softening buffer (10 mM DTT, 100 mM Tris-SO₄, pH 9.4) for 10 min at 30°C with agitation (260 rpm). The cells were collected by centrifugation (2,000g for 5 min) and resuspended in 2 ml of spheroplasting buffer (2.1 M sorbitol, 10 mM potassium phosphate, pH 7.2) containing 10 mM DTT and 0.5% glucose. Zymolyase 20T (Seikagaku, Tokyo) was added at a concentration of 1U per A_{600} unit of the sporulated cells, and the mixture incubated at 30°C for 2 hours with agitation (260 rpm). The spores were collected by centrifugation (2,000g for 10 min) and the supernatant was discarded. The spores were resuspended in 200 μ l sterile Millipore water, to which 0.1 g of glass beads were added, and the mixture incubated at 30°C for 1 hour with agitation (260 rpm). One ml of sterile Millipore water was then added to the suspension and the sample was vortexed at high speed for 2 min. A sample of the cell suspension was examined under a microscope to confirm that the spores were released from the tetrads. The glass beads were allowed to settle, and the spore suspension transferred to a new 1.5 ml Eppendorf tube, collected by centrifugation (5,000g for 5 min), and resuspended in 100 μ l sterile Millipore water. The spore suspension was then vortexed at high speed for 2 min to allow the spores to stick to the walls of the tube. The liquid was removed, and the tube (with attached spores) was washed three times with 1 ml sterile Millipore water. To release the spores from the walls of the tube, 1 ml of sterile 0.01% NP40 was added to the tube, and the tube was sonicated for 1 min in a sonicator bath. The spore suspension was diluted appropriately in 0.01% NP-40 before aliquots were plated on YPD plates and incubated for 3 days to isolate spore clones.

2.15 β -Galactosidase activity assay

To measure the β -galactosidase activity of strains transformed with *lacZ* reporter

genes, 5 ml overnight cultures were grown in 15 ml polypropylene tubes. The cells were collected by centrifugation and washed once with ice-cold Z-buffer (0.06 M Na₂HPO₄, 0.04 M NaH₂PO₄, 0.01 M KCl, 0.001 M MgSO₄, pH 7.0). The cell pellet was resuspended in 5 ml of Z-buffer and placed on ice. To determine cell density, 50 µl of a cell sample was added to 40 µl of H₂O in a microtiter plate, and A_{595} was recorded with an EL_x800 Universal Microplate reader. To permeabilize the cells, chloroform (250 µl) and 0.1% SDS (250 µl) was added to each of the tubes. The cells were vortexed for 5 seconds and stored on ice until use. For the assay, 20 µl of ONPG (4 mg/ml) was added in triplicate to the well of a conical-well polypropylene plate, and the plate placed at 30°C. To start the assay, 100 µl of cell suspension was added to each well at 10-30 seconds intervals. After appropriate color development was observed, the reactions were stopped sequentially by adding 60 µl of 1M Na₂CO₃ to the samples in the original order of addition. The plate was centrifuged to separate the chloroform layer from the cell suspension (2,000g for 5 min), and 90 µl of each sample was transferred to a new polystyrene 96-well plate. The optical density of each sample was recorded with the A_{415} filter of an EL_x800 Universal Microplate reader. β-galactosidase units were determined using the formula for Miller units (MU) = A_{415} /volume of cells (ml) x time of assay (min) x A_{595} x 50.

2.16 Measurement of Mg²⁺ content by Atomic Absorption Spectroscopy (AAS)

Yeast cultures (5 ml) were grown to log phase in SC or YPD media and collected by centrifugation. The cells were washed twice with chilled 10 mM EDTA to remove external Mg²⁺, and twice with chilled Millipore water to remove EDTA. The final pellet was resuspended in 1 ml chilled Millipore water and cell density (A_{600}) was recorded. A 1 ml sample was transferred to a 13 ml glass tube followed by the addition of 1 ml of concentrated nitric acid and the sample was incubated for 16 hours at 95°C. Two ml of 1X LaCl₃ buffer (10 mM LaCl₃, 240 mM HCl) was added to each sample as a “releasing agent”, to prevent phosphate ions from interfering with the estimation of Mg²⁺ concentration. The final volume of the sample was adjusted to 4 ml with Millipore water. Samples were diluted 5 or 10-fold with 0.5X LaCl₃ buffer before measurement of Mg²⁺

concentration with a GBC 904AA AAS instrument. The instrument was calibrated using a set of MgCl_2 standard solutions in 0.5 x LaCl_3 buffer (0-60 μM MgCl_2).

To convert Mg^{2+} concentration values from AAS to mass of Mg^{2+} per cell, the concentration was multiplied by the dilution factor and total volume of the digested cells to obtain the total Mg^{2+} content of the sample, which was then divided by the number of cells in the suspension. A_{595} values for each cell sample were converted into cell number using a standard curve previously generated by comparing numbers of viable cells to cell density measurements.

2.17 Measurement of yeast elemental content using ICP-MS

The cells were processed for ICP-MS analysis using a previously described protocol (Salt, 2004), with some modifications. Aliquots of LMM were inoculated with yeast and grown at 30°C with agitation (260 rpm) until they reached an A_{595} of 0.5-1.0. A 2.5 ml aliquot of each culture was filtered through a nitrocellulose filter (0.45 μm , Millipore, Billerica, MA, USA) under vacuum. The filter was washed twice with 5 ml of wash buffer (20 mM sodium citrate, 1 mM EDTA, pH 4.0) and once with 5 ml sterile Millipore water, then dried under vacuum. The filter was transferred to a 15 ml glass tube followed by the addition of 2.5 ml of concentrated HNO_3 and the filter was digested for 4 hours at 118° C. Each sample was transferred to a polypropylene tube and diluted to 16 ml total volume with water. Elemental content was analyzed on a Thermo Elemental PQ Excell ICP-MS as previously described (Salt, 2004). The elemental content of the membrane was subtracted from the final values obtained (membrane-only controls were performed in parallel).

2.18 Sucrose gradient fractionation of yeast organelles

A modified protocol from one described previously (Perzov et al, 2000) was used to separate yeast organelles via differences in their buoyant density. Cultures for cell fractionation were grown in SC-ura media (500 ml), collected by centrifugation, washed twice with water, and resuspended in 10 ml of sorbitol buffer (10 mM potassium phosphate buffer pH 7.4, 1.2 M sorbitol) containing 10 mM DTT (added fresh). The density (A_{600}) of the cells was measured and Zymolyase 20T (Seikagaku, Tokyo) was

added at a ratio of $1U/A_{600}$ unit of cells. Cells were incubated for 2 hours at 30°C with gentle agitation (100 rpm), and washed twice with ice-cold sorbitol buffer (25 ml) by gentle centrifugation (200g for 5 min). To prevent rupture, the spheroplast pellet was gently dispersed in 5 ml of buffer before addition of more buffer to wash the cells. After the last wash, residual buffer was removed with a pipette and the cells were resuspended in 2 ml of ice-cold cell lysis buffer (10 mM Tris-Cl, pH 7.6, 2 mM $MgCl_2$, 10% sucrose, 10 mM DTT). The suspension was homogenized using 20 strokes in a pre-chilled 7 ml Dounce homogenizer. The extent of lysis was checked using a light microscope. If lysis was incomplete, a $1/3^{rd}$ volume of glass beads was added to the suspension and the mixture vortexed at high speed for 30 seconds. The lysate was centrifuged at low speed at 4°C (200g for 3 min) to pellet unbroken cells and nuclei, and the supernatant containing the organelles was transferred to a new tube.

A continuous 10 ml 20% - 60% sucrose gradient was prepared by using a gradient maker to mix equal volumes of 20% sucrose, 10 mM Tris-Cl pH 7.6, 10 mM DTT, and 60% sucrose in the same buffer. One ml of the organelle suspension was layered on the top of the sucrose gradient and centrifuged at 95,000g for 2 hours at 4°C in the A629 swingout rotor of an OTD70B Ultracentrifuge (Sorvall). One ml fractions of the gradient were collected drip-wise by puncturing the bottom of the tube. If the protein in the fractions was overly dilute, protein was precipitated using the trichloroacetic acid (TCA) method. A 20% solution of ice-cold TCA was added to the fraction and incubated on ice for 2-3 hours. Protein was collected by high speed centrifugation (16,000g for 30 min). To enable collection of protein precipitates from the heavier fractions of the gradient, these were diluted 3-fold with gradient buffer (no sucrose) before centrifugation. The protein pellet was washed twice with cold acetone (200 μ l) to remove residual TCA, and dried in a speed-vac. Proteins were redissolved by adding 100 μ l of protein buffer (Tris-base, 3% SDS, 1 mM PMSF) followed by 5 min treatment at 100°C.

2.19 Protein extraction and immunological detection

2.19.1 Protein extraction using TCA

To isolate protein, 5 ml of overnight culture was grown to the appropriate density (A_{600} of 0.5-1.0) in the appropriate media. The cells were collected by centrifugation

(2,000g for 5 min), washed once with 5 ml of 1 mM EDTA, and once with 1 ml of 1 mM EDTA (in a 1.5 ml tube). The cells were resuspended in 400 μ l of ice-cold TCA extraction buffer (10% TCA, 20 mM Tris pH 8.0, 50 mM ammonium acetate, 2 mM EDTA, and 2 mM PMSF, added fresh from a 100 mM stock in ethanol). Three g of glass beads (Sigma) were added to the suspension and the tube was vortexed at high speed for 10 min at 4°C in a cold room. The glass beads were allowed to settle and the supernatant was collected in a new 1.5 ml Eppendorf tube. An aliquot of TCA extraction buffer (200 μ l) was added to the glass beads, mixed and removed to pool with the original extract.

The broken cells were collected by centrifugation (12,000g for 5 min), and the pellet of broken cells and protein was washed twice with 1 ml acetone to remove excess TCA, and dried in a Speed-Vac. The pellet was then resuspended in SDS-protein buffer (100 mM Tris-base, 3% SDS, 1 mM PMSF) and boiled for 5 min to dissolve the protein. The suspension was centrifuged at high speed (12,000g for 1 min) to pellet insoluble debris, and the supernatant (protein solution) was removed and stored at -80°C.

Protein concentration was measured by using a DC protein assay kit (Bio-Rad) according to the manufacturer's instructions. Colorimetric reactions were quantified using an EL_X800 Universal Microplate Reader at a wavelength of 750 nm. A standard curve was constructed using BSA to calculate protein concentration.

2.19.2 SDS-Polyacrylamide Gel Electrophoresis (PAGE)

SDS-PAGE was used to separate proteins based on their molecular weight. A resolving gel (375 mM Tris-Cl, pH 8.8, 0.1% SDS, 5-10% acrylamide mix [29.2 acrylamide:0.8 bis-acrylamide], 0.1% ammonium persulfate, and 0.1% TEMED) was poured, overlain with butanol and allowed to set. The butanol was removed and the resolving gel was overlain with a 1 cm layer of stacking gel (125 mM Tris-Cl, pH 6.8, 4.5% acrylamide mix, 0.1% SDS, 0.1% ammonium persulfate, and 0.1% TEMED), and a comb inserted. Electrophoresis was performed at 200 volts for approximately 25-35 min in a Mini-PROTEAN III gel rig (Bio-Rad), using Tris-glycine running buffer (25 mM Tris-base, 20 mM glycine, 0.1% SDS). Protein samples were boiled in loading buffer (25 mM Tris-Cl, pH 6.8, 2% SDS, 5% glycerol, 5% β -mercaptoethanol, 0.01% bromophenol blue) for 5 min prior to loading. Depending on application, 30-50 μ g of protein was

loaded per lane. If required, the gel was stained with Coomassie Brilliant Blue R250 (Sigma) to visualize protein bands. The gel was immersed in an aqueous solution of 0.025% Coomassie blue, heated for one minute in a microwave and allowed to cool. The gel was destained by heating for 1 min in destaining solution (40% methanol, 7% acetic acid), then allowing to destain for 30 min to 3 hours. A Kimwipe was included in the destain solution to accelerate this process.

2.19.3 Electroblothing and immunodetection

For the immunodetection of specific proteins, SDS-PAGE gels were blotted to Hybond-N-nitrocellulose membranes (Amersham Biosciences) by electrophoretic wet transfer in a Mini-Trans-Blot Electrophoretic Transfer Cell (Bio-Rad). A gel and membrane sandwich was assembled and inserted into an electrode module. The module was immersed in a transfer cell containing pre-chilled Western transfer buffer (50 mM Tris-base, 380 mM Glycine, 0.1% SDS, and 20% methanol). The blotting cell was placed on ice to prevent overheating, and transfer was performed for 3-4 hours at 63 volts. After disassembly, the nitrocellulose membrane was rinsed three times with 10 ml TBST buffer (50 mM Tris-Cl pH 8.0, 150 mM NaCl, 0.05% Tween 20) and rocked gently in 10 ml blocking buffer (TBST+1% fat free dried milk) overnight to block non-specific protein binding sites. The membrane was washed in 10 ml TBST (once for 20 min and twice for 5 min). The membrane was then incubated with appropriate concentration of primary antibody for 2 hours at room temperature with rocking. Excess primary antibody was removed by washing the blot three times for 10 min each with 10 ml TBST. The membrane was incubated with 10 ml of horseradish peroxidase-conjugated secondary antibody in blocking buffer (usually a 1/5000 dilution) for 2 hours at room temperature. The membrane was then washed three times with TBST buffer as previously described to remove non-specifically bound antibodies. Horseradish peroxidase activity was detected using the ECL (Enhanced Chemiluminescence; Pierce) detection system according to the manufacturer's instructions. After incubation in ECL solution, the membrane was placed between two sheets of cling-film, and light emission was detected by exposure to BioMax scientific imaging film (Kodak) for 5 seconds to 30 min depending on signal intensity. Exposed film was immersed in GBX developer (Kodak) for 5 min with gentle agitation

until bands appeared, washed for 5 min under running tap water for 5 min, then fixed for 5 min with agitation in GBX fixer (Kodak). The film was then washed for 10 min under running tap water and allowed to air-dry.

2.19.4 Indirect immunofluorescence

Indirect immunofluorescence was used to detect the location of epitope-tagged proteins in whole yeast cells. Cells were grown in 25 ml of SC-ura media to an A_{600} of approximately 1.0, collected by centrifugation, and washed twice with 10 ml of 1x PBS (140 mM NaCl, 2.7 mM KCl, 10 mM Na_2HPO_4 , 2 mM NaH_2PO_4). Cells were fixed by treatment with (3%) formaldehyde for 2 hours at 30°C with agitation (260 rpm). The cells were collected by centrifugation, washed twice with ice-cold Solution A (100 mM KHPO_4 , pH 7.0, 1.2 M sorbitol) and resuspended in 2 ml of Solution A containing 10 mM DTT. To remove the cell wall, Zymolyase 20 T enzyme was added (2 U/ A_{600} unit of cells), and the cells incubated at 30°C for 2 hours with gentle agitation (100 rpm). The cells were collected by centrifugation (200g for 5 min), washed twice with 10 ml of Solution A, resuspended in cold methanol (chilled to -20°C) and stored at -20°C for one hour to render the cells permeable to antibodies. The cells were then collected by centrifugation, washed twice with 5 ml cold PBS, and resuspended in 100 μl cold PBS. The wells of microscope slides (Fluorescent Antibody Rite-on, Fisher # 3032) were pre-treated with Poly-L-lysine (PLL) to bind cells. To prepare the slides, each well was treated with 40 μl of 0.1% PLL (Sigma P8920) for 10 min. The excess was removed, leaving a thin layer that was allowed to air-dry. The slides were washed with Millipore water and the excess PLL was removed by gently scrubbing with a Kimwipe. The slides were allowed to air-dry before use. To adhere the cells, a 40 μl aliquot of the cell suspension was applied to a well of the slide, and the slide was left on a wet Kimwipe inside a Petri plate for 1 hour at 4°C. The slides were then rinsed with 1X PBS to remove unbound cells.

To detect the antigen, slides were covered with blocking buffer (1X PBS, 5% non-fat dried milk, 0.1% Tween-20) and incubated overnight at 4°C. Each well was filled with 20 μl of primary antibody in blocking buffer and the antibody allowed to react at room temperature for 1 hour. The slides were given four 10-min washes with 1X PBS/1%

Tween-20 with gentle agitation in a slide bath followed by incubation with appropriate fluorescently-labeled secondary antibody for one hour. The PBS/Tween 20 washes were repeated, and the wells were sealed with one drop (20 μ l) of Mowiol solution and a cover slip (Mowiol was prepared by adding 2.4 g Mowiol [Calbiochem] to 6 g glycerol, 12 mM 0.2 M Tris-Cl, pH 8.5, and 6 ml H₂O and heating until dissolved; 1 ml aliquots of Mowiol were stored at -20°C). Slides were allowed to harden overnight at 4°C. Cells were viewed with a Zeiss Axioscope fluorescence microscope and images captured using the associated software. Image overlays were performed using Photoshop CS (Adobe).

Chapter 3 Role of Mnr2 in ion homeostasis

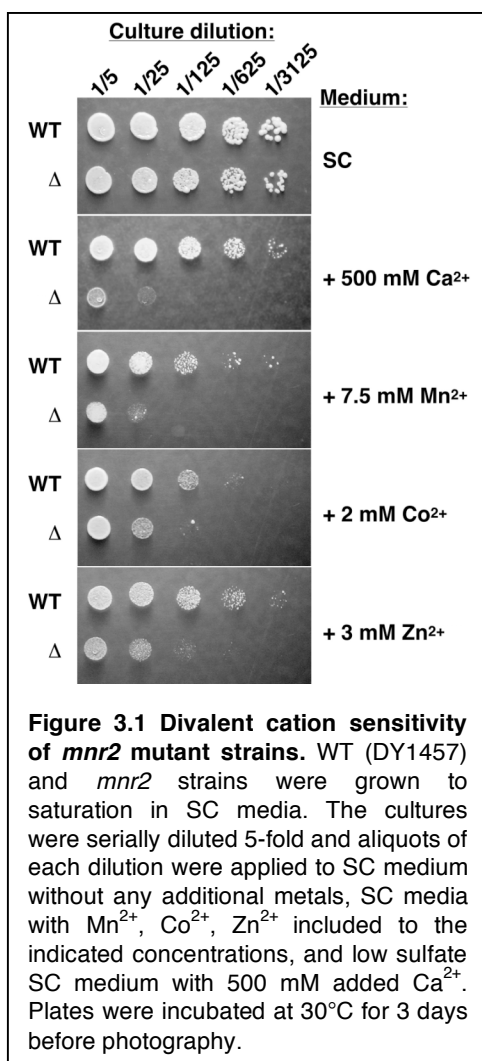
3.1 Introduction

The *YKL064w* reading frame (later designated as *MNR2* for manganese resistance) was first identified during sequencing of yeast chromosome XI (Rasmussen, 1994). Mnr2 is the fifth member of the CorA family in the yeast genome, and it shares approximately 34% protein sequence homology with Alr1 (MacDiarmid & Gardner, 1998). However, unlike the *alr1* mutation, there was no obvious growth defect associated with the *mnr2* mutation, indicating that this gene is not essential in "normal" conditions (MacDiarmid, 1997). This observation suggested that the *ALR* and *MNR2* genes might play distinct and non-overlapping roles in yeast. Further support for this hypothesis comes from a phylogenetic analysis of the CorA family, which indicated that a group of fungal Mnr2-like sequences cluster in a distinct branch of the family (Knoop et al, 2005). This chapter describes several observations that provide support for this model of related but distinct functions for the Alr1 and Mnr2 proteins.

3.2 Effect of the *mnr2* mutation on tolerance to biologically important metal ions

Preliminary experiments suggested that Mnr2 is involved in divalent cation transport. The overexpression or inactivation of the *MNR2* gene altered the sensitivity of yeast to divalent cations such as Ca^{2+} , Mn^{2+} , and Zn^{2+} (MacDiarmid, 1997). The previous study used an *mnr2* mutant strain constructed in the S288C genetic background, which due to inefficient sporulation, is less suitable for genetic studies than the W303 background. For this reason, I decided to determine if these observations could be duplicated using an *mnr2* mutant strain constructed in the W303 background. To construct an *mnr2* mutant strain, an inactivated allele of *MNR2* (*mnr2::KAN^R*) was amplified from a commercially available diploid knockout mutant (Winzeler et al, 1999) and used to transform the haploid strain DY1457 (which is derived from W303). Complete deletion of the *MNR2* coding sequence in this strain was verified using PCR (data not shown). To determine if the new *mnr2* mutant was sensitive to divalent cations,

I assayed growth on plates containing synthetic medium with a range of added metal ions (**Figure 3.1**). Serial dilutions of WT and *mnr2* cultures were applied to the plates and incubated for three days to determine the effect of the metals on growth. Using this assay, I verified that the *mnr2* mutation in the W303 genetic background conferred a strong sensitivity to Ca^{2+} , Mn^{2+} , and Zn^{2+} ions, and a slight sensitivity to Co^{2+} (**Figure 3.1**). The above result suggested that the *mnr2* strain might accumulate higher intracellular levels

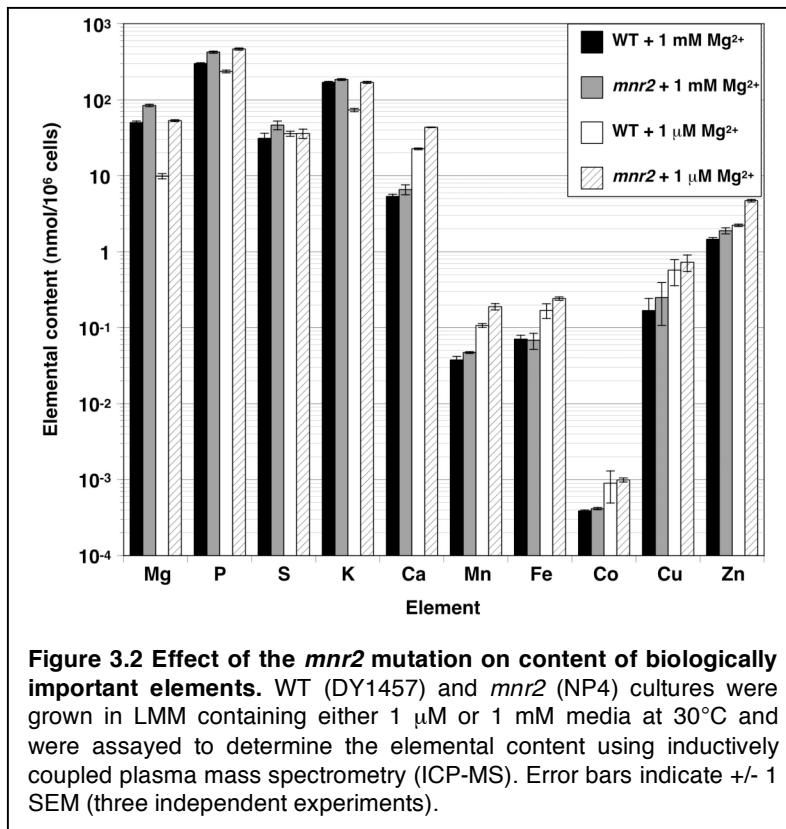


of divalent cations, which might in turn inhibit growth. To test this hypothesis, I directly determined the elemental content of *mnr2* and WT strains using inductively coupled plasma mass spectrometry (ICP-MS). The results of these investigations are shown in **Figure 3.2**. When supplied with a "standard" Mg^{2+} concentration (1 mM), WT and *mnr2* strains displayed relatively large increases in the content of Mg^{2+} and P, but little difference in the content of other elements measured (only those elements which could be reliably quantified are included in the data set shown).

Since the major effect on elemental content seen in the *mnr2* mutant was an increase in Mg^{2+} content, I determined the effect of reducing the Mg^{2+} concentration of the medium on this phenotype. Surprisingly, growth in Mg^{2+} -deficient conditions (1 μM Mg^{2+}) exacerbated the difference in Mg^{2+} content between WT and *mnr2* (**Figure 3.2**). In addition, there was a larger difference in the content of P, K^+ , Ca^{2+} , Mn^{2+} , and Zn^{2+} when strains were grown under Mg^{2+} deficient conditions. Under both Mg^{2+} -deficient and replete conditions however, the primary effect of the *mnr2* mutation was an increase in Mg^{2+} content, implicating Mnr2 in the regulation of Mg^{2+} homeostasis.

3.3 Effect of *mnr2* mutation on growth and Mg^{2+} content

To characterize the effect of the *mnr2* mutation on Mg^{2+} homeostasis in more detail, I measured the growth and intracellular Mg^{2+} content of *mnr2* and WT strains cultured in Low Magnesium containing Medium (LMM) containing a range of Mg^{2+} concentrations, from severely deficient to replete. If Mnr2 played a role in Mg^{2+} homeostasis, the *mnr2* mutation might be associated with a growth defect under Mg^{2+} -deficient conditions, as was observed for *alr1* mutant strains. After 16 hours growth, the



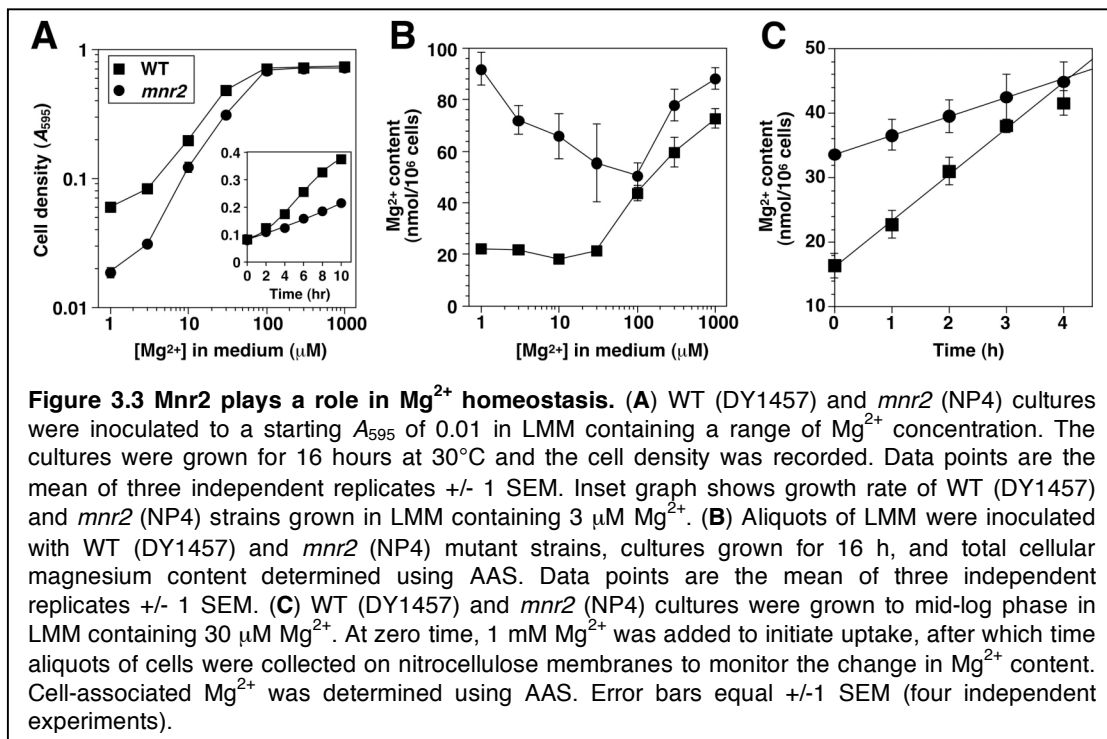
mnr2 strain showed a small but reproducible growth defect under Mg^{2+} -deficient conditions (1-30 μM) (Figure 3.3A). The *mnr2* mutation reduced both the initial growth rate (Figure 3.3A, inset graph) and the final cell density achieved. This data implicated Mnr2 in Mg^{2+} homeostasis under deficient conditions. I then examined the effect of the *mnr2* mutation on

Mg^{2+} content under these conditions. As previously observed in Figure 3.1, compared to the WT, the *mnr2* strain showed an increase in Mg^{2+} content under deficient conditions (1-30 μM) (Figure 3.3B). This difference was most pronounced under extreme Mg^{2+} -deficiency (the difference was approximately 4 fold in 1 μM Mg^{2+}). Together, these results confirm that Mnr2 plays a role in Mg^{2+} homeostasis. The effect of the *mnr2* mutation contrasts with that of the *alr1* mutation. While both mutations caused degrees of Mg^{2+} -dependent growth, they had the opposite effect on Mg^{2+} accumulation (Graschopf et al, 2001; MacDiarmid & Gardner, 1998). These observations suggested that although

both the *ALR1* and *MNR2* genes are required for Mg^{2+} homeostasis, they perform distinct functions.

3.4 Effect of the *mnr2* mutation on Mg^{2+} uptake

The higher intracellular Mg^{2+} content observed in the *mnr2* strain suggested that the rate of Mg^{2+} uptake might be elevated as a consequence of this mutation. To test this hypothesis, WT and *mnr2* strains were grown in relatively Mg^{2+} -deficient conditions (LMM + 30 μM Mg^{2+}) to deplete intracellular stores of Mg^{2+} . When WT cells are depleted of Mg^{2+} in this way, then resupplied with excess Mg^{2+} , they accumulate Mg^{2+}



until their normal content is restored (Graschopf et al, 2001; Lee & Gardner, 2006).

When the same procedure was used to compare Mg^{2+} uptake by a WT and *mnr2* mutant strain, the initial Mg^{2+} content of the *mnr2* strain was twice as high as the WT (**Figure 3.3C**). When the *mnr2* mutant was resupplied with Mg^{2+} , the initial rate of Mg^{2+} accumulation was lower than observed for the WT. Thus, the high intracellular Mg^{2+} content in the *mnr2* strain cannot be solely attributed to an increase in the rate of Mg^{2+} uptake (**Figure 3.3C**).

3.5 Models for Mnr2 function

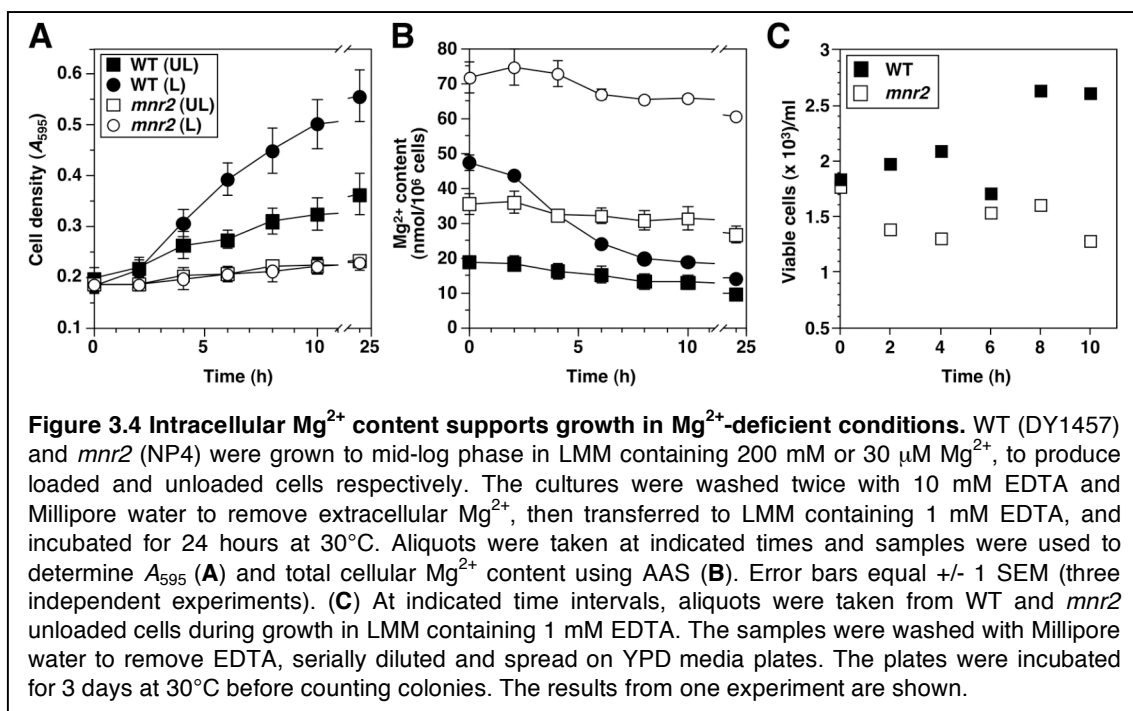
The growth defect seen in the *mnr2* strain under Mg^{2+} deficient conditions could be explained by at least two models. First, the high intracellular Mg^{2+} concentration of the *mnr2* mutant might lead to Mg^{2+} toxicity. However, this explanation seems unreasonable, as *mnr2* and WT strains had a similar level of intracellular Mg^{2+} when grown with a high external Mg^{2+} concentration, but the *mnr2* mutant did not exhibit a growth defect under these conditions (**Figure 3.3A**). A second possible explanation is that under Mg^{2+} -limiting conditions ($< 30 \mu M Mg^{2+}$), the *mnr2* mutant has a defect in cytosolic Mg^{2+} homeostasis, *i.e.* that it cannot maintain the minimum level of Mg^{2+} required for the function of this compartment. If so, it is possible that the higher Mg^{2+} content of the *mnr2* mutant in Mg^{2+} deficient conditions is a consequence of this strain being unable to redistribute Mg^{2+} from an intracellular store to the cytosol. If this model is correct, it predicts that Mnr2 is located in the membrane of an intracellular Mg^{2+} storage compartment, and functions to release Mg^{2+} from this organelle. The *mnr2* mutation would prevent the release of Mg^{2+} from this store upon the transition to deficient conditions, reducing the cytosolic Mg^{2+} concentration and resulting in a growth defect.

The latter model attributes the high intracellular Mg^{2+} content of *mnr2* mutants to Mg^{2+} trapped within an intracellular storage compartment. This model hypothesizes that WT yeast grown in replete conditions contain a significant intracellular store of Mg^{2+} , which can be used to support growth in Mg^{2+} -deficient conditions. If this is the case, when Mg^{2+} -replete WT cells are transferred to Mg^{2+} -free medium, growth of the cells should correspond with a decrease in the intracellular Mg^{2+} content, as the internal store is depleted. In contrast, WT cells that are already Mg^{2+} -deficient should show little growth in Mg^{2+} -free medium, and their intracellular Mg^{2+} content should be stable.

To test these predictions, WT and *mnr2* strains were grown in Mg^{2+} -replete medium (LMM + 200 mM Mg^{2+}) to force Mg^{2+} accumulation and generate "loaded" cells, or a medium with a lower Mg^{2+} content (LMM + 30 $\mu M Mg^{2+}$) to generate "unloaded" cells. **Figure 3.3B** illustrates that WT yeast grown in deficient conditions ($< 30 \mu M Mg^{2+}$) contained approximately 20 nmol $Mg^{2+}/10^6$ cells, which probably corresponds to the minimum amount required for viability. For this reason, it seemed

reasonable to assume that cells supplied with 30 μM Mg^{2+} would not accumulate substantial intracellular Mg^{2+} stores (and could be considered "unloaded" cells). Cultures of loaded and unloaded cells prepared in this way were washed free of extracellular Mg^{2+} , transferred to LMM supplemented with EDTA (to chelate trace quantities of Mg^{2+}), and incubated for up to 24 hours. At intervals during this period, aliquots of cells were taken to monitor the use of stores via measurement of total Mg^{2+} content.

The results show that in Mg^{2+} -free conditions, WT cells loaded with Mg^{2+} grew significantly faster than unloaded cells (**Figure 3.4A**). After 24 hr incubation, cell density of the loaded cells increased 2.75-fold, compared to 1.8-fold for the unloaded cells. At



the start of the experiment, the Mg^{2+} content of the loaded cells was more than 2-fold higher than the unloaded cells, indicating that the pretreatment protocol produced the expected difference in Mg^{2+} content (**Figure 3.4B**). In both WT cultures, Mg^{2+} content decreased with growth, but the loaded cells showed a faster rate of decrease. These observations were consistent with previous reports (Beeler et al, 1997) that intracellular Mg^{2+} stores were used to sustain growth in the absence of an external supply.

I then determined the effect of the *mnr2* mutation on the utilization of intracellular Mg^{2+} . The Mg^{2+} content of both loaded and unloaded cells of the *mnr2* strain was substantially higher than the equivalent WT cells at the start of the experiment (**Figure**

3.4B). Nevertheless, this higher Mg^{2+} content did not translate into a faster growth after transfer to Mg^{2+} -free medium: both loaded and unloaded *mnr2* did not grow under these conditions. In addition, there was little change in the Mg^{2+} content of the *mnr2* cells during the experiment. After 10 hours of growth, a smaller absolute decrease in Mg^{2+} content was observed for the L and UL *mnr2* cells than for the UL WT cells.

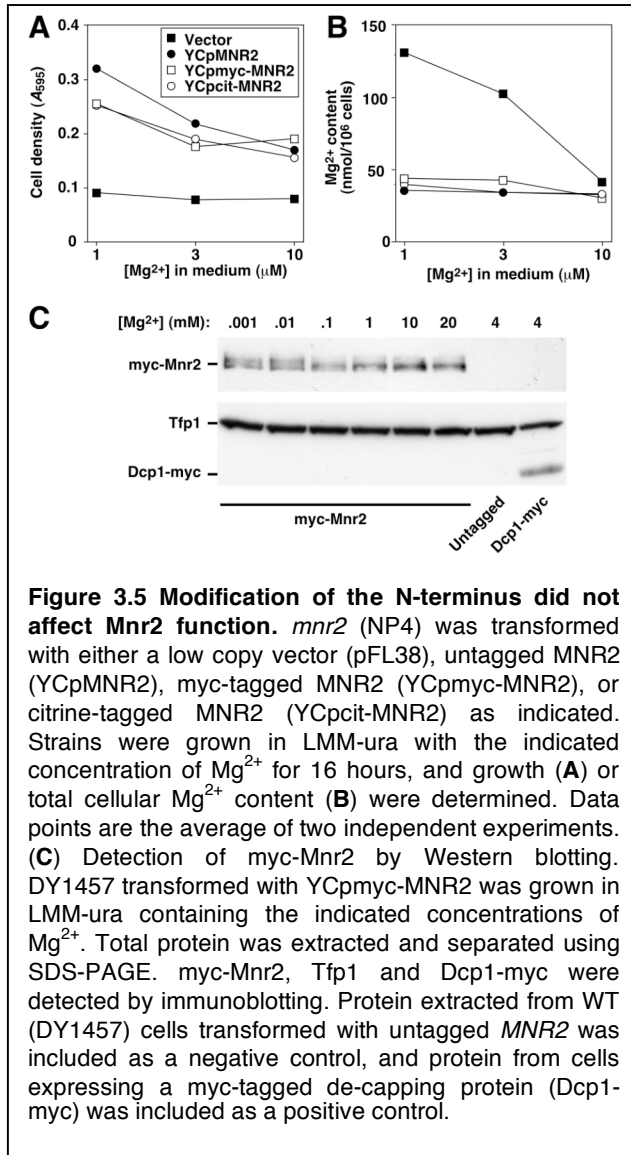
Overall the data shown in **Figure 3.4** suggests that the *mnr2* mutant is unable to utilize intracellular Mg^{2+} to support growth. In fact, the data indicates that the difference in the Mg^{2+} content of WT and *mnr2* strains after growth in deficient conditions appears to be a consequence of the mutant cells retaining the majority of their initial Mg^{2+} content, rather than utilizing it to sustain growth. An alternative explanation is that the elevated Mg^{2+} content reflects an improved ability of the *mnr2* mutant to obtain Mg^{2+} from the environment under deficient conditions. My results do not support this interpretation however, because this effect was observed using a medium that was depleted of trace quantities of Mg^{2+} by the addition of EDTA.

One possible inconsistency between this data and the above model is that, while unloaded *mnr2* cells showed a decrease in intracellular Mg^{2+} content similar to that seen for the WT unloaded cells, the unloaded WT culture still achieved a significantly higher rate of growth than unloaded *mnr2* cells. If the decrease in Mg^{2+} content observed in the WT during this time was due to the redistribution of intracellular stores, then why did the *mnr2* culture not display growth comparable to WT? One possible explanation for the apparent contradiction might be that the viability of the unloaded *mnr2* cells decreased during this experiment, with a consequent release of Mg^{2+} from the dead cells. To test this hypothesis, aliquots of unloaded WT and *mnr2* cells were plated on YPD medium to determine cell viability. Because only one experiment was performed, the data was somewhat variable, but overall the unloaded *mnr2* culture showed a small decrease in viable cell density, while the WT showed a small increase (**Figure 3.4C**). Hence, a decrease in viability may indeed explain the small decrease in Mg^{2+} content of the unloaded *mnr2* cells observed during this experiment.

3.6 Determination of Mnr2 subcellular location

If Mnr2 were a transporter responsible for regulating vacuolar Mg^{2+} storage, it is

likely that this protein would be located in the vacuolar membrane. To test this prediction, I modified a plasmid containing the *MNR2* ORF under the control of the endogenous promoter, adding sequences that would enable detection of the protein by Western blotting or fluorescence microscopy. The N-terminal end of the *MNR2* ORF was fused either to six repeats of the myc-epitope tag, or the fluorescent protein citrine, a



variant of YFP (Griesbeck et al, 2001; Zacharias et al, 2002) (see Ch. 2.6 for details of plasmid construction).

These modified versions of Mnr2 can be considered to be functional if they complement the slow growth and high intracellular Mg²⁺ content phenotypes of *mnr2* mutant strains grown under Mg²⁺ deficient conditions. To test the function of these modified proteins, the two constructs, an untagged *MNR2* construct (YCpMNR2, a positive control) and an empty vector (pFL38, a negative control), were used to transform an *mnr2* deletion mutant. Growth and Mg²⁺ content of these strains were determined after culture in Mg²⁺-deficient conditions. The *mnr2* strain with the empty vector grew little under these conditions, but the same mutant transformed with the

YCpMNR2 (untagged Mnr2), YCpmyc-MNR2 (myc-tagged), or YCpcit-MNR2 (YFP-tagged) constructs displayed a similar level of robust growth (Figure 3.5A). Expression of the tagged versions of Mnr2 also reduced intracellular Mg²⁺ content to a level similar to that observed for the complemented strain (Figure 3.5B). These results indicate that

the addition of sequences to the N-terminal end of the Mnr2 protein does not disrupt its normal function, at least in the case of the myc and citrine tags. In contrast, a construct in which three repeats of the HA tag were fused to the C-terminal end of Mnr2 was not functional, indicating that the C-terminal end is sensitive to modification (data not shown).

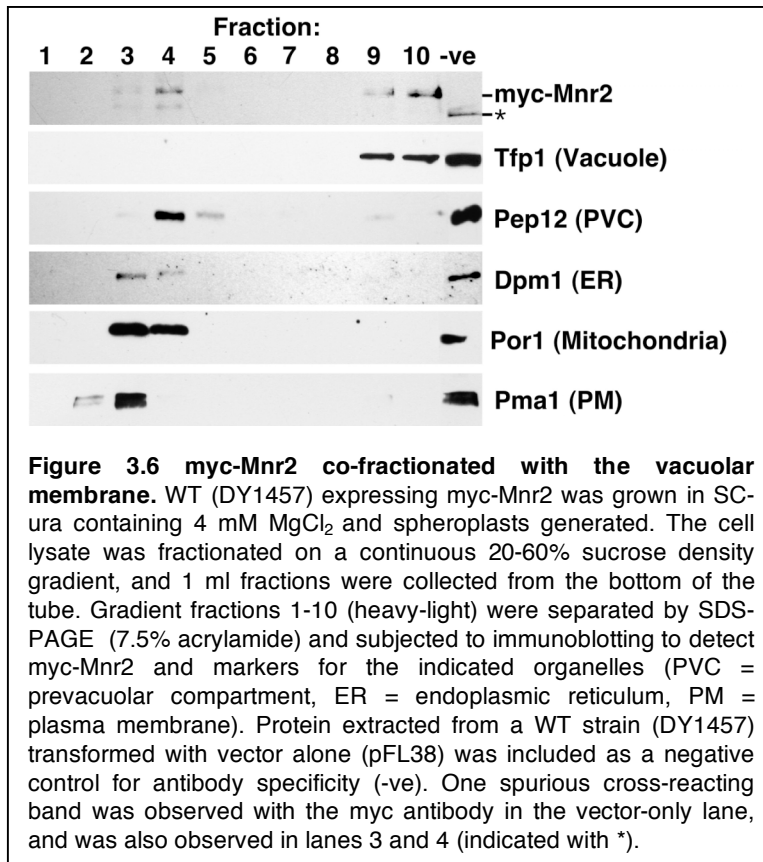
Since the myc-Mnr2 construct was primarily constructed in order to identify Mnr2 using Western blotting, I wanted to determine if myc-Mnr2 was detectable using this method. In addition, I wanted to examine the effect of Mg^{2+} supply on Mnr2 protein accumulation to determine if it was regulated, as previously reported for the Alr1 protein (Graschopf et al, 2001). Mg^{2+} -dependent expression of Mnr2 would be an interesting finding for two reasons. First, it would provide further evidence for a role of Mnr2 in Mg^{2+} homeostasis, and second, it would suggest optimal conditions for the growth of yeast in order to maximize Mnr2 expression (information that may, for example, facilitate the detection of Mnr2 in subsequent experiments).

To perform this experiment, a WT strain expressing myc-Mnr2 was grown over a range of Mg^{2+} concentrations. Total protein was extracted from the cells and separated by SDS-PAGE, then blotted to nitrocellulose. As negative and positive controls, I included protein extracted from a strain that did not express myc-Mnr2, and protein from a strain expressing another myc-tagged protein, Dcp1 (Sean Houshmandi, unpublished data). The myc-Mnr2 protein was detected by using an anti-myc antibody to probe the Western blot, and an anti-Tfp1 antibody was also included to detect this protein as a control for equal lane loading. As shown in **Figure 3.5C**, a band was visible in the lane loaded with protein from the strain expressing myc-Mnr2, but not in the negative control lane. This protein had an apparent molecular weight of approximately 116 kDa, similar to the predicted molecular weight for myc-Mnr2 (120 kDa). In protein from cells grown in Mg^{2+} -deficient conditions, another band appeared with a slightly slower mobility. This lower-mobility band may represent a phosphorylated version of Mnr2, or a product of some other post-translational modification. A comparison of the total signal of these two bands over a range of Mg^{2+} concentrations indicated that there was no appreciable effect of Mg^{2+} supply on Mnr2 accumulation. Thus, this experiment indicated that, unlike Alr1, Mnr2 expression is not regulated by Mg^{2+} concentration. These experiments also

confirmed that the addition of myc-epitope tags allowed detection of the Mnr2 protein in total protein extracts of yeast cells.

3.7 Determination of Mnr2 location using cell fractionation

To determine the subcellular location of Mnr2, I used two independent techniques. The first method was sucrose gradient cell fractionation, which involves separating yeast organelles via differences in their buoyant density (Perzov et al, 2000).



To perform these experiments, a WT strain transformed with YCpmyc-MNR2 was cultured in standard synthetic medium, then processed to extract organelles as described in Materials and Methods (see **Ch. 2.18** for details). The organelles were loaded on a 20-60% sucrose density gradient and subjected to ultracentrifugation. One ml fractions of the gradient were collected, and a 20 μl sample of each was

separated using SDS-PAGE and blotted to nitrocellulose membrane. The myc-Mnr2 protein and known organelle-associated marker proteins were detected using specific primary antibodies.

Sucrose gradient fractionation separates light organelles such as vacuoles to the top (light) fractions, while the heavier organelles, such as mitochondria, endoplasmic reticulum (ER), and plasma membrane are distributed in the heavy fractions. In the sample data **Figure 3.6**, myc-Mnr2 was distributed primarily in the top fractions similar to the vacuolar marker, Tfp1. This observation indicates that the majority of Mnr2 is

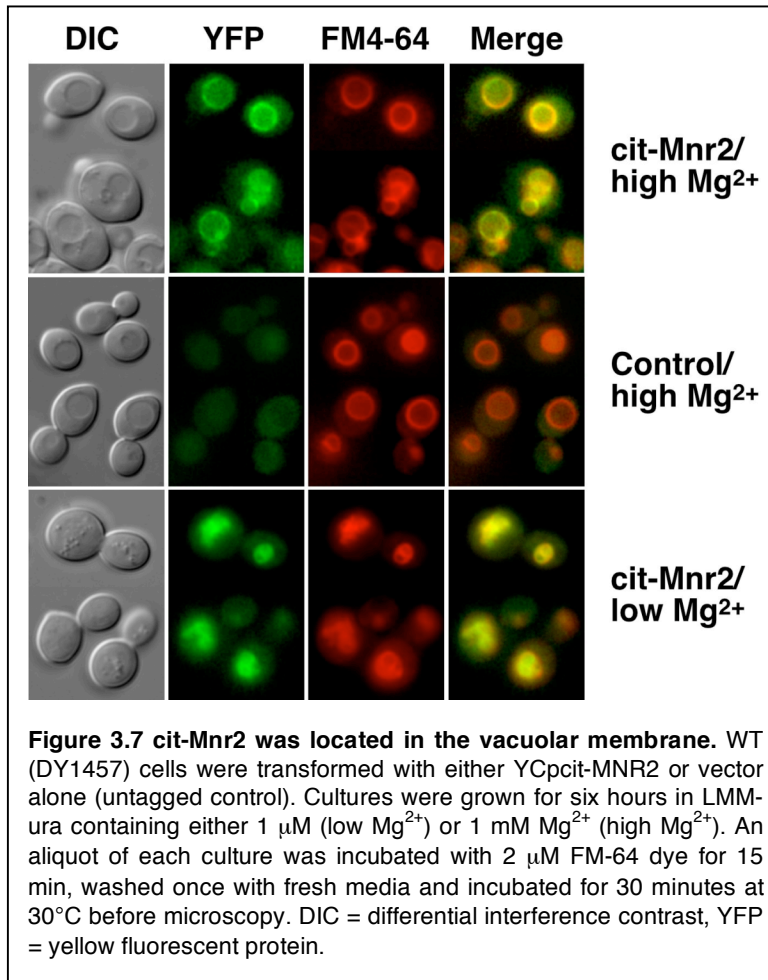
associated with the vacuoles. A small amount of the Mnr2 protein (approximately 20%) appears to be located in the heavier fractions of the gradient, where its distribution overlapped with that of markers for the pre-vacuolar compartment (PVC), mitochondria, and ER. This signal may represent a fraction of the protein that is in transit through the secretory pathway to the vacuolar compartment, or it may be an artifact of poor separation. As expected, protein extracted from the control strain (-ve) showed no signal for myc-Mnr2, confirming the specificity of the anti-myc antibody (previously noted in **Figure 3.5C**). In summary, this data indicates that the bulk of the Mnr2 protein co-fractionated with the vacuolar membrane, consistent with a role in the function of this compartment.

3.8 Determination of Mnr2 location using epifluorescence microscopy

Due to the apparent overlap of some of the myc-Mnr2 protein with ER, mitochondrial, and PVC markers, I used a second, independent technique of epifluorescence microscopy to verify the location of Mnr2. I also wanted to determine if extracellular Mg^{2+} concentration had any effect on the Mnr2 location, and to determine if Mnr2 is present in the vacuole membrane under Mg^{2+} -deficient conditions (as expected if it was responsible for remobilizing vacuolar stores). To detect YFP-tagged Mnr2, a diploid strain (BY4743) was transformed with the YCpcit-Mnr2 construct (an N-terminal fusion of YFP to Mnr2). The citrine variant of yellow fluorescent protein (YFP) was chosen because Mnr2 expression is relatively low, and citrine has an excellent signal/noise ratio when expressed in yeast (Sheff & Thorn, 2004). To mark the location of the vacuolar membrane, I used the lipophilic styryl dye FM4-64. In yeast, FM4-64 is transported from the plasma membrane to yeast vacuoles by an endocytic process (Vida & Emr, 1995). FM4-64 and YFP fluorescence can be distinguished using different filters, allowing these markers to be detected in the same cell. To verify the specificity of the microscope filters, a diploid strain transformed with untagged Mnr2 and labeled with FM4-64 was also examined.

The results shown in **Figure 3.7** revealed that the cells expressing cit-Mnr2 showed a signal around the periphery of the vacuole, as identified by DIC optics and FM4-64 staining. Merging the FM4-64 and YFP images revealed excellent

correspondence between the two signals. Due to fragmentation of the vacuole in Mg^{2+} deficient cells, the morphology of the vacuole was more distinct in replete cells compared with deficient cells, but in deficient cells the FM4-64 signal again corresponded exactly with the YFP signal. Control cells expressing untagged Mnr2 showed low levels of diffuse background autofluorescence, but no obvious vacuolar membrane signal. Despite the relatively low signal intensity of the YFP-tagged Mnr2, the brighter FM4-64 signal



did not "bleed-through" to the YFP channel (see the merged image of control/high Mg^{2+} cells), indicates that the microscope filters separate these signals.

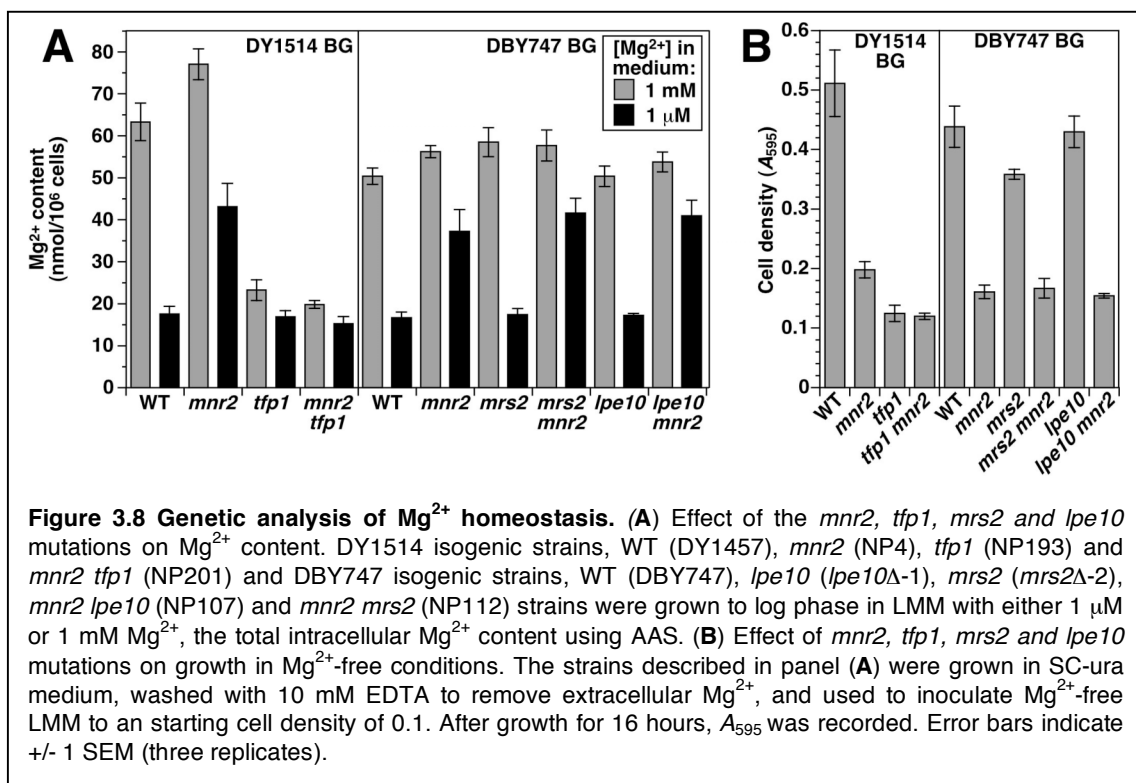
This data confirms that in both Mg^{2+} -replete and deficient cells, Mnr2 is primarily located on the vacuolar membrane consistent with a function in regulating the release of Mg^{2+} from the vacuole. However, it remains possible that a very small amount of Mnr2 is present in other cellular locations

(such as the ER). Later in this work, I describe further experiments undertaken to investigate this possibility (Ch. 3.12)

3.9 Genetic evidence for a role of Mnr2 in vacuole function

Biochemical studies have suggested that a vacuolar Mg^{2+}/H^+ exchanger is responsible for transporting Mg^{2+} into vacuoles (Borrelly et al, 2001). Proton transport to

the vacuole is dependent on V-ATPase activity (Forgac, 1999). Therefore, V-ATPase activity should be required for Mg^{2+} storage in vacuoles, and also for the expression of the *mnr2* Mg^{2+} hyperaccumulation phenotype. In the absence of V-ATPase activity, I expected that the effect of the *mnr2* mutation would be diminished or even eliminated. To test this prediction, I examined the effect of combining the *tfp1* and *mnr2* mutations. The Tfp1 protein is an essential V-ATPase subunit, and loss of this protein eliminates V-ATPase activity (Hirata et al, 1990). As shown in **Figure 3.8A**, an *mnr2* strain grown in Mg^{2+} deficient conditions had a high intracellular Mg^{2+} content compared to the WT. In



contrast, the *tfp1* mutation was associated with a decrease in Mg^{2+} content irrespective of the Mg^{2+} concentration the strain was supplied with, consistent with a defect in Mg^{2+} storage. As expected, the *mnr2 tfp1* double mutant showed Mg^{2+} levels similar to that of the single *tfp1* strain, indicating that the high Mg^{2+} phenotype of *mnr2* was suppressed. This result indicates that, as predicted, the *tfp1* mutation is epistatic to *mnr2*. **Figure 3.8B** shows the effect of the above mutations on cell growth after transfer from Mg^{2+} replete media to deficient media, as an indication of their ability to utilize intracellular stores of Mg^{2+} . While the *mnr2* mutant showed a severe growth defect compared to the WT, the

tfp1 strain shows an even more severe growth defect, consistent with the apparent absence of an intracellular Mg^{2+} store (**Figure 3.8A**). The double mutant showed growth similar to the single *tfp1* mutant, which is again consistent with the apparent lack of internal stores in both these strains.

In mammalian cells, mitochondria may participate in storage of excess Mg^{2+} (Kubota et al, 2005). My cell fractionation studies could not exclude that some portion of Mnr2 was associated with the mitochondria. For this reason, I wanted to examine the possibility that Mnr2 might regulate the Mg^{2+} content of the mitochondria. I constructed a set of strains in the DBY747 background carrying the *mnr2* mutation with or without the *Mrs2* and *Lpe10* proteins. As discussed previously (**Ch. 1.8.1.2**), *Mrs2* and *Lpe10* form a heteromeric complex in the inner mitochondrial membrane, which is thought to transport Mg^{2+} into the mitochondria. Inactivation of either gene reduced mitochondrial Mg^{2+} content, indicating they are both required for mitochondrial Mg^{2+} uptake (Gregan et al, 2001b). As observed previously in the DY1514 genetic background, an *mnr2* mutant in the DBY747 genetic background retained a higher Mg^{2+} content when grown under Mg^{2+} deficient conditions (**Figure 3.8A**). Unlike the *tfp1* mutation, the *mrs2* and *lpe10* single mutations were not associated with a substantial decrease in intracellular Mg^{2+} content under Mg^{2+} replete conditions, suggesting that mitochondrial Mg^{2+} content represents only a minor fraction of total Mg^{2+} content. Additionally, when combined with *mnr2*, the *mrs2* and *lpe10* mutations were not associated with an increase in the severity of the *mnr2* phenotype, suggesting that the increased Mg^{2+} content associated with the *mnr2* mutation is not a consequence of an increase in mitochondrial content. In contrast to the *tfp1* mutation, neither the *mrs2* nor the *lpe10* mutation had any effect on growth, suggesting that these mutants have full access to intracellular Mg^{2+} stores under Mg^{2+} deficient conditions (**Figure 3.8B**), and the combination of *mnr2* with either *lpe10* or *mrs2* mutations did not enhance the *mnr2*-associated growth defect in low Mg^{2+} . These observations support the conclusion that Mnr2 does not regulate the Mg^{2+} content of mitochondria.

3.10 Interaction of the *ALR* and *MNR2* genes

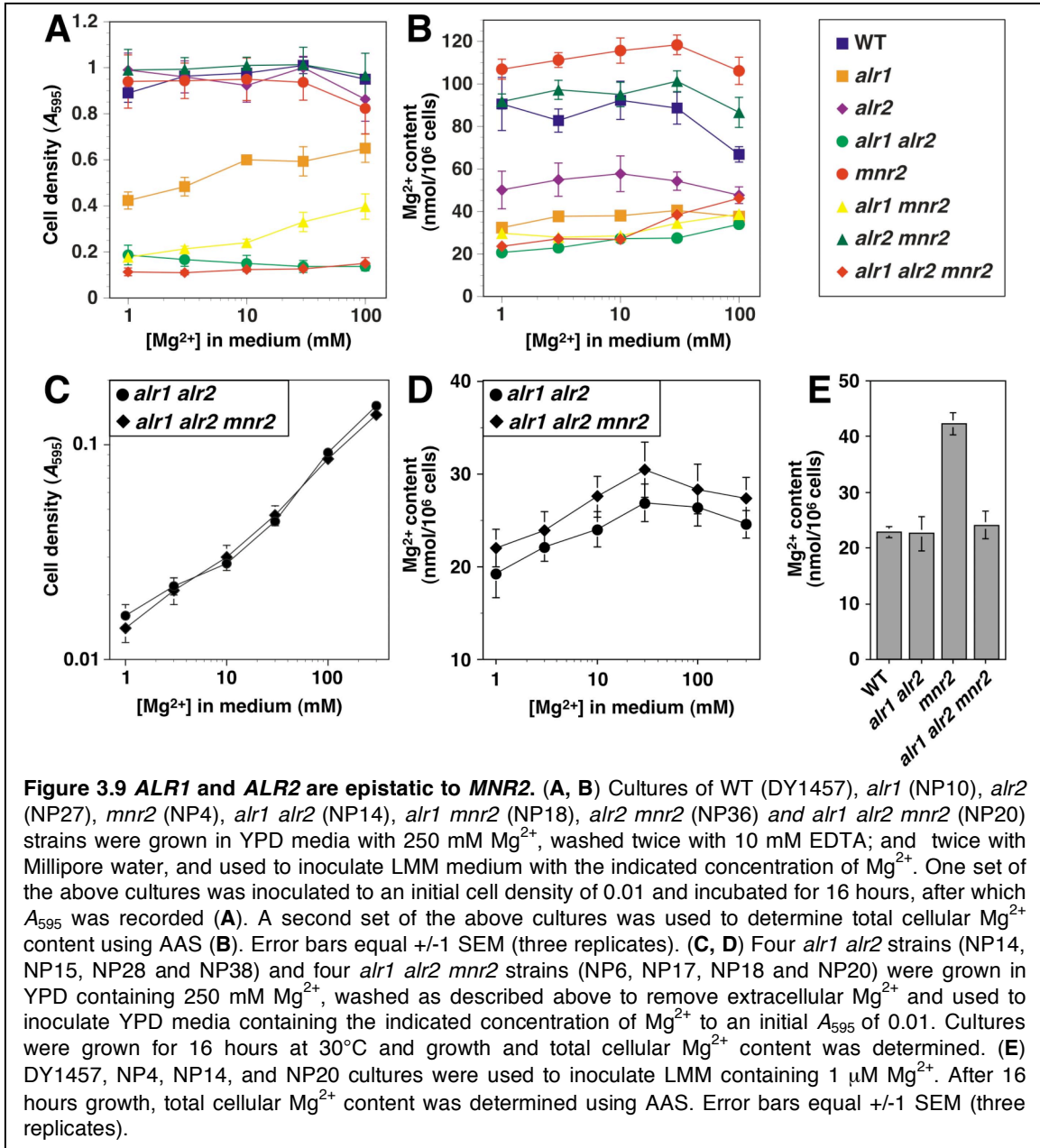
My current model for Mnr2 function proposes that this protein functions to

release Mg^{2+} from the vacuole to buffer the cytoplasmic $[Mg^{2+}]_i$. It is also possible however that the *mnr2* phenotype of higher Mg^{2+} content could result from the activation of a novel (as yet uncharacterized) system responsible for Mg^{2+} uptake. If this model is correct, the *mnr2* phenotype of higher Mg^{2+} content should be independent of the activity of the Alr proteins, the only known systems for Mg^{2+} uptake in yeast. To test if the *mnr2* phenotype was dependent on the Alr proteins, I generated a set of mutants with all possible combinations of the three mutations, and determined their effect on intracellular Mg^{2+} content and Mg^{2+} -dependence for growth. Cultures were initially grown in 250 mM YPD to enable growth of all strains, and washed cells were then used to inoculate aliquots of LMM with a range of Mg^{2+} concentrations. As reported previously (MacDiarmid & Gardner, 1998), the *alr1* mutant showed a growth defect that was ameliorated by supplementation with Mg^{2+} (**Figure 3.9A**). In addition, this strain had a lower intracellular Mg^{2+} content than the WT, and this phenotype was again partially suppressed by Mg^{2+} supplementation. The *alr2* mutation in contrast had no effect on growth, but it significantly reduced Mg^{2+} content (**Figure 3.9B**). Earlier reports had noted that the *alr2* mutation did not significantly affect Mg^{2+} content in the S288C background (Graschopf et al, 2001; MacDiarmid & Gardner, 1998) suggesting that this gene is more active in strains derived from W303. This conclusion is supported by the observation that an *alr1 alr2* double mutant showed a severe growth defect that was not alleviated by Mg^{2+} supplementation. This severe synthetic phenotype suggests that Alr2 plays a significant role in Mg^{2+} uptake in this strain background.

Under the relatively Mg^{2+} -replete conditions used for this experiment, the single *mnr2* mutation was not associated with a growth defect. However, this mutation strongly enhanced the growth defect associated with the *alr1* mutation, which reduced access to extracellular Mg^{2+} . This observation is consistent with the idea that both proteins contribute to regulating the Mg^{2+} concentration of the cytoplasm; Alr1 supplies external Mg^{2+} , and Mnr2 supplies Mg^{2+} from internal stores.

As demonstrated in **Figure 3.9**, eliminating both Alr1 and Alr2 caused a severe reduction in growth and the largest reduction in Mg^{2+} content. The observation that both Mg^{2+} content and growth phenotypes of the *alr1 alr2* mutant were almost insensitive to Mg^{2+} supplementation suggests that this strain has an extremely severe block in Mg^{2+}

uptake. In this genetic background, if the *mnr2* mutation were to cause the activation of another novel Mg^{2+} uptake system, I expected to see this system have an effect on growth and Mg^{2+} content. However, these phenotypes were very similar in the triple and the double mutant strains, which does not support the idea that a novel Mg^{2+} uptake system is



upregulated by the inactivation of *MNR2*. In contrast, the observation that the *alr1* and *alr2* mutations in combination are epistatic to *mnr2* is consistent with my proposed model for *Mnr2* function. I suggest that *alr1 alr2* mutant strains are able to acquire just enough Mg^{2+} to survive, but not enough to accumulate significant stores within the vacuole. For

this reason, the high intracellular Mg^{2+} phenotype of the *mnr2* strain is suppressed in the triple mutant. The inactivation of the *ALR* genes produces an effect similar to the *tfp1* mutation, preventing the cell from accumulating excess Mg^{2+} within the vacuole. Under these conditions, the Mnr2 protein is essentially unnecessary and its inactivation has no effect on homeostasis. Hence, the *ALR* genes are epistatic to *MNR2*.

To further verify that the *mnr2* mutation did not affect growth and Mg^{2+} content phenotypes in the *alr1 alr2* background, I repeated the growth and Mg^{2+} content measurements using four independently isolated strains of double (*alr1 alr2*) and triple mutants (*alr1 alr2 mnr2*) grown over a range of Mg^{2+} concentrations (all strains were derived from sporulation of a triple heterozygous diploid strain). **Figure 3.9C** demonstrates that there was no difference in the growth of double (*alr1 alr2*) versus triple mutants (*alr1 alr2 mnr2*). The *mnr2* mutation was however associated with a slight increase in Mg^{2+} content in an *alr1 alr2* background (**Figure 3.9D**), although this effect was not large enough to be distinguished from random variation.

I also repeated measurements of Mg^{2+} content using cells cultured under severely Mg^{2+} deficient conditions (**Figure 3.9E**), which maximize the effect of the *mnr2* mutation on Mg^{2+} content. Under these conditions, the *mnr2* single mutant had a higher Mg^{2+} content than the WT. However, this phenotype was suppressed in an *alr1 alr2* mutant background, again confirming that the expression of this *mnr2* phenotype is dependent on the function of the Alr proteins.

In summary, these results indicate that the *ALR* genes are epistatic to *MNR2*. This effect can be explained by the observation that in the W303 background, deletion of both of the *ALR* genes induces a severe defect in Mg^{2+} uptake, meaning that such strains are unable to accumulate Mg^{2+} in excess of their minimum requirements for survival. Under these conditions, storage of excess Mg^{2+} in the vacuole is prevented, which suppresses the effect of the *mnr2* mutation.

3.11 Direct assays of cation transport by Mnr2

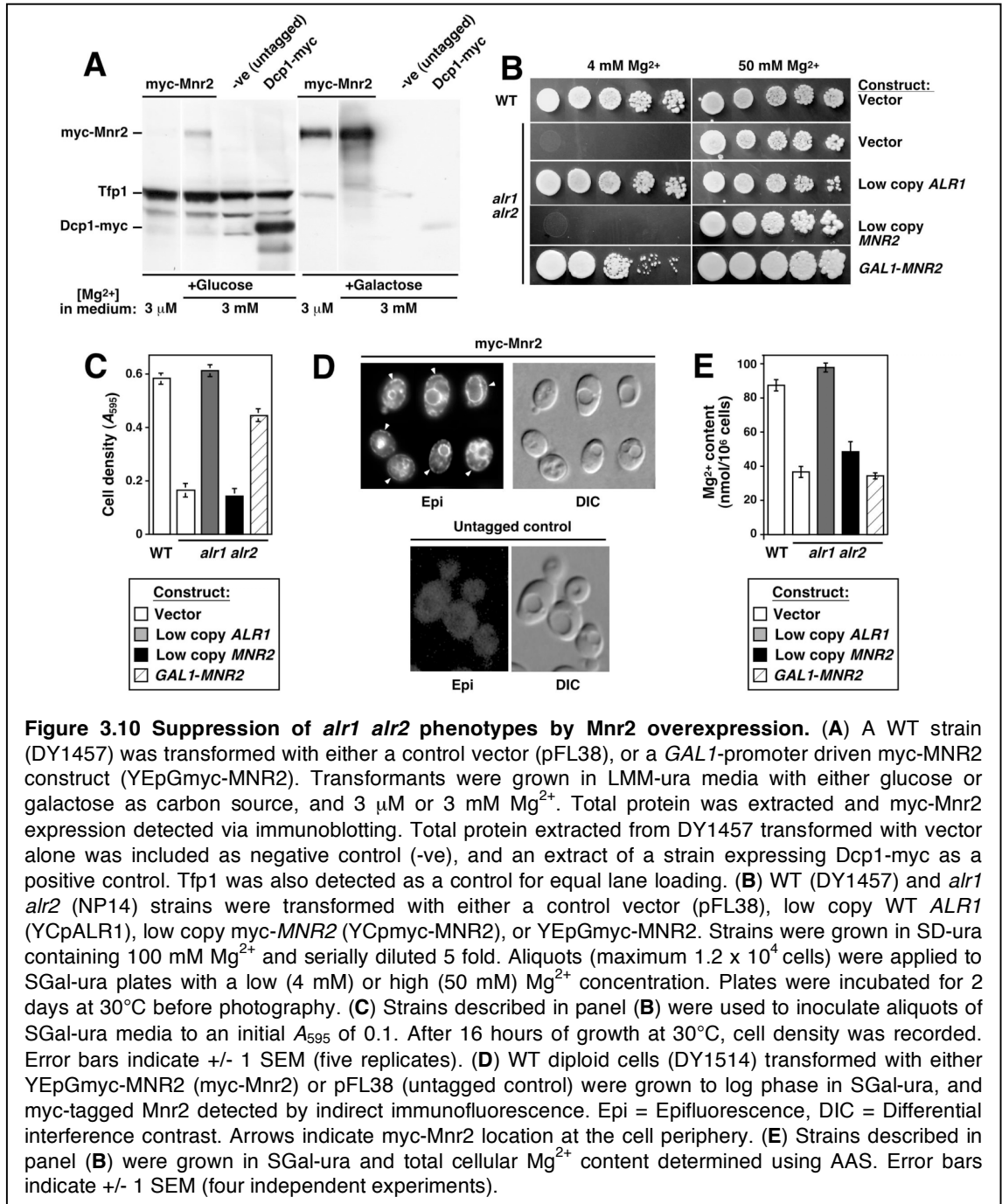
Thus far, my results provide indirect support for a model in which Mnr2 is a transporter responsible for releasing vacuolar Mg^{2+} content. Ideally, it would be possible to demonstrate biochemically that Mnr2 is directly responsible for Mg^{2+} transport.

Isolation of vacuole membranes from yeast is relatively simple, but the probable orientation of Mnr2 in the vacuole membrane, and the lack of suitable radioisotopes of Mg^{2+} makes studies of Mg^{2+} transport by isolated vacuoles technically very difficult. However, I reasoned that if Mnr2 had the same topology as Alr1, it should be capable of mediating Mg^{2+} uptake when relocated to the plasma membrane. Biochemical studies of metal transport using whole yeast cells are theoretically much simpler than utilizing isolated membranes, and would also allow me to determine if there was any functional overlap between the Alr and Mnr2 proteins. For example, if Mnr2 was relocated to the plasma membrane in an *alr1 alr2* mutant strain, the resulting restoration of Mg^{2+} uptake might suppress the *alr1 alr2* phenotypes of slow growth and reduced intracellular Mg^{2+} content.

I suspected that the overexpression of Mnr2 might overcome mechanisms of protein sorting and allow some of the protein to reach the cell surface. To test this prediction, I constructed a plasmid containing the myc-MNR2 coding sequence fused to the strong *GAL1* promoter. Use of a myc-tagged protein would enable me to verify overexpression using Western blotting, and to detect the location of the protein in cells using immunofluorescence. Initially, WT cells were transformed with this construct and grown in LMM-ura medium containing either glucose or galactose as carbon source. Protein was then extracted from the cells and subjected to SDS-PAGE and Western blotting to detect myc-Mnr2. As seen in **Figure 3.10A**, growth of cells in glucose medium drove undetectable levels of Mnr2 in the presence of $3 \mu M Mg^{2+}$, and a low but detectable level of Mnr2 expression relative to the loading control (Tfp1) in presence of $3 mM Mg^{2+}$. Growth in galactose produced a large increase in Mnr2 expression (compare expression of Mnr2 to Tfp1). The effect of galactose was independent of Mg^{2+} supply, although a higher level of Mnr2 was seen in Mg^{2+} -replete cells. Proteins extracted from WT cells expressing untagged Mnr2 and Dcp1-myc were used as negative and positive controls, respectively. No Mnr2 band was detected in the negative control samples, and a band of the appropriate size (26 kDa) was detected in the positive control (Dcp1-myc) samples confirming that the anti-myc antibody was specific for the myc epitope tag.

To determine if the overexpression of Mnr2 in an *alr1 alr2* strain was capable of suppressing the growth defect of this strain, an *alr1 alr2* strain was transformed with the

YEpmyc-Mnr2 plasmid and several control constructs, including an empty vector, a low copy *MNR2* genomic clone, and a low copy *ALR1* genomic clone (**Figure 3.10B**). Growth was then assayed by application of cells to solid synthetic media. All strains grew



at a similar rate to the WT strain in the presence of 2% galactose and excess Mg^{2+} (50 mM) (**Figure 3.10B**), which suppressed the *alr1 alr2* growth defect (MacDiarmid & Gardner, 1998). In the presence of 4 mM Mg^{2+} , the *alr1 alr2* strain transformed with the

empty vector alone did not grow, illustrating the severe growth defect of this strain under normal conditions. I saw no effect of the low copy *MNR2* construct on this phenotype, indicating that a small increase in Mnr2 expression (from an extra 1-2 gene copies/cell) could not suppress the Mg^{2+} uptake defect. In contrast, both the low copy *ALR1* and *GALI-MNR2* constructs conferred robust growth, although Mnr2 overexpression did not completely rescue growth to the WT level. The strong suppression of the growth defect by Mnr2 overexpression indicated that Mnr2 is able to effectively compensate for loss of the *ALR* genes. This suppression was also seen in strains grown in liquid culture with a standard (4 mM) Mg^{2+} supply (**Figure 3.10C**). The low copy *ALR1* construct completely rescued the *alr1 alr2* growth defect, overexpression of Mnr2 restored near-normal rates of growth, and the *alr1 alr2* strain with the low copy *MNR2* construct grew at a similar rate to the uncomplemented strain.

These observations are consistent with the idea that mislocalization of Mnr2 to the plasma membrane could compensate for a loss of plasma membrane uptake systems by transporting Mg^{2+} into the cell. To directly determine the effect of Mnr2 overexpression on its location, I visualized the myc-Mnr2 protein using the technique of immunofluorescence. A diploid strain (BY4743) was transformed with YEpGmyc-MNR2 and YCpMNR2 (as a negative control), and both strains were grown to log phase in SC-ura containing galactose to drive myc-Mnr2 overexpression. The epitope tagged protein was labeled with a fluorescent dye using an indirect immunofluorescence protocol (**Ch. 2.19.4**) and the labeled cells examined using epifluorescence microscopy. Cells overexpressing myc-Mnr2 showed signal around the vacuoles. In addition, the bulk of the cells showed a punctate signal at the plasma membrane (indicated by white arrows in **Figure 3.10D**). Only diffuse background staining was observed in the untagged negative control cells (**Figure 3.10D**). This observation of plasma membrane-localized Mnr2 was in contrast with previous observations of cit-Mnr2 expression, which revealed Mnr2 signal exclusively at the vacuole membrane (**Figure 3.7**). Hence, these observations confirm that Mnr2 overexpression can cause the accumulation of Mnr2 at the plasma membrane, where this protein could potentially mediate Mg^{2+} uptake.

I also examined if Mnr2 overexpression could suppress the reduced Mg^{2+} content of *alr1 alr2* mutants. Expression of *ALR1* restored Mg^{2+} content to a WT level (**Figure**

3.10E). The *MNR2* single copy plasmid was associated with a slight increase in Mg^{2+} content, although Mg^{2+} content of independently isolated *alr1 alr2* mutants varied somewhat (data not shown) and thus this effect is probably not significant. Somewhat surprisingly, overexpression of *Mnr2* did not restore a "WT" level of Mg^{2+} content. However, it is clear that the overexpression of *Mnr2* allowed the *alr1 alr2* strain to accumulate Mg^{2+} at a faster rate than the control strain, because *Mnr2* overexpression allowed much more rapid growth without a consequent decrease in Mg^{2+} content. In order for the *Mnr2* overexpressing strain to grow more quickly than the mutant, while retaining the same Mg^{2+} content, the *Mnr2* overexpressing strain must have obtained Mg^{2+} more efficiently from the environment. In summary, these observations provide strong evidence that the *Mnr2* protein represents an ion channel or transport system that can independently mediate Mg^{2+} transport. Additional discussion on the effect of *Mnr2* overexpression on its activity in the vacuolar membrane, and in turn on the vacuolar Mg^{2+} concentration is included in the summary section (**Ch. 3.13.6**).

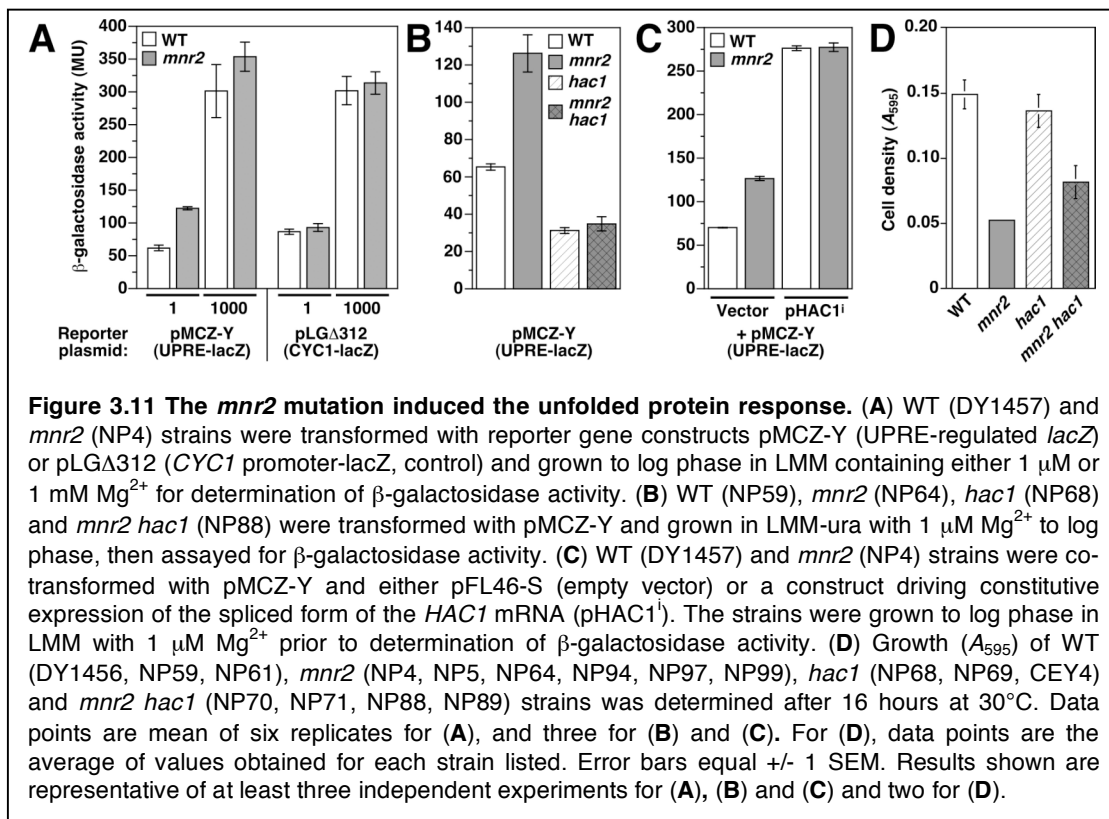
3.12 Effect of the *mnr2* mutation on ER function

My cell fractionation studies (**Figure 3.6**) suggested that a small proportion of *Mnr2* might be present in the secretory pathway. While as previously noted, this observation may be an artifact of the cell fractionation technique, it may also indicate that some of the *Mnr2* protein is resident in these compartments, or is in the process of transport to the vacuolar membrane after synthesis in the ER. If *Mnr2* is required for Mg^{2+} homeostasis within these organelles, the *mnr2* mutation might be deleterious to the function of the secretory pathway.

A commonly used method to determine the health of this compartment is to monitor the activity of the "Unfolded Protein Response" (UPR). The UPR is the induction of a number of coordinately regulated genes in response to a defect in ER function (the signal for which is thought to be the accumulation of unfolded proteins in the ER lumen). The response system consists of two proteins, an ER-localized transmembrane sensor (*Ire1*) and a transcriptional activator (*Hac1*) [reviewed in (Patil & Walter, 2001)]. When secretory pathway function is compromised, unfolded ER proteins activate the endoribonuclease activity of *Ire1*, which then cleaves an intron from the

HAC1 pre-mRNA. The spliced *HAC1* mRNA is translated into a protein (Hac1ⁱ), which functions as a transcriptional activator of UPR target genes (Cox & Walter, 1996; Ellis et al, 2004). The activity of Hac1ⁱ can be measured by using a *lacZ* reporter gene containing UPR-responsive elements in the promoter.

To determine if the *mnr2* mutation induced the UPR, WT and *mnr2* strains were transformed with a UPRE-*lacZ* reporter (Kawahara et al, 1997), and a *CYC1* promoter-*lacZ* reporter (Guarente et al, 1984) as a UPR-insensitive negative control. Strains were grown in LMM containing high (1 μ M) and low (1 mM) Mg²⁺ and β -galactosidase (β -



gal) activity was measured (Figure 3.11A). In both WT and *mnr2* strains, activity of both reporters was significantly reduced in low-Mg²⁺ conditions. I have observed a similar effect of low Mg²⁺ supply on other *lacZ*-fusion constructs, indicating a general negative effect of severe Mg²⁺-deficiency on *lacZ* gene expression (data not shown). For this reason, I could not directly determine the effect of low Mg²⁺ on UPR activity. However, a consistently reproducible increase in reporter activity was seen in the *mnr2* strain under low-Mg²⁺ conditions. In contrast, the control reporter expressed similar levels of β -gal activity in WT and *mnr2* strains regardless of Mg²⁺ supply, indicating that

the increase in UPR reporter activity seen in *mnr2* is not a general effect of this mutation on *lacZ* gene expression.

Since induction of UPR reporter gene activity is an indirect measure of the UPR, I wanted to examine if the induction of the UPR reporter gene in the *mnr2* strain was dependent on a functional response pathway. To do this, I constructed an *mnr2 hac1* double mutant and determined the effect on UPR reporter activity after growth in LMM containing 1 μM Mg^{2+} (**Figure 3.11B**). The *hac1* mutation alone substantially reduced reporter activity, indicating the expected dependence of the system on Hac1 activity. The same low level of activity was observed in the double *mnr2 hac1* strain, indicating that the induction of reporter activity associated with the *mnr2* mutation was dependent on Hac1 activity and the intact UPR signaling pathway.

As a second control, I also examined if the *mnr2* mutation elevated reporter activity by hyperactivating the Hac1ⁱ protein independent of the state of the ER. WT and *mnr2* strains were transformed with a low copy construct containing a version of the *HAC1* gene lacking the intron (pHAC1ⁱ) (Boutry et al, 1989). This construct drives constitutive expression of Hac1ⁱ independent of Ire1 activity. If *mnr2* did affect the activation of Hac1ⁱ independent of Ire1 activity, I expected to see a similar increase in *lacZ* activity in the *mnr2* strain expressing the intron-less pHAC1ⁱ. As expected of strains constitutively expressing Hac1ⁱ, higher reporter activity was observed (**Figure 3.11C**). However, there was no difference in the reporter activity of both WT and *mnr2* strains. This result indicates that *mnr2* does not increase the activity of Hac1ⁱ independent of the Ire1 protein.

Since some strains with severe UPR defects are dependent on the activation of the UPR for growth, I also determined if combining the *hac1* and *mnr2* mutations resulted in a synthetic lethal growth phenotype under Mg^{2+} deficient conditions (where the induction of the UPR was most obvious). Single and double mutant strains were grown in LMM containing 1 μM Mg^{2+} and cell density was recorded after 16 hours of growth. **Figure 3.11E** shows that the *hac1 mnr2* double mutation slightly increased growth compared to *mnr2* alone, indicating that *mnr2* mutants are not dependent on the UPR for growth. This observation is consistent with the small increase in UPR reporter activity seen in *mnr2*, which suggested that this mutation has a relatively mild effect on

secretory pathway function. Nevertheless, these results suggest that in addition to its major role in regulating vacuolar Mg^{2+} storage, Mnr2 is involved in maintaining the function of the ER and secretory pathway under Mg^{2+} -deficient conditions. The contribution of Mnr2 to the maintenance of ER function in Mg^{2+} deficient conditions is further discussed in **Ch. 3.13.8**.

3.13 Summary and discussion

The purpose of this study was to characterize the fifth CorA homolog in the yeast genome, Mnr2, and to understand the role that Mnr2 plays in Mg^{2+} homeostasis. The results reported in this chapter suggest a revised model for Mg^{2+} homeostasis in yeast (**Figure 3.12**). The model suggests that under Mg^{2+} replete conditions, yeast vacuoles function as a storage site for excess Mg^{2+} , and that the Mnr2 protein aids growth in Mg^{2+} -deficient conditions by releasing Mg^{2+} from the vacuole to buffer against cytoplasmic Mg^{2+} deficiency. The evidence supporting this model is discussed below.

3.13.1 The vacuole as a site for storage of excess Mg^{2+}

My work indicates that the vacuole may play a role in the intracellular storage of excess Mg^{2+} ions. Consistent with this model, a recent study showed that the vacuolar Mg^{2+} concentration in Mg^{2+} -replete yeast cells is approximately four-fold higher than the cytoplasmic concentration (Simm et al, 2007). My observations of the effect of the *tfp1* mutation on yeast Mg^{2+} content, and the interaction of the *mnr2* and *tfp1* mutations, are also consistent with a role for the vacuole in Mg^{2+} storage. Transport of Mg^{2+} into the vacuole would require energy input to overcome the charge gradient generated by V-ATPase activity. Although the transporter responsible has not been identified, several lines of evidence suggest that this system is a proton-coupled exchanger. First, mutations that eliminate vacuolar proton-ATPase activity confer Mg^{2+} sensitivity (e.g. *tfp1*, data not shown), as do those that induce defects in vacuole function or morphology (e.g. *vps1*, R. Gardner, personal communication). In addition, mutations inactivating V-ATPase activity substantially reduced Mg^{2+} accumulation [**Figure 3.8A** and (Eide et al, 2005)]. Finally, several studies have identified possible Mg^{2+}/H^+ antiport activities in the vacuole membrane, with apparent K_m values ranging from 0.3 to 1 mM Mg^{2+} (Borrelly et al, 2001; Nishimura et al, 1998; Okorokov et al, 1985). However, it should be noted that the

tfp1 mutant phenotype of reduced Mg^{2+} content may not represent a direct effect of a reduction in Mg^{2+}/H^+ exchanger activity; this phenotype could result from the inhibition of other processes important to Mg^{2+} accumulation in this compartment, such as phosphate storage (Beeler et al, 1997). It is also possible that the *tfp1* mutation prevents the Mg^{2+}/H^+ exchanger from reaching or being correctly assembled in the vacuole membrane. Whatever the mechanism responsible for this effect, these data implicate the

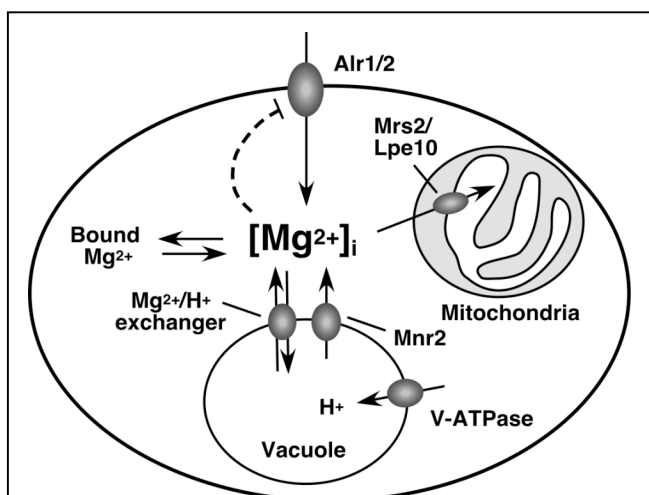


Figure 3.12 Model for Mnr2 function in yeast. The location and function of previously characterized Mg^{2+} transporters and the Mnr2 protein is shown. The Alr proteins regulate the flow of Mg^{2+} into the cell from the external environment, maintaining the concentration of an essential pool of Mg^{2+} within this compartment. Free ionized Mg^{2+} ($[Mg^{2+}]_i$) is in equilibrium with Mg^{2+} bound to proteins and small molecules. Under replete conditions, excess Mg^{2+} entering the cell is diverted into the vacuole, via the activity of an exchanger driven by the vacuolar proton concentration gradient (generated by the V-ATPase). The Mnr2 protein is located at the vacuole membrane, where it regulates the flow of Mg^{2+} from the vacuole lumen to the cytosol. Under deficient conditions, vacuolar stores are allowed to flow back into the cytosolic compartment to buffer the concentration of free ionized Mg^{2+} . Under Mg^{2+} -replete conditions, the bulk of cellular Mg^{2+} is contained within the vacuole.

vacuole in Mg^{2+} storage. In contrast, mutations that prevent mitochondrial Mg^{2+} uptake had no effect on the ability of yeast cells to accumulate intracellular stores of Mg^{2+} , as indicated by the high Mg^{2+} content of these mutants in replete conditions, and subsequent robust growth in Mg^{2+} -free medium (Figure 3.8A and B).

3.13.2 Vacuolar stores of Mg^{2+} can be utilized to offset cytosolic Mg^{2+} deficiency

Previous work (Beeler et al, 1997) as well as data reported here (Figure 3.4) show that the initial Mg^{2+} content of yeast cells affects the rate of growth upon transfer to

Mg^{2+} -free medium, and that Mg^{2+} content rapidly decreases under these conditions. Because approximately 80% of Mg^{2+} in replete cells is vacuolar (Simm et al, 2007), these observations suggest that vacuolar Mg^{2+} can be redistributed to critical cellular compartments to maintain homeostasis. The severe growth defect displayed by *tfp1* cells when transferred to Mg^{2+} -deficient conditions (Figure 3.8B), provides support for this

view.

3.13.3 Mnr2 is required for the release of vacuolar Mg²⁺ stores

Several lines of evidence indicate that Mnr2 is required for the release of vacuolar Mg²⁺ (and more generally, for the regulation of vacuolar Mg²⁺ content). First, *mnr2* mutant strains accumulated more Mg²⁺ than WT during growth in replete conditions (**Figure 3.4**), but this increased content did not translate into improved growth under deficient conditions. Second, genetic interaction studies support the idea that the Mnr2 and Alr proteins both contribute to the maintenance of cytosolic Mg²⁺ concentration. When combined with *alr1*, the *mnr2* mutation conferred a synthetic slow growth phenotype, consistent with both mutations reducing the supply of Mg²⁺ to an essential compartment (most likely the cytosol). The opposite effect of *mnr2* and *alr1/alr2* mutations on Mg²⁺ content, and the location of Mnr2 protein in the vacuolar membrane, is consistent with the model that Mnr2 supplies the cytosol with Mg²⁺ from vacuolar stores, rather than from the external environment. Lastly, the observation that the *tfp1* mutation suppressed the *mnr2* mutant phenotype of high Mg²⁺ content is consistent with this phenotype being due to misregulation of vacuolar Mg²⁺ storage. If the *tfp1* mutation prevents vacuolar Mg²⁺ storage by inhibiting the Mg²⁺ uptake system, the Mnr2 protein would be superfluous.

3.13.4 Mnr2 is directly responsible for Mg²⁺ transport

The direct function of Mnr2 in Mg²⁺ transport is supported by my observation that the redirection of this protein to the plasma membrane effectively suppressed the growth defect of an *alr1 alr2* mutant (**Figure 3.10B-D**), indicating that Mnr2 could substitute for the function of the missing Alr proteins. The increased growth conferred by Mnr2 overexpression had no effect on Mg²⁺ content of the mutant, indicating that it was supported by increased access to external sources of Mg²⁺. The observation that Mnr2 can substitute for the Alr proteins also indicates that Mnr2 does not indirectly affect yeast physiology via the regulation of the activity or expression of the Alr proteins. This is an important point because several examples of regulatory factors orthologous to nutrient transporters have been described in yeast [*e.g.*, Snf3, a plasma membrane glucose sensor, (Forsberg et al, 2001)]. Lastly, in both Mg²⁺-replete and deficient cells, cit-Mnr2 was

detected in the vacuole membrane (**Figure 3.7**), suggesting that it is present in the correct location under the appropriate conditions to regulate the Mg^{2+} content of this organelle.

3.13.5 Cation transport by *mnr2* mutants

Elemental profiling of the *mnr2* strain indicated that under Mg^{2+} -deficient conditions, this strain accumulated a higher content of some divalent cations, including Mn^{2+} , Ca^{2+} and Zn^{2+} (**Figure 3.2**). In addition, sensitivity to the divalent cations Ca^{2+} , Mn^{2+} , Co^{2+} and Zn^{2+} was also increased (**Figure 3.1**). Together, these observations suggested that the *mnr2* mutation resulted in an elevated activity of the cell surface transporters for these metals. Under conditions of cation excess, an increased rate of accumulation via these systems might cause increased sensitivity. This model raises the question of why the *mnr2* mutation has this effect on cation uptake.

Several explanations could be proposed. First, it is possible that the *mnr2* mutation increased the expression of high affinity transport systems that are specific for all these divalent cations. A second model is that the Mnr2 protein itself is responsible for homeostasis of some of these cations (in addition to Mg^{2+}), and that an increase in cation accumulation occurs for the same reason as Mg^{2+} accumulation (the cations are trapped in the vacuole compartment). This explanation seems possible given that CorA family proteins have the ability to transport other divalent cations with low affinity (e.g. Co^{2+}) (Hmiel et al, 1986; Payandeh & Pai, 2006; Snavely et al, 1989a). A third model is that the *mnr2* mutation increases the expression or activity of systems involved in Mg^{2+} homeostasis, indirectly leading to an increase in the activity of a relatively non-specific low affinity cation uptake system.

Looking at these models in turn, I prefer model 3, for the following reasons. Model 1 seems implausible, given the multiple complex systems in place to regulate the activity of high affinity cation uptake systems for such potentially toxic cations as Mn^{2+} and Zn^{2+} . The expression or activity of these systems would have to be coordinated by the inactivation of a single gene. At least one of these systems in particular is dependent on a single well-characterized factor (e.g., Zap1 for zinc regulation) (Zhao et al, 1998; Zhao & Eide, 1997), and there seems to be no clear mechanism by which Mnr2 could have a global affect on the function of all of these disparate systems.

Model 2 (trapping of cations in the vacuole) does not easily explain both phenotypes (high cation content and associated sensitivity), since a block in the release of divalent cations from the vacuole is not likely to increase sensitivity to those cations. In fact, the opposite effect might be expected since increased trapping of cations in the vacuole would be expected to decrease their concentration in the cytosol, thus increasing resistance. In addition, there are other systems known to release divalent cations from the vacuole. For example, Zn^{2+} storage is regulated by Zrt3 (MacDiarmid et al, 2000), while Mn^{2+} storage is regulated by Smf2 (Culotta et al, 2005). Expression of both these proteins is upregulated by a deficiency of their respective substrates. In this context, any effect of the Mnr2 transporter on storage of these metals would be expected to be minor. However, I cannot rule out some contribution of this effect to the elevated cation content of the mutant strain.

The last model (that the *mnr2* mutation increases the activity of a non-specific cation uptake system) seems the most plausible. Although homeostasis of Mg^{2+} is not well understood compared to that of other nutrient metals, it has been reported that the expression of the Alr1 protein is regulated by Mg^{2+} availability. Both transcriptional and post-translational mechanisms were proposed to explain this regulation (Graschopf et al, 2001). Other systems regulating the expression of cation transporters are generally coupled to the cytosolic cation concentration, for example via the activity of cation-sensing transcriptional regulators like the Zap1 protein (Lyons et al, 2000; Zhao & Eide, 1997). If this is also the case for Alr1, then a reduction in the cytosolic Mg^{2+} concentration might be expected to increase the accumulation of this protein at the cell surface. If my proposed model for Mnr2 function that it serves as vacuolar Mg^{2+} efflux transporter is correct, it appears likely that the *mnr2* mutation reduces cytosolic Mg^{2+} availability (an idea which is supported by the observation that the *mnr2* mutation enhanced the growth defect associated with the *alr1* mutation). As a consequence of this perceived Mg^{2+} deficiency, *mnr2* mutant cells may up-regulate the expression of Alr1 to compensate. A previous study showed that the overexpression of Alr increased the rate of Co^{2+} uptake and induced a strong sensitivity to this cation, as well as several other divalent cations (including Ca^{2+} , Mn^{2+} and Zn^{2+}) (MacDiarmid & Gardner, 1998). The effect of increased Alr1 expression on cation homeostasis is consistent with my

observations (**Figure 3.1** and **3.2**). In addition, it is important to note that reducing Mg^{2+} availability enhanced the effect of the *mnr2* mutation on cation content. This effect could have two possible explanations: first, due to the absence of competitive inhibition by Mg^{2+} , a low Mg^{2+} concentration may promote the uptake of other cations by the Alr1 protein; second, the cellular Mg^{2+} -deficiency induced by growth in low Mg^{2+} medium may stimulate an increase in Alr1 activity, further enhancing uptake of other divalent cations. Although not much is known about the specific regulation of Alr1 activity, the activity of other CorA proteins (such as Mrs2) is reportedly regulated by cytosolic Mg^{2+} availability (Romani et al, 1991; Romani & Scarpa, 2000; Schindl et al, 2007). In Chapter 4, I describe the results of my experiments designed to test some of these predictions (for example, the effect of the *mnr2* mutation on Alr1 expression).

3.13.6 Mg^{2+} storage is not restored by the overexpression of Mnr2

The observation that an *alr1 alr2* mutant overexpressing Mnr2 could grow rapidly under normally non-permissive conditions, while still retaining the same Mg^{2+} content as the corresponding mutant strain, indicates that Mnr2 overexpression increased the rate at which the mutant could obtain Mg^{2+} from the environment. However, Mnr2 overexpression did not restore the Mg^{2+} content of the mutant to the level of a WT strain grown under replete conditions, suggesting that Mnr2 overexpression did not fully substitute for the loss of the Alr proteins. There are at least two possible explanations for this observation.

First, my experiments (**Figure 3.3B**) as well as previous work (Beeler et al, 1997) indicate that in replete cells, 50-80% of total cellular Mg^{2+} is not required for growth. Consistent with this idea, I observed that *tfp1* mutants cultured in Mg^{2+} -replete or deficient conditions accumulated approximately the same Mg^{2+} content as WT strains grown under severely deficient conditions (approximately 20 nmol/ 10^6 cells), indicating that this value probably represents the minimum Mg^{2+} content required for viability. In *alr1 alr2* strains overexpressing Mnr2, the rate of Mg^{2+} influx may be sufficient to supply this minimal requirement and support growth, but not sufficient for the cell to refill intracellular stores. In this regard, it is important to note that Mnr2 overexpression did not completely suppress the growth defect of the *alr1 alr2* strain (**Figure 3.10C**). Second, in

addition to causing mislocalization of Mnr2, overexpression of this protein substantially increased its accumulation in the vacuole membrane (**Figure 3.10D**). If Mnr2 is responsible for the efflux of Mg^{2+} from the vacuole, the resulting increase in activity may counteract the storage of Mg^{2+} in this compartment. Thus, there are at least two valid reasons why Mnr2 overexpression might return the cytosolic Mg^{2+} concentration to a near-normal level and restore a near-normal growth rate, but not allow significant refilling of vacuolar stores. Interestingly, the expression of some plant Mg^{2+} transporters (e.g. AtMrs2-1) in yeast *alr1 alr2* mutants was reported to facilitate growth without significantly altering Mg^{2+} content (da Costa et al, 2007), indicating that this effect is not unique to Mnr2.

3.13.7 Role of Alr2 in Mg^{2+} homeostasis

My work also provides some new insights into the role of the Alr2 transporter. Alr2 function is somewhat controversial; its apparently minor contribution to homeostasis (da Costa et al, 2007; Gräschopf et al, 2001; MacDiarmid & Gardner, 1998; Wachek et al, 2006) has been attributed to lower expression (MacDiarmid & Gardner, 1998) or to a mutation that reduces its activity compared to Alr1 (Wachek et al, 2006). This work demonstrates that Alr2 does contribute to homeostasis independent of Alr1, at least in the W303 genetic background (**Figure 3.9B**). Deletion of *ALR2* alone significantly reduced Mg^{2+} accumulation, but did not affect growth. The effect of the *ALR2* deletion on Mg^{2+} content was consistently observed in several independently isolated mutant strains, indicating that it was reproducible. One possible explanation for this phenotype is that in cells grown under replete conditions, Alr2 promotes the influx of Mg^{2+} in excess of normal cellular requirements. This could be simply due to the contribution to total Alr protein activity provided by this gene, or it could reflect a specific effect of the Alr2 protein on the activity of heteromeric complexes formed with Alr1 (Wachek et al, 2006). Whatever the mechanism, if the Alr2 protein has this effect, then the *alr2* mutation would prevent the cell from completely filling intracellular stores. In contrast, the *alr1* deletion had a larger effect on Mg^{2+} content, and conferred a strong growth defect, suggesting that Alr1 is essential for the routine maintenance of the cytosolic Mg^{2+} concentration.

3.13.8 Mnr2 may be required for the maintenance of ER function in Mg²⁺-deficient conditions

In addition to its role in the release of vacuolar Mg²⁺ stores, I obtained evidence suggesting that Mnr2 may also be required for the function of other endomembrane compartments. This experiment was suggested by the observation that a fraction of the Mnr2 protein may not be associated with the vacuole membrane (**Figure 3.6**). A portion of Mnr2 co-fractionated with markers for the late endosome, ER and mitochondrial compartments in density gradients, suggesting it could not be assigned unequivocally to any of these compartments. However, I did not observe any obvious alternative location for cit-Mnr2 in cells examined with fluorescence microscopy (**Figure 3.7**). For these reasons, the exact location of this fraction of the protein could not be determined, and it remains possible that it simply represents an artifact of the cell fractionation technique. However, given that Mnr2 would still be expected to transit through the ER and secretory pathway on its way to the vacuole, I decided to investigate the effect of the *mnr2* mutation on secretory pathway function. I observed that the *mnr2* mutation increased the activity of a UPR-regulated *lacZ* reporter gene in Mg²⁺-deficient conditions (**Figure 3.11A**), suggesting that Mnr2 is important for ER function. Although little is known about the role of Mg²⁺ ions in the ER compartment, there is good reason to believe that Mg²⁺ may be required for ER function. The lumen of the ER is a site where newly synthesized proteins are folded and modified, and some of the enzymes essential for these processes are Mg²⁺-dependent. Two examples are the yeast ER-localized protein chaperones Kar2 and Lhs1 (Steel et al, 2004). Kar2 is required for the process of ER-associated protein degradation (ERAD), which exports misfolded proteins from the ER lumen (Nishikawa et al, 2001), while Lhs1 plays a role in refolding denatured luminal proteins (Hamilton et al, 1999; Hanninen et al, 1999). Both Kar2 and Lhs1 require Mg²⁺ to enable the ATP hydrolysis essential for refolding their substrates (Hamilton et al, 1999; Tokunaga et al, 1992).

In light of this information, I suggest two models that may explain the apparent ER defect associated with *mnr2* mutation. First, Mnr2 may play a direct role in regulating the Mg²⁺ content of the ER lumen, perhaps by supplying Mg²⁺ to this compartment. Since

Mnr2 is likely to represent a channel, the direction of Mg^{2+} flow through this system would be dependent in part on Mg^{2+} concentration, and under appropriate conditions, the opening of the channel may equalize the concentration between the cytosol and the lumen of the ER. In support of this model, we note that the highest induction of the UPR reporter was observed under severely Mg^{2+} -deficient conditions (under which the supply of Mg^{2+} to the ER and secretory pathway compartments may be more critical).

Second, it is possible that the apparent cytosolic Mg^{2+} deficiency associated with the *mnr2* mutation (as a consequence of a block in the release of Mg^{2+} stores) could indirectly inhibit the function of the secretory pathway, by decreasing the supply of Mg^{2+} to the ER. Since defects in components of the ERAD pathway have been shown to induce the UPR (Travers et al, 2000), the inhibition of Kar2 function in the *mnr2* mutant might explain the induction that we observed. However, we note that in WT yeast, microarray experiments did not reveal the induction of known UPR target genes by Mg^{2+} deficiency, (Wiesenberger et al, 2007) suggesting that Mnr2 may play a more specific role in the maintenance of ER function. A definitive test of these models will require the development of reliable methods to measure the Mg^{2+} concentration of both cytosolic and secretory pathway compartments in yeast.

Chapter 4 Effect of intracellular Mg²⁺ storage on Alr1 regulation and modification

4.1 Introduction

In **Ch. 3.5**, I described evidence suggesting that the Mnr2 protein regulates intracellular Mg²⁺ stores by releasing Mg²⁺ from the vacuole under Mg²⁺-deficient conditions. One of the phenotypes of the *mnr2* mutant strain was sensitivity to divalent cations such as Ca²⁺, Mn²⁺, Zn²⁺, and Co²⁺ (**Figure 3.1**). An examination of the elemental content of WT and *mnr2* mutant strains revealed an increase in the content of Ca²⁺, Mn²⁺, and Zn²⁺, most notably under Mg²⁺ deficient conditions (**Figure 3.2**). To explain the above two observations, I suggested that the *mnr2* mutation causes an increase in the expression or activity of a non-specific divalent cation transport system in the plasma membrane (**Ch. 3.13.5**).

Alr1, like other members of CorA family proteins, has been reported to mediate low affinity transport of various divalent cations (e.g. Co²⁺) (MacDiarmid & Gardner, 1998; Maguire, 2006) making this protein a potential candidate for the induced non-specific divalent cation transport system. Additional support for this model comes from a previous study (Graschopf et al, 2001) reporting that Alr1 expression is regulated by Mg²⁺ availability. The level of Alr1 protein in WT cells was induced under Mg²⁺ deficient conditions, and upon exposure to higher Mg²⁺ concentrations, the Alr1 protein underwent rapid degradation. Since the *mnr2* mutation may deplete the cytosolic Mg²⁺ concentration, I suspected that Alr1 expression might be induced to a higher level in this mutant. This change might in turn have resulted in a higher rate of accumulation of other divalent cations via the Alr1 protein.

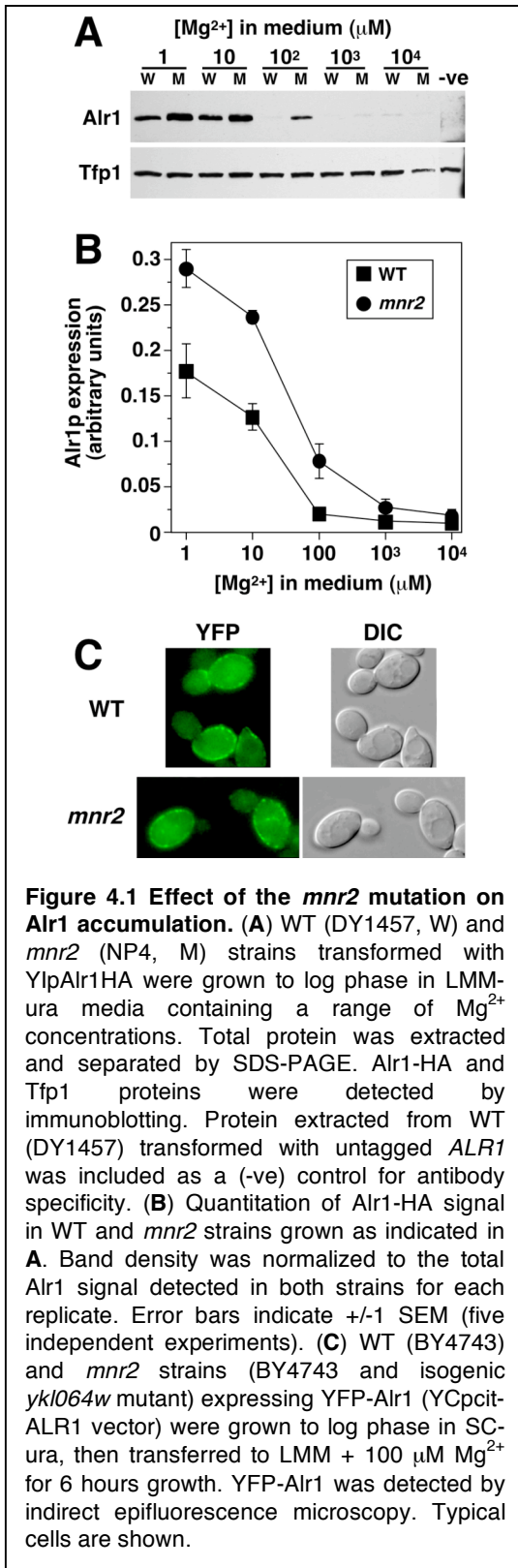
In this chapter, I describe experiments performed to understand the effect of the *mnr2* mutation on Alr1 expression and activity, and by extension on cytoplasmic Mg²⁺ homeostasis.

4.2 Effect of Mg²⁺ supply and the *mnr2* mutation on Alr1 protein accumulation

To determine if the *mnr2* mutation increased Alr1 accumulation, WT and *mnr2*

strains expressing an epitope-tagged Alr1 protein (Graschopf et al, 2001) were grown in LMM containing a range of Mg^{2+} concentrations. Protein was extracted from the cells, separated with SDS-PAGE, and subjected to immunoblotting to detect epitope-tagged Alr1. As previously observed (Graschopf et al, 2001), my experiments showed that in WT yeast, Alr1 protein levels were elevated after growth in Mg^{2+} deficient conditions ($< 100 \mu M Mg^{2+}$) (Figure 4.1A). I also observed that Alr1 accumulation was significantly elevated in the *mnr2* strain. The difference in Alr1 accumulation was most obvious under moderately deficient conditions, but was observed to some extent at all Mg^{2+} concentrations tested. This observation supports the hypothesis that the *mnr2* mutation causes the cell to sense a change in Mg^{2+} availability, via mechanisms that regulate *ALR1* gene expression or protein accumulation.

The observation that Alr1 protein accumulation was increased as a consequence of the *mnr2* mutation is consistent with the model proposed to explain the increased divalent cation content of this mutant. However, it was not clear whether the additional Alr1 protein was located at the plasma membrane, or if it was accumulated in some other location. To



verify the location of Alr1 in the *mnr2* strain, I determined the location of a version of the Alr1 protein tagged with YFP (citrine) on the N-terminus (**Ch. 2.5.1**). This N-terminally tagged version of Alr1 is fully functional (Abhinav Pandey, unpublished data) and its expression is usually regulated from the native *ALR1* promoter. As previously reported (Graschopf et al, 2001), when expressed in a WT strain, YFP-Alr1 signal was predominantly detected as a punctate signal at the plasma membrane, with a smaller amount of punctate intracellular signal observed in a minority of cells. In the *mnr2* mutant expressing YFP-Alr1, the distribution of signal was not significantly altered (**Figure 4.1C**). In control cells without the tagged *ALR1* construct, only a weak diffuse cytosolic background signal was observed (data not shown). Since these observations were made using cells grown in LMM with 100 μM Mg^{2+} , any difference in location associated with the difference in Alr1 expression should have been readily visible. The normal (plasma membrane) distribution of Alr1 in the *mnr2* strain also demonstrated that the growth defect associated with this mutation in Mg^{2+} -deficient conditions (**Figure 3.3A**) could not be attributed simply to Alr1 mislocalization and a consequent reduction in Mg^{2+} uptake.

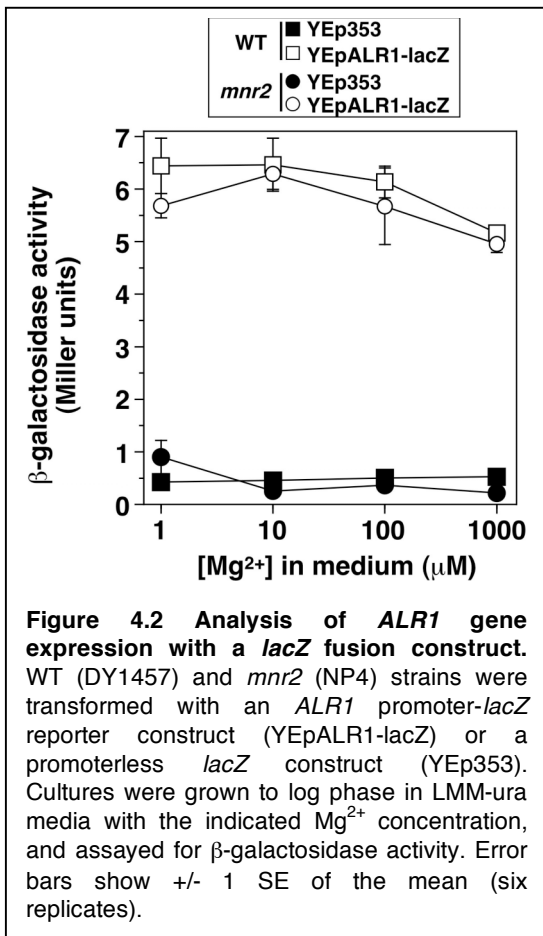
Together, these observations are consistent with the explanation for the increased divalent cation content of *mnr2* mutants proposed above, specifically the increased expression of the Alr1 low-affinity divalent cation uptake system. This increased Alr1 expression may also explain the divalent cation sensitivity of *mnr2* mutants (**Figure 3.1**). Although cation sensitivity was assayed under Mg^{2+} -replete conditions, where Alr1 expression was relatively low, an increase in Alr1 expression in the *mnr2* strain was still observed under replete conditions (100 μM -10 mM Mg^{2+} , **Figure 4.1B**). In addition, the elevated cation content of the *mnr2* strain was significantly enhanced under conditions of severe Mg^{2+} -deficiency (**Figure 3.2** and **Figure 3.3B**), where an increase in Alr1 expression was clearly observed (**Figure 4.1A**).

4.3 Mechanism of Alr1 regulation

Since the *mnr2* mutation affected Alr1 expression, I wanted to understand how this effect occurred. For this reason, it was necessary to study the mechanism by which Alr1 is regulated in response to Mg^{2+} supply. In doing so, I also hoped to develop tools to

investigate the physiological role of Mnr2 in more detail.

The expression of many yeast metal transporters (e.g. Zn^{2+} transporters) has been linked to the intracellular content of the corresponding metal ion (Eide et al, 2005). This regulation prevents deficiency of essential metal ions, while limiting their overaccumulation in replete conditions. Transporter regulation is often mediated at several levels, with both transcriptional and post-translational components (Eide, 2006; Gaither & Eide, 2000). In most cases, these systems respond to the intracellular



concentration of the metal ion (rather than the external supply). For example, the Zap1 protein, a transcriptional activator, senses the availability of Zn^{2+} within the cytosol and mediates transcriptional regulation of the zinc transporter, Zrt1. Zap1 mediates its effect on Zrt1 gene expression by binding to recognition sites in the promoters of the *ZRT1* and other Zn^{2+} -regulated genes (Lyons et al, 2000). This transporter and other examples suggested that transcriptional control might be important for Alr1 regulation.

In a previous study, the authors reported an increase in *ALR1* mRNA under deficient conditions, based on RT-PCR quantification of *ALR1* transcript levels (Graschopf et al, 2001). However, when

others in this laboratory attempted to replicate these results using the more direct technique of mRNA extraction and Northern blotting, no consistent regulation of the *ALR1* transcript level was observed (Aandahl Achari and Colin MacDiarmid, unpublished data). These observations were made using the same strain described in the original report (FY1679, which is derived from the S288C genetic background), as well as when using the DY1457 strain (which is derived from the W303 genetic background)

(Aandahl Achari, unpublished data). These results cast doubt on the earlier report of *ALRI* transcriptional regulation in response to Mg^{2+} supply.

To further investigate *ALRI* transcription using an independent approach, I generated a construct containing the entire *ALRI* promoter region fused to the *lacZ* reporter gene (**Ch. 2.6**). This construct was introduced into WT and *mnr2* strains, which were then grown in media supplied with a range of Mg^{2+} concentrations and assayed for β -gal activity. Two observations are evident from this data in **Figure 4.2**. First, consistent with the results of the Northern analysis, there was no significant increase in reporter activity under deficient conditions, confirming that *ALRI* promoter activity is not responsive to Mg^{2+} supply. Second, there was no major difference in β -gal activity between the WT and *mnr2* strains at any of the Mg^{2+} concentrations tested (**Figure 4.2**).

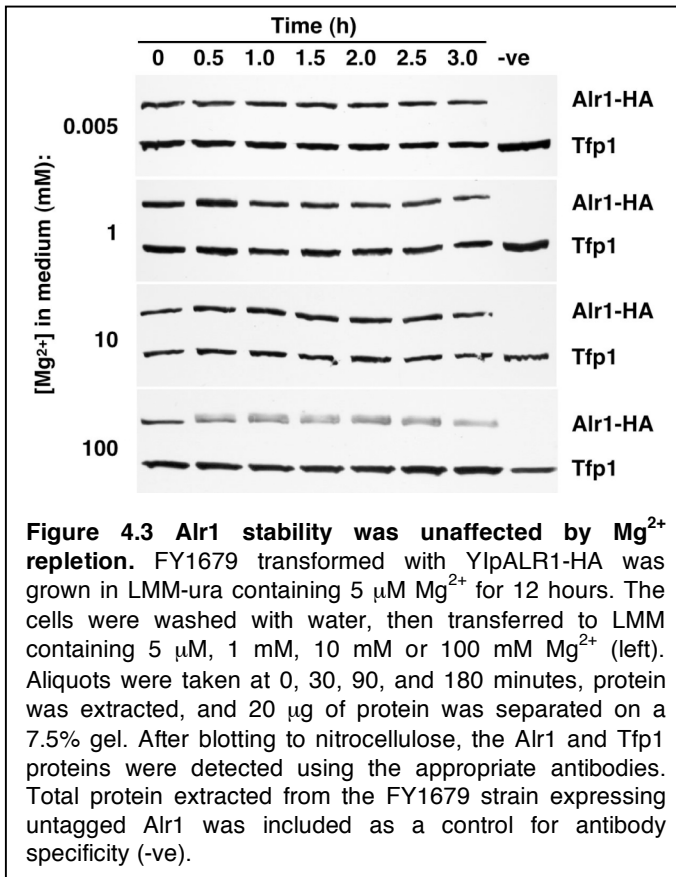
From these results it is possible to draw two conclusions. First, the elevated Alr1 protein accumulation under deficient conditions is not a consequence of an increase in *ALRI* gene expression. The increase in Alr1 protein might instead be achieved by an alternative mechanism, such as the post-translational control of protein stability, or the rate of Alr1 translation. Second, the increase in Alr1 accumulation seen in the *mnr2* mutant does not appear to be a consequence of an increase in *ALRI* gene expression. This increase may again result from a change in the efficiency of some downstream regulatory process, such as the regulation of Alr1 protein stability.

4.4 Effect of Mg^{2+} concentration on Alr1 stability

A previous report proposed that the accumulation of the Alr1 protein was post-translationally regulated by Mg^{2+} supply (Graschopf et al, 2001). They observed that in deficient cells exposed to high Mg^{2+} , Alr1 was rapidly degraded. This process was dependent both on endocytosis, and the activity of the Rsp5 ubiquitin ligase (degradation was inhibited in *end3* and *npi1* mutant strains). To duplicate these results, I obtained the yeast strain carrying the epitope-tagged Alr1 construct used in the study (FY1679 transformed with a construct for expression of the *ALRI* gene, fused to three repeats of the HA epitope at the C-terminal end). This strain was grown in LMM-ura medium containing 5 μ M Mg^{2+} for 12 hours to allow Alr1 expression, and the culture was then transferred to LMM-ura media containing different concentrations of Mg^{2+} (5 μ M and 1-

100 mM) (**Figure 4.3**). In contrast to the previous report, I observed no difference in Alr1 stability between cells transferred to replete (1-100 mM Mg^{2+}) and those transferred to fresh deficient medium (5 μM Mg^{2+}).

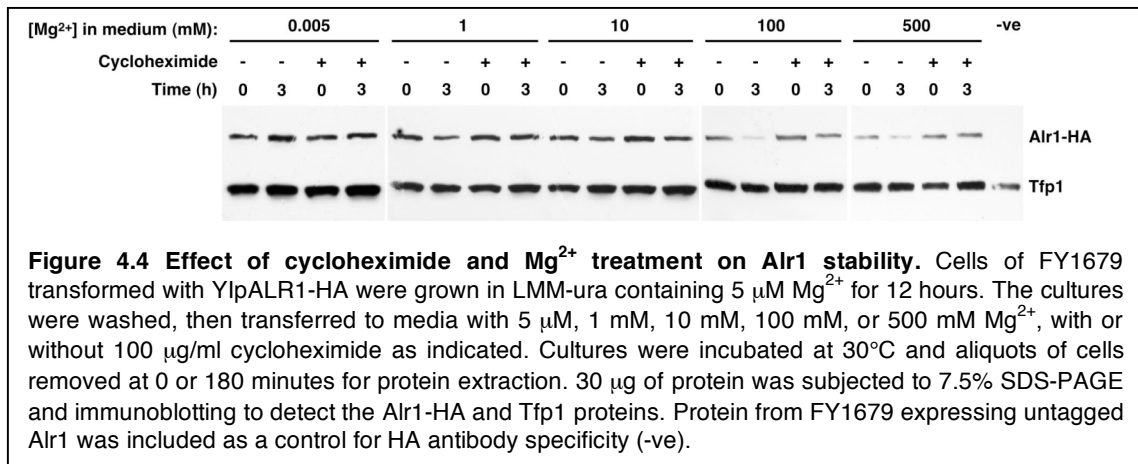
In the above experiments, I deviated from the published protocol (Graschopf et al, 2001) by omitting cycloheximide from the Mg^{2+} -replete medium. I believed that the rapid degradation previously reported upon exposure to Mg^{2+} would overwhelm the contribution of new Alr1 synthesis during this time, making the use of this antibiotic



unnecessary. However, the high stability of the Alr1 protein in my experiments suggested that new protein synthesis during the time course might have counteracted the effect of Mg^{2+} on Alr1 stability. To determine if this was the case, I added 100 $\mu g/ml$ cycloheximide to the Mg^{2+} -replete medium before transferring the cells. In this experiment (**Figure 4.4**), a three-hour exposure of deficient cells to Mg^{2+} concentrations up to 500 mM did not result in a reproducible decrease in the protein compared to controls. Although a small

decrease in the stability of the protein from the cells exposed to high Mg^{2+} concentrations (100 and 500 mM) in the absence of cycloheximide was observed in this individual experiment, the previous experiment (**Figure 4.3**) failed to show decrease in the protein stability in cells exposed to 100 mM Mg^{2+} concentration.

These results cast doubt on one published finding, that the stability of the existing pool of Alr1 in deficient cells is dependent on Mg^{2+} supply. In support of my findings, other workers in this laboratory have generated similar results (Aandahl Achari, Colin MacDiarmid, unpublished results), as has an independent laboratory (Richard Gardner, unpublished results). Others in this laboratory subsequently performed experiments to investigate the mechanism of Alr1 regulation and obtained results that were consistent with the stability of Alr1 observed here. The results of some of these experiments, and how they relate to an overall model of Alr1 regulation, are discussed in the summary section. However, in subsequent investigations, I decided to focus on other interactions of the *MNR2* and *ALR1* genes, as outlined below.



4.5 Post-translational modification of Alr1

During the above experiments, I noticed an interesting effect of Mg^{2+} on the Alr1 protein. On exposure of Mg^{2+} deficient cells to Mg^{2+} replete conditions, the single band of Alr1-HA protein seen in Western blot underwent rapid change to a form with slower mobility (**Figure 4.3**) (henceforth, the change in the mobility of the Alr1-HA protein is alternatively referred as "modification" in this report). The modification was most obvious when proteins were separated via SDS-PAGE gels containing a lower percentage of acrylamide (5%) than was normally used (7.5-10%). In the experiment shown, this effect was predominantly seen in the cells exposed to 100 mM Mg^{2+} (**Figure 4.3**), possibly due to an extended run time for this electrophoresis experiment (other

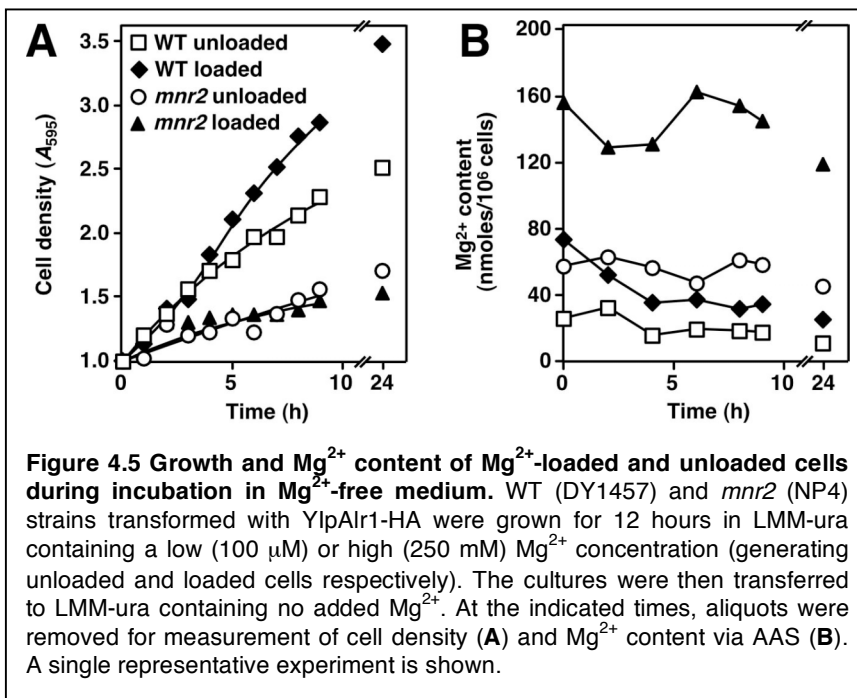
experiments indicated that as little as 1 mM Mg^{2+} could trigger this change). This change occurred within 30 minutes of exposure to Mg^{2+} , consistent with a previous study of Alr1 regulation (Graschopf et al, 2001). The change in Alr1 mobility suggests that the Alr1 protein is post-translationally modified on exposure to Mg^{2+} , for example by phosphorylation or ubiquitination. Many plasma membrane nutrient transporters (e.g. Zrt1) have been shown to undergo such modifications in response to elevated concentrations of their substrates (Gitan et al, 1998). However, the apparent stability of Alr1 suggests that this modification is not ubiquitination (since the addition of ubiquitin would be expected to trigger rapid degradation of the protein). A recent report attributed the change to phosphorylation, based on a reduction in the abundance of the lower mobility form after treatment with lambda protein phosphatase (Wachek et al, 2006). These observations suggested that the lower mobility form of Alr1 (with the higher apparent molecular weight) is the phosphorylated form.

Modification of Alr1 in response to Mg^{2+} could occur as a consequence of a change in conformation that exposes sites capable of being phosphorylated. The Mg^{2+} -binding sites visualized in the CorA structure are likely to be present in the Alr1 protein, since the residues responsible for interaction with Mg^{2+} in *T. maritima* CorA are tightly conserved in Alr1 (data not shown). I hypothesize that when cytosolic Mg^{2+} availability increases, the Alr1 protein can bind Mg^{2+} at these conserved sites. Occupancy of these sites may in turn change the conformation of the Alr1 complex, and trigger phosphorylation by an unidentified kinase. If this model is correct, the extent of Alr1 modification might provide an indirect measure of cytosolic Mg^{2+} availability. In addition, modification may contribute in part to the regulation of Alr1 activity. For this reason, I believed it was important to study the effect of *mnr2* mutation on this Mg^{2+} -dependent Alr1 modification.

I first examined the effect of decreasing the intracellular Mg^{2+} content on the rate at which the Alr1 protein was modified. I predicted that if Alr1 was modified in response to decreasing Mg^{2+} availability, a WT strain with a lower Mg^{2+} store would show a faster rate of Alr1 modification when compared to cells having higher internal stores. In addition, I predicted that (irrespective of their intracellular Mg^{2+} content), *mnr2* cells would display a faster rate of Alr1 modification than WT, because of the inaccessibility

of the intracellular Mg^{2+} store in this mutant.

To perform this experiment, WT and *mnr2* strains expressing epitope-tagged Alr1 were grown in LMM media containing either low (100 μ M) or high (250 mM) Mg^{2+} concentration for 12 hours. These treatments generated either Mg^{2+} -unloaded or loaded cells respectively. The 100 μ M concentration was chosen because this medium should significantly deplete Mg^{2+} stores while still allowing active growth. The cells were then transferred to a medium containing no Mg^{2+} to study the effect of depleting intracellular Mg^{2+} stores on the Alr1 protein. Aliquots of cells were taken to measure cell density and Mg^{2+} content during the experiment (**Figure 4.5A** and **B**). Directly after transfer to fresh



medium and at intervals thereafter, aliquots of the cells were removed and protein was extracted under denaturing conditions (to prevent any subsequent modification of the Alr1 protein *in vitro*). Alr1-HA and

control proteins were separated by SDS-PAGE and detected by Western blotting (**Figure 4.6**).

As expected, loading cells with Mg^{2+} generated a 2-fold difference in the Mg^{2+} content of WT cells at the start of the experiment (**Figure 4.5B**). WT loaded cells grew 30% more than unloaded cells over 24 hours, and depleted their intracellular Mg^{2+} content to \sim 50% of its starting value during this time. This observation is consistent with my previous experiments (**Figure 3.4A** and **B**) showing that Mg^{2+} -replete cells have excess Mg^{2+} content that can be used to support growth under deficient conditions. I concluded that the initial difference in Mg^{2+} stores between loaded and unloaded WT

cells was significant enough to produce variation in the Mg^{2+} concentration of the cytosol during their subsequent incubation in Mg^{2+} -free conditions.

As previously observed (**Figure 3.4A**), *mnr2* cells displayed a growth defect when transferred to deficient conditions (**Figure 4.5A**). Despite differences in their initial Mg^{2+} content, both loaded and unloaded *mnr2* cells showed the same slow rate of growth in Mg^{2+} -free medium. In addition, the Mg^{2+} content of both loaded and unloaded *mnr2*

cells did not decrease during growth, remaining similar to the starting values even after 24 hours of incubation. These observations are consistent with *mnr2* mutant lacking the ability to access intracellular Mg^{2+} stores to support growth.

In protein extracts of WT loaded and unloaded cells at the zero time point, two major bands of Alr1-HA were detected. Initially, the predominant band (**Figure 4.6A**, band 1) had a lower mobility, but over time, this low-mobility band was completely replaced by a higher-mobility band (**Figure**

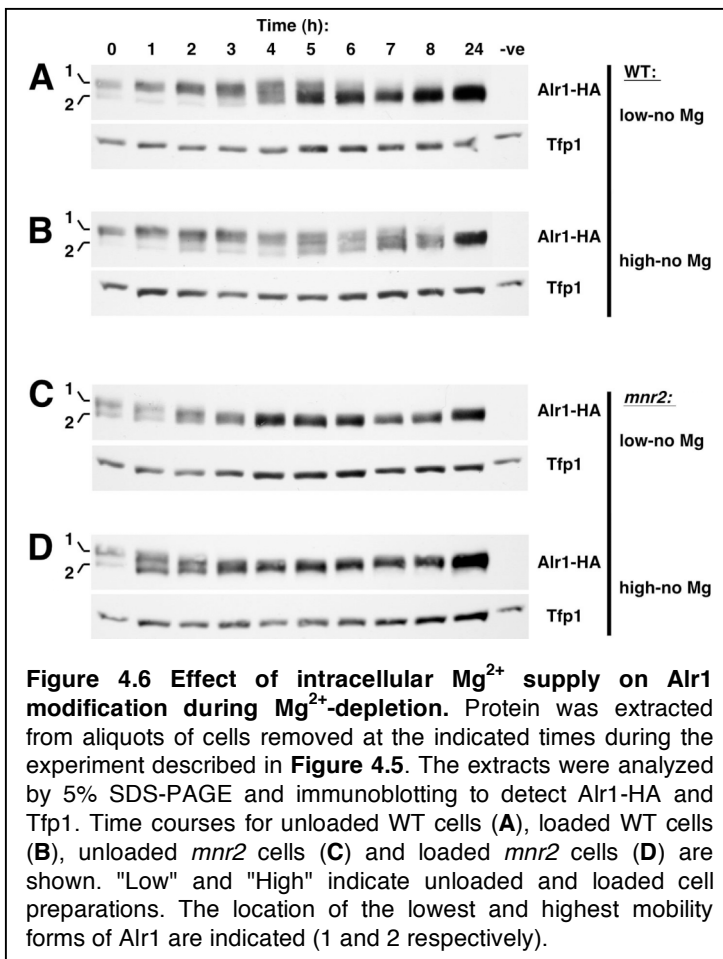
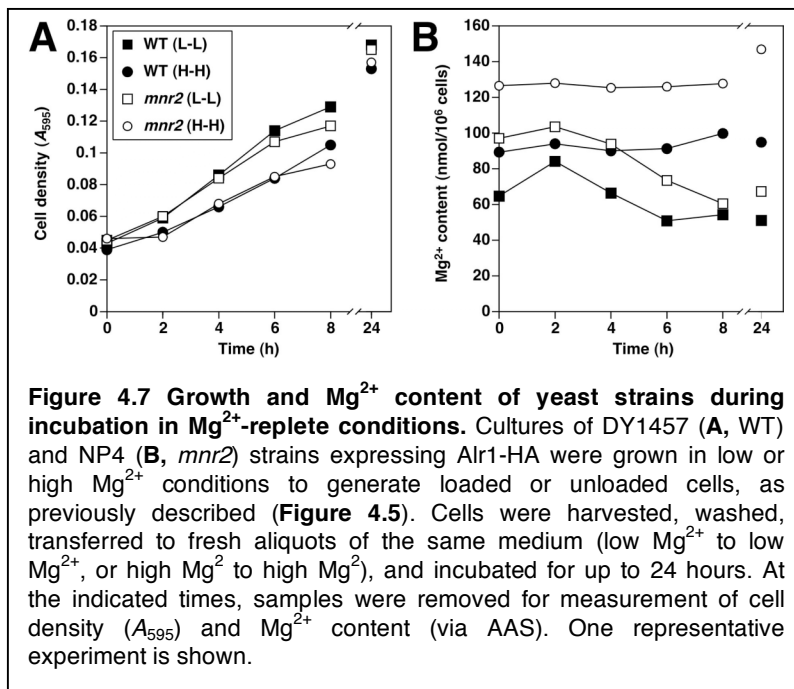


Figure 4.6 Effect of intracellular Mg^{2+} supply on Alr1 modification during Mg^{2+} -depletion. Protein was extracted from aliquots of cells removed at the indicated times during the experiment described in **Figure 4.5**. The extracts were analyzed by 5% SDS-PAGE and immunoblotting to detect Alr1-HA and Tfp1. Time courses for unloaded WT cells (**A**), loaded WT cells (**B**), unloaded *mnr2* cells (**C**) and loaded *mnr2* cells (**D**) are shown. "Low" and "High" indicate unloaded and loaded cell preparations. The location of the lowest and highest mobility forms of Alr1 are indicated (1 and 2 respectively).

4.6A, band 2). I suggest that this change indicates a gradual change in the form of the Alr1 protein in response to Mg^{2+} -deficient conditions (it is also possible that some of the newly formed band was contributed by newly-synthesized Alr1, but this fraction was also in a different form from the original protein). This modification was the opposite of that observed when cells were transferred from deficient to replete conditions (**Figure 4.3**) (Graschopf et al, 2001). In extracts from WT unloaded cells (low-no Mg, **Figure 4.6A**),

the transition to the new form was essentially complete by 6 hours. However, the loaded WT cells (high-no Mg, **Figure 4.6B**) showed a slower rate of Alr1 modification, and lower mobility forms were still present 8 hours after transfer. This difference in the rate of Alr1 modification between loaded and unloaded cells was consistently observed in several different experiments (data not shown). Since no Mg^{2+} was available in the medium, this observation suggests that the form of the Alr1 protein depends upon intracellular Mg^{2+} availability, rather than the external concentration.

When the response of the *mnr2* mutant was determined, I observed a very clear difference from WT. At the start of the time course, there appeared to be slightly more of

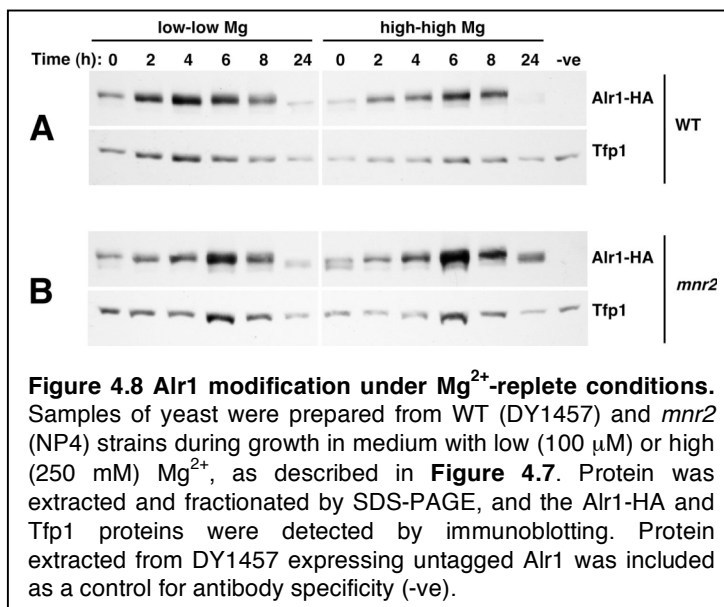


the higher mobility form of Alr1 present in both loaded and unloaded *mnr2* cells. This observation suggests that even replete *mnr2* cells may exhibit a slight cytosolic Mg^{2+} deficiency compared to WT. After transfer to Mg^{2+} deficient conditions, both unloaded (low-no Mg,

Figure 4.6C) and loaded (high-no Mg, **Figure 4.6D**) *mnr2* mutant cells showed similar rapid rates of Alr1 modification. Modification to the higher mobility form was essentially complete within 2 to 3 hours. The observation that a major variation in the initial Mg^{2+} store had no effect on the rate of this transition appears to provide further evidence that the *mnr2* mutation prevents intracellular stores from contributing to Mg^{2+} homeostasis.

I also performed control experiments to confirm that the change in Alr1 modification that I observed was a consequence of Mg^{2+} -deficiency (and for example, not simply a response to transferring the cells to fresh growth medium). In these experiments, the cells were transferred to fresh media containing the same concentration of Mg^{2+} as the

original culture (100 μM or 250 mM). As before, I monitored growth and Mg^{2+} content of the cells during the time course (**Figure 4.7**). Both strains exhibited robust growth in either Mg^{2+} concentration, although the higher concentration had a minor inhibitory effect on growth (an effect that I have observed in other experiments). Mg^{2+} content at the start of the experiment matched that expected for the conditions and genotypes used. During the experiment, content fluctuated somewhat, but was not substantially altered by the end of the time course. Alr1 modification was also monitored for up to 24 hours (**Figure 4.8A and B**). In extracts from either loaded or unloaded WT cells, the lower mobility form of Alr1 predominated for the entire time course. In the *mnr2* mutant, I observed the same slight increase in the higher mobility form in both loaded and



unloaded cells at the start of the time course. Interestingly, after transfer to fresh medium, the small amount of the higher mobility form that was present previously rapidly disappeared, and the lower mobility form predominated for the remainder of the time course. Thus, when either WT or *mnr2* cells were supplied with adequate Mg^{2+}

throughout the time course, I did not observe a transition to the higher mobility form, as would be expected if this change reflected the induction of Mg^{2+} deficiency.

4.6 Summary and discussion

The initial goal of the experiments reported in this chapter was to investigate the effect of inactivating the *MNR2* gene on one aspect of Mg^{2+} homeostasis, the regulation of *ALR1* gene and protein expression. The rationale behind these investigations was that since *ALR1* expression had been reported to respond to Mg^{2+} availability, I expected that a loss of Mnr2 function would cause disruptions in Mg^{2+} homeostasis, which might in

turn perturb Alr1 regulation. If so, this effect might in part explain some other phenotypes of *mnr2* mutants, in particular their higher content of divalent cations such as Ca^{2+} and Mn^{2+} , and their sensitivity to these cations. In the longer term, these investigations might provide novel tools to study other aspects of Mg^{2+} homeostasis in yeast, such as Mg^{2+} -responsive reporter genes. The results of these studies appear to establish that the *mnr2* mutation does affect some aspects of Alr1 regulation and biology, in particular the level of Alr1 protein accumulation, but has no effect on *ALR1* gene expression. I also identified an effect of the *mnr2* mutation on the gel mobility of the Alr1 protein, suggesting that the altered Mg^{2+} levels resulting from this mutation affects the post-translational modification of Alr1. These findings, and their relevance to the model previously proposed to explain Mnr2 function (**Figure 3.12** and **Ch. 3.5**), are summarized below.

4.6.1 Alr1 modification and Mg^{2+} homeostasis

Another finding described in this work was that Alr1 underwent an apparent post-translational modification in response to Mg^{2+} supply resulting in a change in its mobility in SDS-PAGE. In Mg^{2+} -replete conditions ($\text{Mg}^{2+} > 100 \mu\text{M}$), the Alr1 protein was primarily present in a lower-mobility form, while under Mg^{2+} -deficient conditions the mobility of the protein was increased. Most interestingly, the rate at which this modification occurred was influenced by the *mnr2* mutation, suggesting a dependence on intracellular Mg^{2+} availability. A previous study attributed the change in Alr1 mobility to phosphorylation of the protein (Graschopf et al, 2001; Wachek et al, 2006), but these experiments were poorly controlled, and it is possible that the observed effect was due to the degradation of this protein during the assay. Despite this uncertainty, I believe that Alr1 is likely to be phosphorylated in replete conditions for the reasons outlined below. First, when Mg^{2+} -deficient cells were transferred to replete medium, there was a rapid conversion of the low form of Alr1 to the high form (within 30 minutes in 100 mM, **Figure 4.3**, and data not shown). The speed of this transition was consistent with a post-translational modification like phosphorylation rather than a slower process such as the *de novo* synthesis of an alternative form of the protein. Second, a previous survey of the yeast proteome identified a peptide derived from Alr1 that was phosphorylated at serine residue 190 (Peng et al, 2003). I suggest that this peptide is unlikely to represent the only

site of Alr1 modification, as only a small number of peptides derived from Alr1 were identified in the Peng study. In addition, several intermediate forms of Alr1 are visible on Western blots (**Figure 4.6**) implying that several different residues are modified. Third, a recent study determined the ability of various purified yeast kinases to phosphorylate the yeast proteome *in vitro* (Ptacek et al, 2005). These researchers reported that Alr1 was phosphorylated by several purified kinases (Fus3, Tos3, Atg1, Tpk1 and Ptk2). Although these results do not prove that Alr1 is a target for these kinases *in vivo*, they do demonstrate that recognition sites for these kinases are present in the protein. Interestingly, the same study also demonstrated the *in vitro* phosphorylation of Alr2 by the Atg1, Ptk2 and Tpk1 kinases, and of Mnr2 by the Ptk2, Sky1, Pho85/Pho80, Tpk1, Tpk2, and Tpk3 kinases. The Tpk1 kinase (which can phosphorylate all three proteins) is one of three isoforms of protein kinase A (PKA) in yeast (cAMP-dependent protein kinase) [reviewed in (Hardie et al, 2006)]. PKA regulates many different processes broadly connected with cell growth, including the response to essential nutrients. Another kinase identified in this study, Ptk2, is involved in regulating polyamine transport in yeast, which is a process that some studies have connected with Mg²⁺ transport via the Alr proteins (Maruyama et al, 1994). Thus, phosphorylation of these proteins by PKA and Ptk2 could very well have a significant role in regulating Alr1 function.

4.6.2 The *mnr2* mutation increased Alr1 accumulation

As previously reported (Graschopf et al, 2001), I observed that Alr1 accumulation was elevated in Mg²⁺-deficient conditions, suggesting that yeast cells can regulate *ALR1* expression according to Mg²⁺ supply. Since a previous report attributed this regulation in part to changes in *ALR1* mRNA levels, I initially suspected that the *mnr2* mutation exerted its effect on Alr1 protein accumulation primarily via an effect on gene regulation. However, Northern blotting and hybridization experiments failed to provide evidence for an effect of Mg²⁺-supply on the expression of the *ALR1* gene (Aandahl Achari and Colin MacDiarmid, unpublished data). When an *ALR1* promoter-*lacZ* fusion construct was used to measure *ALR1* promoter activity, no effect of Mg²⁺ supply was observed (**Figure 4.2**) and the *mnr2* mutation also had no effect on the activity of this reporter construct. Based on this data, I concluded that the previous report of *ALR1* gene regulation was inaccurate,

and that the effect of the *mnr2* mutation was not mediated through an effect on *ALR1* gene expression.

If Alr1 protein levels were not determined by mRNA level, then what mechanism is responsible for the effect of Mg^{2+} and the *mnr2* mutation on Alr1 protein accumulation? One possibility is that the Alr1 protein is post-translationally regulated via the control of protein stability (Graschopf et al, 2001). According to this model, the stability of the Alr1 protein is high in Mg^{2+} deficient cells, but is reduced upon repletion. When Mg^{2+} availability increases, plasma membrane-localized Alr1 is modified by ubiquitination, rapidly internalized by endocytosis, trafficked to the vacuole, and degraded in a Pep4-dependent process. However, based on my experiments and those of others in this laboratory, it appears that the stability of the existing pool of Alr1 protein in deficient cells is unaffected by exposure to excess Mg^{2+} .

My results raise the question of why key observations in a previous report were not reproducible (Graschopf et al, 2001). My experiments to analyze the effect of Mg^{2+} on Alr1 stability were performed under conditions in which Mg^{2+} accumulation is known to occur (**Figure 3.3B**) (Lee & Gardner, 2006), suggesting that inefficient Mg^{2+} uptake was not responsible for the absence of Alr1 degradation. In addition, similar experiments performed in parallel with another metal-regulated protein (the Zn^{2+} transporter, Zrt1) were successful in demonstrating its destabilization by Zn^{2+} (Aandahl Achari, unpublished data), indicating that the stability of Alr1 was not a consequence of some fundamental flaw in the experimental strategy. As previously noted, independent research groups also failed to reproduce key observations in the previous report (Richard Gardner, personal communication).

An independent approach to studying the effect of Mg^{2+} on Alr1 stability is to examine its effect on protein location. When a YFP-tagged version of the Alr1 protein (YCpcit-ALR1) was expressed in Mg^{2+} -deficient WT yeast, and the cells were then transferred to replete medium, signal was initially observed at the plasma membrane as expected (Lauren Stein, unpublished observations). After 2 hours of incubation in high Mg^{2+} medium, no internalization of the Alr1 protein was observed, indicating that Mg^{2+} supplementation did not accelerate endocytosis of Alr1. In addition, the *end3* mutation (which blocks endocytosis) (Raths et al, 1993) had no effect on the distribution of the

protein after two hours (in both WT and *end3* strains, it remained on the plasma membrane). Thus, even using an independent experimental approach, rapid internalization and degradation of Alr1 in response to Mg^{2+} was not observed.

Another finding of the previous report (Graschopf et al, 2001) was that various genetic changes affected Alr1 regulation. For example, the *end3*, *rsp5*, *npi1* and *pep4* mutations were reported to prevent Alr1 degradation following Mg^{2+} repletion. Other workers in this laboratory also attempted to replicate these observations, with mixed success (Aandahl Achari, Abhinav Pandey, and Colin MacDiarmid, unpublished observations).

Since we could not detect any Mg^{2+} -stimulated degradation of Alr1, the effect of the mutations (*end3*, *rsp5* (*npi1*) and *pep4*) on the steady-state accumulation of Alr1 in Mg^{2+} -deficient and replete conditions were determined. From these experiments, it was concluded that the *rsp5* mutation (which prevents ubiquitin-protein ligase (Rsp5) mediated protein degradation) (Graschopf et al, 2001; Hein et al, 1995) and the *pep4* mutation (which prevents protein turnover in vacuoles) (Jones et al, 1982) did in fact inhibit the regulation of Alr1 accumulation (Abhinav Pandey, unpublished observations). These observations are consistent with the initial model (Graschopf et al, 2001), which proposed that in replete conditions Alr1 was ubiquitinated (via an Rsp5-dependent process), internalized, and delivered to the vacuole for degradation (a Pep4-dependent process). The possible involvement of ubiquitination in Alr1 regulation is also supported by a recent proteomic survey (Peng et al, 2003), which identified Alr1 as a component of a mixture of ubiquitin (Ub)-conjugated proteins. In contrast to the previous report however (Graschopf et al, 2001), the *end3* and *dim1* mutations that prevent endocytosis had no effect on regulation (Aandahl Achari, Abhinav Pandey and Colin MacDiarmid, unpublished observations). These observations are consistent with the lack of response of the YFP-tagged Alr1 protein to high Mg^{2+} in both WT and *end3* strains (see above), and together suggest that plasma membrane-localized Alr1 is resistant to internalization and degradation in response to high Mg^{2+} concentrations.

4.6.3 Revised model for Alr1 regulation

Given the above observations, how is the steady-state regulation of Alr1 protein

level achieved? (**Figure 4.1A**). Although the plasma membrane localized pool of YFP-tagged version of Alr1 is apparently relatively insensitive to high Mg^{2+} concentration (Lauren Stein, unpublished observations), factors implicated in the regulation of protein stability and sorting (Pep4 and Rsp5) are required for regulation. In addition, the effect of *mnr2* mutation on Alr1 accumulation (**Figure 4.1A**) is most easily explained based on a model in which Alr1 accumulation is coupled to the cytosolic Mg^{2+} concentration.

Taking the above factors into consideration, I suggest a revised model for Alr1 regulation outlined here. I propose that upon translation of the Alr1 protein and its subsequent insertion in the ER membrane, the yeast cell makes a decision about the fate of the protein that is based on the current level of cytosolic Mg^{2+} . In Mg^{2+} -deficient cells, the protein follows a "default" sorting pathway and accumulates in the plasma membrane, where it can mediate Mg^{2+} uptake. In Mg^{2+} -replete cells, the protein is modified by the addition of ubiquitin, and is then sorted to the vacuole for degradation. In *pep4* and *npi1* mutants, the protein is either ubiquitinated and accumulates in the vacuole lumen (in *pep4*), or fails to be ubiquitinated and follows the default pathway to the cell surface (in *npi1*). If cytosolic Mg^{2+} homeostasis is perturbed genetically (by the *mnr2* mutation), the proportion of Alr1 sorted to the vacuole is reduced, and the steady state level of the protein increases. Similar processes of regulation have been observed for some other regulated yeast transporters. For example, in non-permissive conditions, the Gap1 amino acid transporter is also directly sorted from the Golgi to the vacuole for degradation, without transit through the plasma membrane (Scott et al, 2004). Thus, precedent for this mode of regulation exists in yeast.

One argument that might be made against the above model is that the stability of the Alr1 protein in deficient cells was not affected by Mg^{2+} status (**Figure 4.4**) and in some way is misleading. For example, the Alr1 protein may have been internalized in response to Mg^{2+} repletion, but not degraded. However, I do not believe this is the case, for the following reasons. First, as previously noted, the rate of Mg^{2+} uptake by deficient cells is constant for at least three hours (**Figure 3.3C**). Second, as previously discussed, other workers in this laboratory examined the location of Alr1 directly (Lauren Stein, Frank Donovan and Colin MacDiarmid, unpublished observations). When a YFP-tagged version of Alr1 (YCpcit-ALR1) was expressed in Mg^{2+} -deficient yeast cells, it was

present at the cell surface as expected. Subsequent exposure of the cells to Mg^{2+} -replete medium for up to three hours did not appreciably change the location of the protein. Thus, since Alr1 remains on the plasma membrane after Mg^{2+} exposure, any down-regulation of the activity of the protein would require its modification *in situ*.

4.6.4 Genetic tests of the trafficking model

Other work in this laboratory appears to provide additional support for the above model. For example, several other genes have been identified as required for the regulation of Alr1 accumulation (Abhinav Pandey and Colin MacDiarmid, unpublished data). As previously reported (Graschopf et al, 2001), other members of this laboratory have also observed a dependence on the *PEP4* gene for Alr1 regulation, indicating a requirement for vacuolar proteases (an observation which is consistent with post-translational regulation). The *npil* and *doa4* mutations are both associated with an increased accumulation of Alr1 in Mg^{2+} -replete conditions. Both of these genes are required for correct regulation of ubiquitination in yeast (Belgareh-Touze et al, 2008; Swaminathan et al, 1999). The *npil* mutation reduces the activity of the essential Rsp5 gene by 90% (Springael & Andre, 1998). This mutation is associated with reduced ubiquitination of many regulated membrane proteins and a consequent increase in their stability (Galan et al, 1996; Springael et al, 2002). The *doa4* mutation eliminates the activity of an enzyme required for the cleavage of Ub from modified proteins before their delivery to the vacuolar lumen for degradation. As with *npil*, this mutation stabilizes many plasma membrane proteins (Dupre & Haguenaer-Tsapis, 2001). Although this mutation reduces the level of free Ub within the cell, a reduction in Ub availability is not thought to be the reason for the effect of the mutation on protein stability. Instead, recent studies implicate the role of Doa4 as a sorting factor required for the delivery of ubiquitinated proteins to the vacuole lumen (Nikko & Andre, 2007). In the absence of Doa4, these proteins are sorted from the vacuolar membrane back to the plasma membrane via retrograde transport pathways (Nikko & Andre, 2007).

In addition to these factors, genes required for the correct function of protein sorting pathways (specifically, the sorting of ubiquitinated proteins to the vacuole) were also found to be required for Alr1 regulation. For example, a strain lacking the *VPS27*

gene, and one lacking both the *GGA1* and *GGA2* genes, were defective in Alr1 regulation. *VPS27* is required for sorting of ubiquitinated proteins from the pre-vacuolar compartment (PVC) to the vacuole (Piper et al, 1995), while *GGA1* and *GGA2* are partially redundant genes required for the sorting of ubiquitinated proteins from the late-Golgi to the PVC (Scott et al, 2004). The effect of these mutations on Alr1 regulation is consistent with my proposed model that in replete conditions, ubiquitinated Alr1 follows a pathway from the late-Golgi direct to the vacuole. Ubiquitination of Alr1 could occur in the Golgi under replete conditions, mediated by Rsp5. Further evidence for this model of direct sorting from Golgi to vacuole were provided by experiments showing that the *end3* and *dim1* mutations, which prevent endocytosis, had no effect on Alr1 regulation, consistent with a model in which regulation primarily occurs via trafficking directly from Golgi to vacuole.

If the above model is correct, it does raise the question of why plasma membrane-localized Alr1 would not be targeted for ubiquitination and internalized upon Mg^{2+} repletion, as is the case for many other regulated nutrient transporters (Roberg et al, 1997). One possibility is that, because of the relatively non-toxic nature of Mg^{2+} ions, such a "rapid-response" system for Alr1 downregulation is simply unnecessary. It is also possible that the Alr1 protein at the plasma membrane can sense and respond to increased cytosolic Mg^{2+} by immediately lowering its activity, as has been reported for bacterial CorA channels (Payandeh et al, 2008). This model would make sense in light of the rather slow uptake of Mg^{2+} by deficient yeast (**Figure 3.3C**). I previously suggested that this slow Mg^{2+} uptake is limited by the ability of the cell to sequester Mg^{2+} in the vacuole. Given that Alr1 is a cation channel, and should display the rapid transport characteristics of such proteins, the slow rate of uptake observed suggests that transport via Alr1 is not the rate-limiting step in Mg^{2+} accumulation. Instead, I suggest that the rate of sequestration in the vacuole determines the rate of overall uptake. By this model, uptake would proceed until cytosolic Mg^{2+} concentrations reached a critical level, at which time the Alr1 channel would close. When sufficient sequestration had taken place to lower the cytosolic level, Alr1 would open again and allow Mg^{2+} influx. Such a regulated uptake process might prevent the overaccumulation of cytosolic Mg^{2+} , and thus reduce the possibility of Mg^{2+} toxicity during repletion.

Chapter 5 Summary and future directions

5.1 Summary and significance of this work

My studies involving Mnr2 characterization have provided new information on Mg^{2+} homeostasis in yeast and other eukaryotes. As summarized in **Figure 3.12**, the data presented in this dissertation are consistent with a model in which Mnr2 functions as a cation efflux system in the vacuole membrane. Under conditions of cytosolic Mg^{2+} deficiency, the Mnr2 protein allows the release of Mg^{2+} from stores held in the vacuolar compartment. This released Mg^{2+} can then be utilized to allow cells to continue growth for a short time in the absence of an external Mg^{2+} supply. Mnr2 also participates in Mg^{2+} homeostasis over a range of Mg^{2+} concentrations, as indicated by the higher Mg^{2+} content of *mnr2* mutants grown in replete conditions. However, the primary importance of Mnr2 (and vacuolar Mg^{2+} stores in general) is evident from the phenotypes of *mnr2* deletion mutants, which were unable to deplete intracellular Mg^{2+} stores under deficient conditions, and displayed a severe growth defect. The *mnr2* mutation was also associated with two other phenotypes suggestive of lower intracellular Mg^{2+} availability, the increased accumulation of the Mg^{2+} -responsive Alr1 protein, and an increase in the abundance of a higher-mobility form of this protein associated with Mg^{2+} deficiency. This work provides the first description of a transporter that regulates Mg^{2+} homeostasis by controlling access to an intracellular Mg^{2+} store. In this chapter, I will describe experiments that might be performed to further test this basic model, and discuss the general implications of my findings to the field of Mg^{2+} homeostasis and to biotechnology in general.

5.2 Role of Mnr2 in homeostasis of other divalent cations

In addition to its clear role in Mg^{2+} homeostasis, the *mnr2* mutant also showed sensitivity to, and increased content of, other divalent cations, notably Mn^{2+} and Ca^{2+} . These phenotypes of the *mnr2* mutant suggest that Mnr2 may also participate in the homeostasis of these cations. In some respects this observation is not surprising, given the relatively broad specificity of CorA-family proteins for divalent cations (Graschopf et al, 2001; MacDiarmid & Gardner, 1998). Based on the observations reported here, there

are at least two models that could explain the above phenotypes. First, it is possible that the *mnr2* mutation has the same effect on the intracellular storage of other divalent cations as it does on Mg^{2+} storage; *i.e.*, the *mnr2* mutation could block the release of these cations from the vacuolar compartment. It is clear from published work that the vacuole is a major site for storage of potentially toxic cations such as Zn^{2+} , Fe^{2+} and Ca^{2+} (Dunn et al, 1994; MacDiarmid et al, 2000; Paidhungat & Garrett, 1998; Simm et al, 2007). Transport systems responsible for storage of these cations (Li et al, 2001a; MacDiarmid et al, 2000; Pozos et al, 1996) as well as systems responsible for their release from the vacuole under deficient conditions have been identified (e.g. Zrt3 for Zn^{2+} , Smf3 for Fe^{2+} , and Yvc1 for Ca^{2+}) (Denis & Cyert, 2002; MacDiarmid et al, 2000; Palmer et al, 2001; Portnoy et al, 2000). In addition to these specific systems, it is possible that under appropriate conditions, Mnr2 provides a "low-affinity" system that allows efflux of these metals from the vacuole when they are present at high concentrations. This observation would not be unusual, as redundancy of low and high affinity transport systems is a feature of ion homeostasis in yeast (Waters & Eide, 2002). If Mnr2 does play this role, loss of its activity could result in higher levels of cation accumulation in the vacuole. This effect might be more obvious under conditions in which rates of metal influx into the cell are high and vacuolar stores are filled (for example, when cells are grown with very high concentrations of metals, or when a low environmental Mg^{2+} allows elevated influx of other divalent cations via Alr1).

A second possible explanation for the higher divalent cation content of the *mnr2* mutant is that it occurs as a consequence of another effect on Mg^{2+} homeostasis. I observed several different effects of the *mnr2* mutation on the major Mg^{2+} transport system of yeast, Alr1. The *mnr2* mutation is associated with a significant increase in the accumulation of the Alr1 protein in the cell without any change in the subcellular distribution of the protein (as determined by fluorescence microscopy). This observation suggested that *mnr2* mutants might have a higher activity of Alr1 at the cell surface. If so, this protein might provide a route for increased influx of various divalent cations into the cell, particularly under conditions of low external Mg^{2+} content. Previous work has shown that the overexpression of Alr1 increased both the rate of $^{57}Co^{2+}$ uptake and sensitivity to this cation as well as conferring sensitivity to many other divalent cations

(including Mn^{2+} , Ca^{2+} , Ni^{2+} , and Zn^{2+}) (MacDiarmid & Gardner, 1998). Reducing the Mg^{2+} concentration of yeast media enhances the toxicity of most divalent cations, suggesting that these cations compete with Mg^{2+} for transport via Alr1 (Blackwell et al, 1997; Eitinger et al, 2000; Joho et al, 1991).

5.3 Measurement of Alr1 activity

To distinguish between the above two models, it would be best to directly examine the effect of the *mnr2* mutation on Alr1 activity. If increased activity of Alr1 at the plasma membrane is responsible for increased divalent cation uptake (model 2), it should be possible to measure this difference directly by measuring the initial rate of cation uptake. Currently it is possible to measure Mg^{2+} uptake by monitoring the total Mg^{2+} content of yeast cells after transfer from deficient to replete conditions (**Figure 3.3C**). From published work, it is clear that this process is dependent on the Alr proteins (Lee & Gardner, 2006). However, the rate of this uptake process is very slow (**Figure 3.3C**), suggesting that it may be limited by the rate of sequestration in the intracellular store rather than the activity of Alr1, per se. In addition, because detection of this uptake requires that cells first be depleted of Mg^{2+} stores, it is not possible to use this protocol to compare the rate of uptake (and hence Alr1 activity) in replete and deficient cells, or to compare strains that vary in their initial Mg^{2+} content under these conditions. For example, this technique could not be used to measure uptake in WT vs *mnr2* mutants (**Figure 3.3C**), as the substantial stores present in Mg^{2+} -deficient *mnr2* cells complicated the subsequent measurement of Mg^{2+} uptake rate in replete conditions (as well as the interpretation of the results).

Although one study described the use of electrophysiological techniques for measurement of Alr1 activity (Liu et al, 2002), the use of such methods in yeast is technically very demanding. In addition, this technique required the overexpression of Alr1, which would prevent its use to study normal variations in Alr1 expression and activity. A simple quantitative method to measure Alr1 activity in yeast is required to better understand how Alr1 contributes to Mg^{2+} homeostasis, and to investigate the role of phosphorylation in this process. Previous studies of Alr1 activity utilized a radioactive cobalt isotope ($^{57}Co^{2+}$) to measure a relatively rapid uptake process possibly mediated by

the Alr proteins (MacDiarmid & Gardner, 1998). These studies demonstrated that the overexpression of Alr1 or Alr2 resulted in a substantial increase in the rate of $^{57}\text{Co}^{2+}$ accumulation, while *ALR1* deletion reduced this activity. The authors concluded that the Alr proteins provided a "low affinity" Co^{2+} uptake system, and that $^{57}\text{Co}^{2+}$ was therefore a useful tracer for studies of Alr activity. These studies were inconclusive however, in that they did not fully define the contribution of the Alr proteins to total Co^{2+} uptake.

Although the mutant strain showed reduced uptake activity, this decrease could have been a consequence of a general decline in the viability of this strain in response to the defect in Mg^{2+} homeostasis associated with this mutation. This is an important caveat because as several systems are known to accumulate Co^{2+} in yeast (Li & Kaplan, 1998; Liu et al, 1997), and Co^{2+} uptake may be a relatively non-specific assay for Alr activity.

Despite this uncertainty about Co^{2+} however, the use of alternative substrates to study the activity of the Alr proteins has a lot of potential. Several divalent cations have been suggested to be substrates for the Alr proteins, based on the enhanced sensitivity of strains overexpressing these proteins (MacDiarmid & Gardner, 1998). It may be possible to identify a divalent cation for which transport is almost entirely mediated by the Alr proteins under a particular condition. Such a cation might be identified by utilizing known or potential inhibitors of the Alr proteins to define the proportion of total uptake contributed by the Alr proteins. For example, hexaminecobalt (III) chloride has been shown to be a very effective and specific inhibitor of bacterial (Kucharski et al, 2000), fungal (Kolisek et al, 2003) and plant (Li et al, 2001b) CorA-family proteins. Although the effect of this inhibitor on Alr activity has not been tested, it seems likely that it would also be an effective inhibitor of these systems. Another possible Alr inhibitor is Al^{3+} ion (MacDiarmid & Gardner, 1998), although the specificity of this inhibitor for CorA-type proteins is not as well defined. Finally, Mg^{2+} itself should competitively inhibit the uptake of other divalent cations via the Alr proteins, although it may not be as effective as the above two candidates. A simple screen for metal uptake could be performed by incubating yeast cells with a mixture of all potential Alr substrates (Ni^{2+} , Co^{2+} , Zn^{2+} , Mn^{2+} , and Ca^{2+}) in the presence or absence of inhibitors. A change in the content of all the cations over time could be measured simultaneously by using ICP-MS. The cation showing the most robust uptake in the absence of inhibitor, but minimal uptake in the

presence of the inhibitor would be selected for further study. Control experiments could then be performed to verify the specificity of the tracer. For example, I would expect that in strains overexpressing the protein, uptake of the substrate would be enhanced, and that this increased activity would also be sensitive to inhibition.

Once a suitable tracer is identified, it may be possible to measure the activity of the Alr proteins in yeast over relatively short time periods (so as to measure the initial rate of the uptake process). Measurement of the initial rate of uptake would be essential to ensure that the activity of the Alr protein itself was being studied rather than the rate of secondary processes, such as the intracellular sequestration of the cation. Using a radioactive isotope of the metal may facilitate measurement of initial rates of transport (isotopes of Ni^{2+} and Mn^{2+} are available that would be suitable for this task). Rapid measurements may also be possible using ICP-MS. The effect of the *mnr2* mutation on uptake activity could then be determined. As controls, I would include a strain that overexpressed the Alr1 protein (I would expect this strain to show faster uptake of the tracer used). In addition, it would be advisable to determine the level of Alr1 expression observed in the various strains. This would enable me to definitively determine if the increased activity was due to increased expression under the exact conditions used in the experiment, or if it could be due to another effect (for example, the post-translational modification of Alr1, as discussed below).

5.4 Identifying phosphorylated residues in Alr1

Before we can understand the physiological role of the post-translational modification of Alr1, it will be necessary to demonstrate that the modification observed is primarily phosphorylation. The conventional method to determine if a protein is phosphorylated is to purify it. For example, immunoprecipitation could be used to purify small amounts of an epitope-tagged version of the protein. The purified protein could then be subjected to Western blotting using antibodies that recognize the epitope tag (as a positive control), and phosphorylated residues such as phosphoserine or phosphothreonine. In this way, it could be directly demonstrated that the slow-mobility form was phosphorylated, as only this form would be expected to react with the antibody. Controls could be included in this experiment to show that the slower-mobility form

could be transformed into the faster form by treating the purified protein with a phosphatase enzyme, such as calf intestinal phosphatase (Heredia et al, 2001). I would expect that this faster form would not react with antibodies specific to phosphorylated residues.

The above experiment would demonstrate that the protein was phosphorylated, and might suggest which class of residue was involved (serine, threonine or tyrosine), but it would not identify the specific residue(s) that are modified. It is clear from my work that several residues may be modified, and the large number of potential phosphorylation sites in Alr1 identified by software tools such as NetPhosYeast (Ingrell et al, 2007) makes identifying the exact sites of phosphorylation a difficult task. A recent study used an evolutionary approach to predict phosphorylation sites for PKA in yeast proteins (Budovskaya et al, 2005). As the consensus recognition site for PKA is R-[KR]-X-S, potential sites can be identified using simple sequence database searches. Although such sites will occur randomly in any protein sequence with fairly high frequency, functional sites will tend to be conserved between closely related homologs from different yeast species. The authors found that a consensus PKA recognition site within the Alr1 sequence (RRKTM, at T612) is conserved in Alr1 homologs from several closely related species (Budovskaya et al, 2005). The location of this site differed from that previously identified as phosphorylated by Peng et al. (Peng et al, 2003), and there is no direct evidence for Alr1 modification at this location. Nevertheless, the identification of these sites provides a useful starting point for any genetic analysis of phosphorylation.

Interestingly, potential sites for PKA were also found at amino acid (aa) 611 of Alr2, and at aa 162 and 618 of Mnr2. During my work on Mnr2, I noticed that this protein also shows an apparent Mg^{2+} -dependent modification (**Figure 3.5C**). In Western blots, a lower mobility form of Mnr2 is observed in low Mg^{2+} ($< 100 \mu M$). This observation suggests that Mg^{2+} -dependent modification, most likely via phosphorylation, is not restricted to Alr1 but may instead represent a general strategy for regulation of these channels.

The fastest way to identify specific sites of Mg^{2+} -dependent phosphorylation in Alr1 may be to purify the protein and utilize mass spectrometry for analysis. A polyhistidine tract (Hengen, 1995) or Tandem Affinity Purification tag (Tagwerker et al,

2006) could be added to the N-terminal end of the protein to allow its purification from cell lysates. Cells expressing these constructs could be grown in Mg^{2+} -deficient and replete conditions to generate cell extracts containing predominantly one or the other form of Alr1. The Alr1 protein would be purified from each extract under conditions designed to prevent dephosphorylation (for example, using denaturing conditions to inactivate endogenous phosphatases). Western analysis of the protein would be used to verify that the purified protein showed the same difference in mobility as I observed in crude protein extracts. Enough of the protein would need to be purified for it to be visualized on SDS-PAGE gels. Both bands could then be excised from the gel, purified, and subjected to protease digestion (to obtain peptides) prior to mass spectrometry. The peptides derived from high Mg^{2+} and low Mg^{2+} samples would be compared for a mass shift of 80 Daltons in serine, threonine and tyrosine residues indicative of phosphorylation. This approach was successful on a much larger scale in yeast (Peng et al, 2003), even to the extent of identifying Alr1 peptides in a digest of the entire yeast proteome. As an added advantage, this approach may also allow to identify other post-translational modifications of Alr1, including ubiquitination, which has been implicated in the regulation of Alr1 accumulation.

The necessity of the above strategy may have been preempted by recent progress in yeast proteomics however. Many general studies have now been performed to characterize the yeast phosphoproteome using mass spectroscopy (Ficarro et al, 2002). The results of these studies have been collated into web databases such as PeptideAtlas (King et al, 2006) and Phosphopep (Bodenmiller et al, 2007) to provide a resource for the preliminary identification of defined phosphorylation sites on yeast proteins. Searching the database of compiled results for Alr1 phosphorylation sites revealed five phosphorylated residues, including two serine residues (S847 and S850) in the C-terminal cytosolic domain. Interestingly, work in this laboratory has revealed a possible role for this domain in the regulation of Alr1 protein accumulation by Mg^{2+} supply (Abhinav Pandey, personal communication). In addition, alignment of the C-terminal domain sequence with closely regulated Alr1 homologs reveals that the potentially phosphorylated S847 and S850 residues are very tightly conserved (identical in 10/10 fungal sequences). The existence of these conserved residues at the C-terminal end of

Alr1 suggests that they might play a role in regulating Alr1 stability. For example, the phosphorylation of Alr1 may be a prerequisite for its ubiquitination. Genetic evidence suggests that ubiquitination plays a role in the regulation of Alr1 stability (Graschopf et al, 2001), and there are several examples from yeast of phosphorylation (or dephosphorylation) preceding the ubiquitination of post-translationally regulated membrane proteins (e.g. Gap1) (Garrett, 2008). Modifying these residues to determine their importance to regulation would be one way to test this model.

5.5 Known functions of ion channel phosphorylation

In addition to its potential role in regulating Alr1 stability, phosphorylation might also allow the activity of the Alr1 channel to be modulated according to Mg^{2+} availability. Studies of other channels have revealed that such modification can affect channel activity via different mechanisms. These include changing the sensitivity of a ligand-dependent channel to activation by its ligand, changing the activity of the channel directly (via alteration of the open probability), or changing the degree to which regulatory subunits (inhibitory or stimulatory) associate with the core channel. For example, the inositol 1,4,5-trisphosphate receptor (IP_3R) is a Ca^{2+} channel located in the ER membrane responsible for the release of Ca^{2+} from ER stores in response to an increased cytosolic concentration of the IP_3 signaling molecule (Vanderheyden et al, 2008). The IP_3R is phosphorylated at several sites by at least 12 different protein kinases. Although the function of this phosphorylation in many cases remains unclear, some clear effects have been documented. For example, phosphorylation of the IP_3R subunit 1 by protein kinase A has been shown to result in an increase in channel sensitivity to IP_3 (the receptor ligand) (Tang et al, 2003). This channel also serves as an example of how phosphorylation can affect channel interactions with other regulatory proteins. PKA phosphorylation of the IP_3R1 subunit is thought to reduce its interaction with calmodulin, enhancing channel activity (Tang et al, 2003).

Another good example of the effect of phosphorylation on channel activity is the Kir3 protein, one of a family of inward rectifying potassium channels regulating heart function. Phosphorylation of Kir3 by PKA was reported to modulate the response of the channel to cAMP-dependent activation. Mutation of the S385 residue of the Kir3 protein,

which prevented phosphorylation, strongly reduced its activation by the cAMP pathway (Rusinova et al, 2009). The activity of several other inwardly rectifying Kir channels are also modulated by phosphorylation by PKA or PKC (Karle et al, 2002; Keselman et al, 2007). These kinases phosphorylate different residues in the proteins, and have different effects on function (either stimulating or suppressing activity).

The mammalian TRPM6 and TRPM7 proteins form another class of channel specific for Mg^{2+} ions [(reviewed in (Cao et al, 2008a)]. As outlined previously (**Ch. 1.9.1**), these proteins are primarily responsible for Mg^{2+} uptake by mammalian cells, and play an important role in whole-body Mg^{2+} homeostasis through their function in regulating Mg^{2+} reabsorption by the kidney (Schlingmann & Gudermann, 2005). The TRPM proteins are unusual in having a cytoplasmic domain consisting of an active protein kinase of an unusual type (the α -kinase domain). This domain has been demonstrated to phosphorylate associated channel subunits, and is also capable of autophosphorylation. Genetic studies have suggested that the kinase domain is important for the interaction of TRPM channels with a regulatory protein, RACK1 (Cao et al, 2008b), which modulates channel activity. Thus, phosphorylation may play a role in regulating the primary mechanism of Mg^{2+} uptake in mammalian systems. Use of the yeast model system to study the physiological role of Mg^{2+} transporter modification may also throw light on the role of this modification in mammalian cells.

5.6 Genetic analysis of phosphorylation

Although a role for phosphorylation in regulating Alr1 activity is an interesting model, it should be noted that there is as yet little evidence that Alr1 activity is modified by Mg^{2+} availability. As previously discussed, this absence of information is primarily due to the lack of simple and accurate techniques for such measurements. Once a reliable method for the measurement of Alr1 activity is established, it would be possible to perform studies to measure the effect of Mg^{2+} supply on Alr1 activity, and to determine if the predominant form of the Alr1 protein affects this activity. In addition, it would also become possible to perform genetic studies to define the role of specific residues on Alr1 activity. For example, once residues modified by phosphorylation were identified, it would be possible to mutate these residues to either prevent or simulate modification of

the protein. Replacement of a phosphorylated serine by alanine for example, would prevent its modification, while replacement with aspartate would simulate constitutive phosphorylation of that residue. The modified versions could then be reintroduced into yeast to measure the effect of the mutations on activity (or some other parameter such as protein stability). The advantage of this approach is that it allows the effect of the modification to be measured in cells grown under identical conditions, removing the variable of Mg^{2+} supply from the interpretation of the results. Development of this assay would also allow a determination of the effect of the *mnr2* mutation on Alr1 activity. The *mnr2* mutation altered both Alr1 accumulation and the degree of Alr1 modification. Either of these effects may have increased Alr1 activity, an effect that might explain the increase in divalent cation content of the *mnr2* mutant detected with ICP-MS.

A second question raised by this work is to identify which protein kinases (and protein phosphatase enzymes) are responsible for Alr1 modification. Identification of phosphorylated residues may provide clues to the kinases responsible, because these enzymes generally recognize consensus sequences within proteins (as discussed above for PKA). Identifying the kinase responsible for Alr1 modification may be as simple as screening kinase mutants to determine which strains are unable to phosphorylate the Alr1 protein. Some clues to the identity of the kinase are already available in the form of studies performed to determine the *in vitro* substrate specificity of yeast kinases (described above). Assuming that phosphorylation does play a role in Alr1 regulation by Mg^{2+} supply, identification of the kinase(s) responsible may provide clues to the signal transduction pathway that senses Mg^{2+} availability. This response may represent a specific reaction to the absence of Mg^{2+} , or it may reflect a more general physiological response to nutrient limitation, or a decreased growth rate. Either way, such findings would provide interesting insights into this poorly understood area.

5.7 Parallels between Mg^{2+} homeostasis in yeast and plants

In contrast to yeast, where only five different CorA transporters are present, there are many different CorA family genes in plants. In sequence, these proteins are most closely related to the yeast Mrs2 and Lpe10 channels of the mitochondrial membrane (Gregan et al, 2001a). However, characterization of several of the *Arabidopsis* proteins

has demonstrated that they play diverse roles, including mediating Mg^{2+} uptake over the plasma membrane and transport into chloroplasts. The function of majority of these proteins is unknown at present, but it is very likely that one or more members of this family are involved in regulating vacuolar Mg^{2+} content. Differentiated plant cells contain large vacuoles that, as in yeast, play an important role in the storage of essential inorganic nutrients [reviewed in (Martinoia et al, 2007)].

One interesting parallel observed between my work and plant biology is in the field of ionomics. The ionome is the content of inorganic nutrients in an organism. Possible variation in the yeast ionome was previously determined by screening a collection of approximately 4500 viable yeast deletion mutants for those mutations that affect elemental content (Eide et al, 2005). The screening defined a set of 212 mutant strains that had an altered content of at least one of 13 elements measured when grown under "replete" conditions. Some interesting correlations between these different mutants were observed. For example, most of the mutants identified showed variation in content in several different elements indicating that the mutations were generally pleiotropic. In fact, only four out of the 212 mutations affected only one element. This observation suggests that processes essential for general homeostasis of a variety of different elements, rather than more specific transport functions, were altered by the mutations. In agreement with this conclusion, a major class of mutants affected vacuolar formation or function, for example, by preventing the generation of the vacuolar proton gradient. A particular feature of this class of mutants is a decrease in Mg^{2+} , P, Ni^{2+} and Co^{2+} content, presumably because the vacuole was less able to accumulate these elements. Since the proton gradient is essential for the transport of cations into the vacuole, and the content of this compartment has a large influence on overall elemental content, it is understandable that the content of several elements is affected in these mutants.

This type of analysis has also been extended to plant systems (Lahner et al, 2003). In this study, mutant populations of *A. thaliana* were subjected to systematic ICP-MS analysis to identify novel mutations affecting elemental content. Fifty-one mutants were isolated in this screen, and many of these plants had alterations in Mg^{2+} content, meaning that this could be a useful method for analysis of Mg^{2+} homeostasis in *Arabidopsis*. A similar study was performed recently in *Lotus japonicus* (Chen et al, 2008), indicating

that this method is applicable not just to model plant systems. Interestingly, in the later study, a subgroup of mutations with pleiotrophic effects on Mg^{2+} , Co^{2+} , Ni^{2+} and P content was identified. These mutations may identify genes involved in vacuolar function, as observed in yeast. ICP-MS analysis of the *mnr2* mutant revealed that this mutation was also pleiotrophic, altering yeast content of Mn^{2+} , Zn^{2+} , Ca^{2+} and P in addition to Mg^{2+} . Since my work showed that Mnr2 affects vacuolar ion homeostasis, it seems possible that some of the mutations now being identified in plants have similar effects, and may even encode members of the CorA-family.

The description of the ionome in plants, and the characterization of genes encoding specific element transport systems is an essential step towards the biotechnological manipulation of elemental content. Making specific changes in the degree to which plants accumulate and store various elements would facilitate many biotechnological advances. As an indication of the importance of this information, it is clear that many modern high-yielding crops have a significantly lower content of many inorganic nutrients (Davis, 2009) including Mg^{2+} , Fe^{2+} , Cu^{2+} and Ca^{2+} . For some elements, reduction in the nutrient content is substantial (for example, in one comparison of modern and "classic" varieties of 20 vegetable crops, copper content decreased an average of 80%). Much of this decrease is likely a consequence of selection for higher yield and bulk, without co-selection for nutrient content. The definition of model plant and crop plant ionomes would facilitate reversing this trend by the use of specific genome modifications, potentially without altering valuable traits for high yield. In this context, pleiotrophic mutations that alter content of several elements at once may be very useful, as modification or addition of only a single gene could promote the accumulation of several different elements.

One gene family that represents a good example of this idea was described recently (Uauy et al, 2006). The NAM genes from wheat affect the redistribution of nutrients from the plant to the developing seed. Three NAM genes were shown to be important for this transfer process, and plants lacking NAM genes function stored less nitrogen, Zn^{2+} and Fe^{2+} in the seed. The NAM genes encode transcription factors that may regulate the expression of transport systems required for nutrient redistribution from leaf cells. Given the importance of seed nutrient content to agriculture and human

nutrition, the identification of the NAM genes represents a major advance, and the identification of other genes that affect nutrient content will hopefully follow.

Another major application for genes affecting elemental content is the bioaccumulation of valuable or toxic soil components. Some plants have been developed as tools for accumulating elements from soil, a process called phytoextraction [reviewed in (Chaney et al, 2007)]. In this technique, a plant variety capable of hyperaccumulating a potentially toxic element (and which is generally very tolerant to the element) is grown in soil containing a high concentration of that element. Such soils can occur naturally or as a result of human activity (for example, due to contamination with mine or factory waste). Harvesting the plant allows it to be disposed of at a safe location, removing the toxic element from the soil. Repeated cycles of this process eventually lead to the rehabilitation of the site, with minimal human intervention. In some cases, the element can be recovered from the harvested plant material, providing a profitable means of "mining" the metal.

Nickel (Ni^{2+}) is one such element for which this process has been proven to be economically viable. Ni^{2+} hyperaccumulator species (e.g. *Alyssum murale*) can accumulate 100-fold more Ni^{2+} in the shoot than other crop plants without a decrease in yield. When *Alyssum murale* was grown in naturally Ni^{2+} -rich serpentine soils, the ash derived from burning the crop consisted of 25-50% Ni^{2+} (Tappero et al, 2007). The relatively pure Ni^{2+} present in this material makes it the richest Ni^{2+} ore available for smelters. Hyperaccumulators that show specific ability to accumulate various elements have been described, including those for Zn^{2+} , Co^{2+} , Cd^{2+} , Mn^{2+} and Ni^{2+} . The tolerance and hyperaccumulation phenotypes of these species have been attributed to higher activity of metal transport systems (Pence et al, 2000) as well as the biosynthesis of metal chelating metabolites such as nicotianamine or histidine (Pianelli et al, 2005), although the specific contribution of many of these compounds to tolerance is still controversial. Ionic analysis of hyperaccumulator species may be one way to identify the genes involved in these processes. One feature of bioaccumulators that does seem clear is that the metal ions tend to be stored in the vacuoles of the plant cells (Tappero et al, 2007), an observation which again demonstrates the parallels between basic mechanisms of metal homeostasis in yeast and plants.

BIBLIOGRAPHY

- Beeler T, Bruce K, Dunn T (1997) Regulation of cellular Mg^{2+} by *Saccharomyces cerevisiae*. *Biochim Biophys Acta* **1323**(2): 310-318
- Belgareh-Touze N, Leon S, Erpapazoglou Z, Stawiecka-Mirota M, Urban-Grimal D, Haguenaer-Tsapis R (2008) Versatile role of the yeast ubiquitin ligase Rsp5p in intracellular trafficking. *Biochem Soc Trans* **36**(Pt 5): 791-796
- Bennett W (1997) *Nutrient deficiencies and toxicities in crop plants*, St. Paul, MN: APS Press, The American Phytopathological Society.
- Benz I, Kohlhardt M (1991) Modulation of single cardiac Na^+ channels by cytosolic Mg^{++} ions. *Eur Biophys J* **20**(4): 223-228
- Bird AJ, Zhao H, Luo H, Jensen LT, Srinivasan C, Evans-Galea M, Winge DR, Eide DJ (2000) A dual role for zinc fingers in both DNA binding and zinc sensing by the Zap1 transcriptional activator. *EMBO J* **19**(14): 3704-3713.
- Blackwell KJ, Tobin JM, Avery SV (1997) Manganese uptake and toxicity in magnesium-supplemented and unsupplemented *Saccharomyces cerevisiae*. *Appl Microbiol Biotechnol* **47**(2): 180-184
- Blanc-Potard AB, Groisman EA (1997) The *Salmonella* selC locus contains a pathogenicity island mediating intramacrophage survival. *Embo J* **16**(17): 5376-5385
- Blanc-Potard AB, Lafay B (2003) MgtC as a horizontally-acquired virulence factor of intracellular bacterial pathogens: evidence from molecular phylogeny and comparative genomics. *J Mol Evol* **57**(4): 479-486
- Bodenmiller B, Malmstrom J, Gerrits B, Campbell D, Lam H, Schmidt A, Rinner O, Mueller LN, Shannon PT, Pedrioli PG, Panse C, Lee HK, Schlapbach R, Aebersold R (2007) PhosphoPep--a phosphoproteome resource for systems biology research in *Drosophila* Kc167 cells. *Mol Syst Biol* **3**: 139
- Bonneaud N, Ozier-Kalogeropoulos O, Li GY, Labouesse M, Minvielle-Sebastia L, Lacroute F (1991) A family of low and high copy replicative, integrative and single-stranded *S. cerevisiae*/*E. coli* shuttle vectors. *Yeast* **7**(6): 609-615
- Borrelly G, Boyer JC, Touraine B, Szponarski W, Rambier M, Gibrat R (2001) The yeast mutant *vps5D* affected in the recycling of Golgi membrane proteins displays an enhanced vacuolar Mg^{2+}/H^+ exchange activity. *Proc Natl Acad Sci USA* **98**(17): 9660-9665.
- Boutry M, Michelet B, Goffeau A (1989) Molecular cloning of a family of plant genes encoding a protein homologous to plasma membrane H^+ -translocating ATPases. *Biochem*

Biophys Res Commun **162**: 567-574

Brannan PG, Vergne-Marini P, Pak CY, Hull AR, Fordtran JS (1976) Magnesium absorption in the human small intestine. Results in normal subjects, patients with chronic renal disease, and patients with absorptive hypercalciuria. *J Clin Invest* **57**(6): 1412-1418

Buchmeier N, Blanc-Potard A, Ehrt S, Piddington D, Riley L, Groisman EA (2000) A parallel intraphagosomal survival strategy shared by mycobacterium tuberculosis and *Salmonella enterica*. *Mol Microbiol* **35**(6): 1375-1382

Budovskaya YV, Stephan JS, Deminoff SJ, Herman PK (2005) An evolutionary proteomics approach identifies substrates of the cAMP-dependent protein kinase. *Proc Natl Acad Sci U S A* **102**(39): 13933-13938

Bui DM, Gregan J, Jarosch E, Ragnini A, Schweyen RJ (1999) The bacterial magnesium transporter CorA can functionally substitute for its putative homologue Mrs2p in the yeast inner mitochondrial membrane. *J Biol Chem* **274**(29): 20438-20443.

Butler MG (1990) Prader-Willi syndrome: current understanding of cause and diagnosis. *Am J Med Genet* **35**(3): 319-332

Cao G, Hoenderop JG, Bindels RJ (2008a) Insight into the molecular regulation of the epithelial magnesium channel TRPM6. *Curr Opin Nephrol Hypertens* **17**(4): 373-378

Cao G, Thebault S, van der Wijst J, van der Kemp A, Lasonder E, Bindels RJ, Hoenderop JG (2008b) RACK1 inhibits TRPM6 activity via phosphorylation of the fused alpha-kinase domain. *Curr Biol* **18**(3): 168-176

Chai JH, Locke DP, Grealley JM, Knoll JH, Ohta T, Dunai J, Yavor A, Eichler EE, Nicholls RD (2003) Identification of four highly conserved genes between breakpoint hotspots BP1 and BP2 of the Prader-Willi/Angelman syndromes deletion region that have undergone evolutionary transposition mediated by flanking duplicons. *Am J Hum Genet* **73**(4): 898-925

Chaney RL, Angle JS, Broadhurst CL, Peters CA, Tappero RV, Sparks DL (2007) Improved understanding of hyperaccumulation yields commercial phytoextraction and phytomining technologies. *J Environ Qual* **36**(5): 1429-1443

Chen Z, Watanabe T, Shinano T, Okazaki K, Osaki M (2008) Rapid characterization of plant mutants with an altered ion-profile: a case study using *Lotus japonicus*. *New Phytol*

Chubanov V, Waldegger S, Mederos y Schnitzler M, Vitzthum H, Sassen MC, Seyberth HW, Konrad M, Gudermann T (2004) Disruption of TRPM6/TRPM7 complex formation by a mutation in the TRPM6 gene causes hypomagnesemia with secondary hypocalcemia. *Proc Natl Acad Sci USA* **101**(9): 2894-2899

- Cole DE, Quamme GA (2000) Inherited disorders of renal magnesium handling. *J Am Soc Nephrol* **11**(10): 1937-1947
- Cowan JA (1995) Introduction to the biological chemistry of the magnesium ion. In *The Biological Chemistry of Magnesium*, Cowan JA (ed), pp 1-23. New York: VCH Publishers
- Cowan JA (2002) Structural and catalytic chemistry of magnesium-dependent enzymes. *Biometals* **15**(3): 225-235
- Cox JS, Walter P (1996) A novel mechanism for regulating activity of a transcription factor that controls the unfolded protein response. *Cell* **87**(3): 391-404
- Culotta VC, Yang M, Hall MD (2005) Manganese transport and trafficking: lessons learned from *Saccharomyces cerevisiae*. *Eukaryot Cell* **4**(7): 1159-1165
- da Costa BM, Cornish K, Keasling JD (2007) Manipulation of intracellular magnesium levels in *Saccharomyces cerevisiae* with deletion of magnesium transporters. *Appl Microbiol Biotechnol* **77**(2): 411-425
- Dai LJ, Quamme GA (1991) Intracellular Mg^{2+} and magnesium depletion in isolated renal thick ascending limb cells. *J Clin Invest* **88**(4): 1255-1264
- Dai LJ, Ritchie G, Kerstan D, Kang HS, Cole DE, Quamme GA (2001) Magnesium transport in the renal distal convoluted tubule. *Physiol Rev* **81**(1): 51-84.
- Davis DR (2009) Declining Fruit and Vegetable Nutrient Composition: What is the Evidence? . *HortScience*(44): 15-19
- de Rouffignac C, Quamme G (1994) Renal magnesium handling and its hormonal control. *Physiol Rev* **74**(2): 305-322
- Deheinzelin D, Negri EM, Tucci MR, Salem MZ, da Cruz VM, Oliveira RM, Nishimoto IN, Hoelz C (2000) Hypomagnesemia in critically ill cancer patients: a prospective study of predictive factors. *Braz J Med Biol Res* **33**(12): 1443-1448
- Delhaize E, Ryan PR (1995) Aluminum Toxicity and Tolerance in Plants. *Plant Physiol* **107**(2): 315-321
- Deng W, Luo K, Li D, Zheng X, Wei X, Smith W, Thammina C, Lu L, Li Y, Pei Y (2006) Overexpression of an Arabidopsis magnesium transport gene, AtMGT1, in *Nicotiana benthamiana* confers Al tolerance. *J Exp Bot* **57**(15): 4235-4243
- Denis V, Cyert MS (2002) Internal Ca^{2+} release in yeast is triggered by hypertonic shock and mediated by a TRP channel homologue. *J Cell Biol* **156**(1): 29-34

Dix DR, Bridgham JT, Broderius MA, Byersdorfer CA, Eide DJ (1994) The *FET4* gene encodes the low affinity Fe(II) transport protein of *Saccharomyces cerevisiae*. *J Biol Chem* **269**(42): 26092-26099

Drummond R, Tutone A, Li Y, Gardner R (2006) A putative magnesium transporter AtMRS2-11 is localized to the plant chloroplast envelope membrane system *Plant Science* **170**: 78-89

Dunn T, Gable K, Beeler T (1994) Regulation of cellular Ca²⁺ by yeast vacuoles. *J Biol Chem* **269**(10): 7273-7278

Dupre S, Haguenaer-Tsapis R (2001) Deubiquitination step in the endocytic pathway of yeast plasma membrane proteins: crucial role of Doa4p ubiquitin isopeptidase. *Mol Cell Biol* **21**(14): 4482-4494

Eide DJ (1998) The molecular biology of metal ion transport in *Saccharomyces cerevisiae*. *Annu Rev Nutr* **18**: 441-469

Eide DJ (2006) Zinc transporters and the cellular trafficking of zinc. *Biochim Biophys Acta* **1763**(7): 711-722

Eide DJ, Clark S, Nair TM, Gehl M, Gribskov M, Guerinot ML, Harper JF (2005) Characterization of the yeast ionome: a genome-wide analysis of nutrient mineral and trace element homeostasis in *Saccharomyces cerevisiae*. *Genome Biol* **6**(9): R77

Eitinger T, Degen O, Bohnke U, Muller M (2000) Nic1p, a relative of bacterial transition metal permeases in *Schizosaccharomyces pombe*, provides nickel ion for urease biosynthesis. *J Biol Chem* **275**(24): 18029-18033

Elin RJ (1987) Assessment of magnesium status. *Clin Chem* **33**(11): 1965-1970

Ellis CD, Wang F, MacDiarmid CW, Clark S, Lyons T, Eide DJ (2004) Zinc and the Msc2 zinc transporter protein are required for endoplasmic reticulum function. *J Cell Biol* **166**(3): 325-335

Eshaghi S, Niegowski D, Kohl A, Martinez Molina D, Lesley SA, Nordlund P (2006) Crystal structure of a divalent metal ion transporter CorA at 2.9 angstrom resolution. *Science* **313**(5785): 354-357

Ferreira A, Rivera A, Romero JR (2004) Na⁺/Mg²⁺ exchange is functionally coupled to the insulin receptor. *J Cell Physiol* **199**(3): 434-440

Fiaccadori E, Del Canale S, Coffrini E, Melej R, Vitali P, Guariglia A, Borghetti A (1988) Muscle and serum magnesium in pulmonary intensive care unit patients. *Crit Care Med* **16**(8): 751-760

- Ficarro SB, McClelland ML, Stukenberg PT, Burke DJ, Ross MM, Shabanowitz J, Hunt DF, White FM (2002) Phosphoproteome analysis by mass spectrometry and its application to *Saccharomyces cerevisiae*. *Nat Biotechnol* **20**(3): 301-305
- Flatman PW, Smith LM (1990) Magnesium transport in ferret red cells. *J Physiol* **431**: 11-25
- Flatman PW, Smith LM (1996) Magnesium transport in magnesium-loaded ferret red blood cells. *Pflugers Arch* **432**(6): 995-1002
- Forgac M (1999) Structure and properties of the vacuolar (H⁺)-ATPases. *J Biol Chem* **274**(19): 12951-12954
- Forsberg H, Hammar M, Andreasson C, Moliner A, Ljungdahl PO (2001) Suppressors of *ssy1* and *ptr3* null mutations define novel amino acid sensor-independent genes in *Saccharomyces cerevisiae*. *Genetics* **158**(3): 973-988
- Froschauer EM, Kolisek M, Dieterich F, Schweigel M, Schweyen RJ (2004) Fluorescence measurements of free [Mg²⁺] by use of MagFura-2 in *Salmonella enterica*. *FEMS Microbiol Lett* **237**(1): 49-55
- Fuhrmann G-F, Rothstein A (1968) The transport of Zn²⁺, Co²⁺ and Ni²⁺ into yeast cells. *Biochim Biophys Acta* **163**: 325-330
- Gadd GM, Laurence OS (1996) Demonstration of high affinity Mn²⁺ uptake in *Saccharomyces cerevisiae*: specificity and kinetics. *Microbiol* **142**: 1159-1167
- Gaither LA, Eide DJ (2000) Functional expression of the human hZIP2 zinc transporter. *J Biol Chem* **275**(8): 5560-5564.
- Galan JM, Moreau V, Andre B, Volland C, Haguenaer-Tsapis R (1996) Ubiquitination mediated by the Npi1p/Rsp5p ubiquitin-protein ligase is required for endocytosis of the yeast uracil permease. *J Biol Chem* **271**(18): 10946-10952
- Garcia Vescovi E, Soncini FC, Groisman EA (1996) Mg²⁺ as an extracellular signal: environmental regulation of *Salmonella* virulence. *Cell* **84**(1): 165-174.
- Gardner RC (2003) Genes for magnesium transport. *Curr Opin Plant Biol* **6**(3): 263-267
- Garrett JM (2008) Amino acid transport through the *Saccharomyces cerevisiae* Gap1 permease is controlled by the Ras/cAMP pathway. *Int J Biochem Cell Biol* **40**(3): 496-502
- Gibson MM, Bagga DA, Miller CG, Maguire ME (1991) Magnesium transport in *Salmonella typhimurium*: the influence of new mutations conferring Co²⁺ resistance on the CorA Mg²⁺ transport system. *Mol Microbiol* **5**(11): 2753-2762

- Gitan RS, Lou H, Rodgers J, Broderius M, Eide D (1998) Zinc-induced inactivation of the yeast *ZRT1* zinc transporter occurs through endocytosis and vacuolar degradation. *J Biol Chem* **273**: 28617-28624
- Goytain A, Hines RM, El-Husseini A, Quamme GA (2007) NIPA1 (SPG6), the basis for autosomal dominant form of hereditary spastic paraplegia, encodes a functional Mg²⁺ transporter. *J Biol Chem* **282**(11): 8060-8068
- Goytain A, Hines RM, Quamme GA (2008) Functional characterization of NIPA2, a selective Mg²⁺ transporter. *Am J Physiol Cell Physiol* **295**(4): C944-953
- Goytain A, Quamme GA (2005a) Functional characterization of ACDP2 (ancient conserved domain protein), a divalent metal transporter. *Physiol Genomics* **22**(3): 382-389
- Goytain A, Quamme GA (2005b) Functional characterization of human SLC41A1, a Mg²⁺ transporter with similarity to prokaryotic MgtE Mg²⁺ transporters. *Physiol Genomics* **21**(3): 337-342
- Goytain A, Quamme GA (2005c) Functional characterization of the human solute carrier, SLC41A2. *Biochem Biophys Res Commun* **330**(3): 701-705
- Goytain A, Quamme GA (2005d) Identification and characterization of a novel mammalian Mg²⁺ transporter with channel-like properties. *BMC Genomics* **6**(1): 48
- Goytain A, Quamme GA (2008) Identification and characterization of a novel family of membrane magnesium transporters, MMgT1 and MMgT2. *Am J Physiol Cell Physiol* **294**(2): C495-502
- Graschopf A, Stadler JA, Hoellerer MK, Eder S, Sieghardt M, Kohlwein SD, Schweyen RJ (2001) The yeast plasma membrane protein Alr1 controls Mg²⁺ homeostasis and is subject to Mg²⁺-dependent control of its synthesis and degradation. *J Biol Chem* **276**(19): 16216-16222
- Grauer UE HW (1992) Modelling cation amelioration of aluminium phytotoxicity. *Soil Science Society of America Journal* **56**
- Gregan J, Bui DM, Pillich R, Fink M, Zsurka G, Schweyen RJ (2001a) The mitochondrial inner membrane protein Lpe10p, a homologue of Mrs2p, is essential for magnesium homeostasis and group II intron splicing in yeast. *Mol Gen Genet* **264**(6): 773-781.
- Gregan J, Kolisek M, Schweyen RJ (2001b) Mitochondrial Mg²⁺ homeostasis is critical for group II intron splicing *in vivo*. *Genes Dev* **15**(17): 2229-2237.

Griesbeck O, Baird GS, Campbell RE, Zacharias DA, Tsien RY (2001) Reducing the environmental sensitivity of yellow fluorescent protein. Mechanism and applications. *J Biol Chem* **276**(31): 29188-29194

Groenestege WM, Hoenderop JG, van den Heuvel L, Knoers N, Bindels RJ (2006) The epithelial Mg²⁺ channel transient receptor potential melastatin 6 is regulated by dietary Mg²⁺ content and estrogens. *J Am Soc Nephrol* **17**(4): 1035-1043

Groisman EA (2001) The pleiotropic two-component regulatory system PhoP-PhoQ. *J Bacteriol* **183**(6): 1835-1842

Grubbs RD (2002) Intracellular magnesium and magnesium buffering. *Biometals* **15**(3): 251-259

Guarente L, Lalonde B, Gifford P, Alani E (1984) Distinctly regulated tandem upstream activation sites mediate catabolite repression of the *CYC1* gene of *S. cerevisiae*. *Cell* **36**(2): 503-511

Gunn JS, Miller SI (1996) PhoP-PhoQ activates transcription of *pmrAB*, encoding a two-component regulatory system involved in *Salmonella typhimurium* antimicrobial peptide resistance. *J Bacteriol* **178**(23): 6857-6864

Gunzel D, Kucharski LM, Kehres DG, Romero MF, Maguire ME (2006) The MgtC virulence factor of *Salmonella enterica* serovar Typhimurium activates Na(+),K(+)-ATPase. *J Bacteriol* **188**(15): 5586-5594

Hamilton TG, Norris TB, Tsuruda PR, Flynn GC (1999) Cer1p functions as a molecular chaperone in the endoplasmic reticulum of *Saccharomyces cerevisiae*. *Mol Cell Biol* **19**(8): 5298-5307

Handy RD, Gow IF, Ellis D, Flatman PW (1996) Na-dependent regulation of intracellular free magnesium concentration in isolated rat ventricular myocytes. *J Mol Cell Cardiol* **28**(8): 1641-1651

Hanninen AL, Simola M, Saris N, Makarow M (1999) The cytoplasmic chaperone hsp104 is required for conformational repair of heat-denatured proteins in the yeast endoplasmic reticulum. *Mol Biol Cell* **10**(11): 3623-3632

Hardie DG, Hawley SA, Scott JW (2006) AMP-activated protein kinase--development of the energy sensor concept. *J Physiol* **574**(Pt 1): 7-15

Hein C, Springael JY, Volland C, Haguenaer-Tsapis R, Andre B (1995) *NP11*, an essential yeast gene involved in induced degradation of Gap1 and Fur4 permeases, encodes the Rsp5 ubiquitin-protein ligase. *Mol Microbiol* **18**(1): 77-87

Heithoff DM, Conner CP, Hentschel U, Govantes F, Hanna PC, Mahan MJ (1999)

- Coordinate intracellular expression of Salmonella genes induced during infection. *J Bacteriol* **181**(3): 799-807
- Hengen P (1995) Purification of His-Tag fusion proteins from Escherichia coli. *Trends Biochem Sci* **20**(7): 285-286
- Heredia J, Crooks M, Zhu Z (2001) Phosphorylation and Cu⁺ coordination-dependent DNA binding of the transcription factor Mac1p in the regulation of copper transport. *J Biol Chem* **276**(12): 8793-8797
- Hermans C, Verbruggen N (2005) Physiological characterization of Mg deficiency in Arabidopsis thaliana. *J Exp Bot*
- Hirata R, Ohsumi Y, Nakano A, Kawasaki H, Suzuki K, Anraku Y (1990) Molecular structure of a gene, VMA1, encoding the catalytic subunit of H⁺-translocating adenosine triphosphatase from vacuolar membranes of Saccharomyces cerevisiae. *J Biol Chem* **265**: 6726-6733
- Hmiel SP, Snavelly MD, Florer JB, Maguire ME, Miller CG (1989) Magnesium transport in Salmonella typhimurium: genetic characterization and cloning of three magnesium transport loci. *J Bacteriol* **171**(9): 4742-4751
- Hmiel SP, Snavelly MD, Miller CG, Maguire ME (1986) Magnesium transport in *Salmonella typhimurium*: characterization of magnesium influx and cloning of a transport gene. *J Bacteriol* **168**(3): 1444-1450
- Hua SB, Qiu M, Chan E, Zhu L, Luo Y (1997) Minimum length of sequence homology required for in vivo cloning by homologous recombination in yeast. *Plasmid* **38**(2): 91-96
- Ingrell CR, Miller ML, Jensen ON, Blom N (2007) NetPhosYeast: prediction of protein phosphorylation sites in yeast. *Bioinformatics* **23**(7): 895-897
- Johnson JD, Hand WL, King-Thompson NL (1980) The role of divalent cations in interactions between lymphokines and macrophages. *Cell Immunol* **53**(2): 236-245
- Joho M, Tarumi K, Inouhe M, Tohoyama H, Murayama T (1991) Co²⁺ and Ni²⁺ resistance in *Saccharomyces cerevisiae* associated with a reduction in the accumulation of Mg²⁺. *Microbios* **67**(272-273): 177-186
- Jones EW, Zubenko GS, Parker RR (1982) PEP4 gene function is required for expression of several vacuolar hydrolases in *Saccharomyces cerevisiae*. *Genetics* **102**(4): 665-677
- Karle CA, Zitron E, Zhang W, Wendt-Nordahl G, Kathofer S, Thomas D, Gut B, Scholz E, Vahl CF, Katus HA, Kiehn J (2002) Human cardiac inwardly-rectifying K⁺ channel Kir(2.1b) is inhibited by direct protein kinase C-dependent regulation in human isolated cardiomyocytes and in an expression system. *Circulation* **106**(12): 1493-1499

- Kawahara T, Yanagi H, Yura T, Mori K (1997) Endoplasmic reticulum stress-induced mRNA splicing permits synthesis of transcription factor Hac1p/Ern4p that activates the unfolded protein response. *Mol Biol Cell* **8**(10): 1845-1862
- Kerstan D, Quamme, G.A. (2002) *Physiology and pathophysiology of intestinal absorption of magnesium*
- Keselman I, Fribourg M, Felsenfeld DP, Logothetis DE (2007) Mechanism of PLC-mediated Kir3 current inhibition. *Channels (Austin)* **1**(2): 113-123
- King NL, Deutsch EW, Ranish JA, Nesvizhskii AI, Eddes JS, Mallick P, Eng J, Desiere F, Flory M, Martin DB, Kim B, Lee H, Raught B, Aebersold R (2006) Analysis of the *Saccharomyces cerevisiae* proteome with PeptideAtlas. *Genome Biol* **7**(11): R106
- Kinraide TB, Parker DR (1987) Cation Amelioration of Aluminum Toxicity in Wheat. *Plant Physiol* **83**(3): 546-551
- Knauer R, Lehle L (1999) The oligosaccharyltransferase complex from *Saccharomyces cerevisiae*. Isolation of the *OST6* gene, its synthetic interaction with *OST3*, and analysis of the native complex. *J Biol Chem* **274**(24): 17249-17256
- Knoop V, Groth-Malonek M, Gebert M, Eifler K, Weyand K (2005) Transport of magnesium and other divalent cations: evolution of the 2-TM-GxN proteins in the MIT superfamily. *Mol Genet Genomics* **274**(3): 205-216
- Kolisek M, Launay P, Beck A, Sponder G, Serafini N, Brenkus M, Froschauer EM, Martens H, Fleig A, Schweigel M (2008) SLC41A1 is a novel mammalian Mg²⁺ carrier. *J Biol Chem* **283**(23): 16235-16247
- Kolisek M, Zsurka G, Samaj J, Weghuber J, Schweyen RJ, Schweigel M (2003) Mrs2p is an essential component of the major electrophoretic Mg²⁺ influx system in mitochondria. *EMBO J* **22**(6): 1235-1244
- Kozak JA, Cahalan MD (2003) MIC channels are inhibited by internal divalent cations but not ATP. *Biophys J* **84**(2 Pt 1): 922-927
- Kubota T, Shindo Y, Tokuno K, Komatsu H, Ogawa H, Kudo S, Kitamura Y, Suzuki K, Oka K (2005) Mitochondria are intracellular magnesium stores: investigation by simultaneous fluorescent imagings in PC12 cells. *Biochim Biophys Acta* **1744**(1): 19-28
- Kucharski LM, Lubbe WJ, Maguire ME (2000) Cation hexaamines are selective and potent inhibitors of the CorA magnesium transport system. *J Biol Chem* **275**(22): 16767-16773
- Lahner B, Gong J, Mahmoudian M, Smith EL, Abid KB, Rogers EE, Guerinot ML,

Harper JF, Ward JM, McIntyre L, Schroeder JI, Salt DE (2003) Genomic scale profiling of nutrient and trace elements in *Arabidopsis thaliana*. *Nat Biotechnol* **21**(10): 1215-1221

Lanza H, Afonso-Cardoso SR, Silva AG, Napolitano DR, Espindola FS, Pena JD, Souza MA (2004) Comparative effect of ion calcium and magnesium in the activation and infection of the murine macrophage by *Leishmania major*. *Biol Res* **37**(3): 385-393

Laurant P, Touyz RM (2000) Physiological and pathophysiological role of magnesium in the cardiovascular system: implications in hypertension. *J Hypertens* **18**(9): 1177-1191

Lawley TD, Chan K, Thompson LJ, Kim CC, Govoni GR, Monack DM (2006) Genome-wide screen for *Salmonella* genes required for long-term systemic infection of the mouse. *PLoS Pathog* **2**(2): e11

Lee JM, Gardner RC (2006) Residues of the yeast *ALR1* protein that are critical for magnesium uptake. *Curr Genet* **49**(1): 7-20

LeFurgey A, Ingram P, Blum JJ (1990) Elemental composition of polyphosphate-containing vacuoles and cytoplasm of *Leishmania major*. *Mol Biochem Parasitol* **40**(1): 77-86

Li L, Chen OS, McVey Ward D, Kaplan J (2001a) *CCCI* is a transporter that mediates vacuolar iron storage in yeast. *J Biol Chem* **276**(31): 29515-29519

Li L, Kaplan J (1998) Defects in the yeast high affinity iron transport system result in increased metal sensitivity because of the increased expression of transporters with a broad transition metal specificity. *J Biol Chem* **273**(35): 22181-22187.

Li L, Sokolov, L. Yang, Y. Li, D., Ting, J., Pandey, G. and Luan, S (2008) A Mitochondrial Magnesium Transporter Functions in *Arabidopsis* Pollen Development. *Molecular Plant* **1**(4): 675-685

Li L, Tutone AF, Drummond RS, Gardner RC, Luan S (2001b) A novel family of magnesium transport genes in *Arabidopsis*. *Plant Cell* **13**(12): 2761-2775.

Li M, Jiang J, Yue L (2006) Functional characterization of homo- and heteromeric channel kinases TRPM6 and TRPM7. *J Gen Physiol* **127**(5): 525-537

Liu GJ, Martin DK, Gardner RC, Ryan PR (2002) Large Mg(2+)-dependent currents are associated with the increased expression of ALR1 in *Saccharomyces cerevisiae*. *FEMS Microbiol Lett* **213**(2): 231-237

Liu XF, Supek F, Nelson N, Culotta VC (1997) Negative control of heavy metal uptake by the *Saccharomyces cerevisiae* *BSD2* gene. *J Biol Chem* **272**(18): 11763-11769

Lombeck I, Ritzl F, Schnippering HG, Michael H, Bremer HJ, Feinendegen LE,

Kosenow W (1975) Primary hypomagnesemia. I. Absorption Studies. *Z Kinderheilkd* **118**(4): 249-258

Lunin VV, Dobrovetsky E, Khutoreskaya G, Zhang R, Joachimiak A, Doyle DA, Bochkarev A, Maguire ME, Edwards AM, Koth CM (2006) Crystal structure of the CorA Mg²⁺ transporter. *Nature* **440**(7085): 833-837

Lyons TJ, Gasch AP, Gaither LA, Botstein D, Brown PO, Eide DJ (2000) Genome-wide characterization of the Zap1p zinc-responsive regulon in yeast. *Proc Natl Acad Sci U S A* **97**(14): 7957-7962.

Ma H, Kunes S, Schatz PJ, Botstein D (1987) Plasmid construction by homologous recombination in yeast. *Gene* **58**(2-3): 201-216

MacDiarmid CW (1997) Aluminium toxicity and resistance in *Saccharomyces cerevisiae*., Cellular and Molecular Biology, University of Auckland, Auckland

MacDiarmid CW, Gaither LA, Eide D (2000) Zinc transporters that regulate vacuolar zinc storage in *Saccharomyces cerevisiae*. *EMBO J* **19**(12): 2845-2855.

MacDiarmid CW, Gardner RC (1996) Al toxicity in yeast. A role for Mg? *Plant Physiol* **112**(3): 1101-1109

MacDiarmid CW, Gardner RC (1998) Overexpression of the *Saccharomyces cerevisiae* magnesium transport system confers resistance to aluminum ion. *J Biol Chem* **273**(3): 1727-1732

MacDiarmid CW, Milanick MA, Eide DJ (2002) Biochemical properties of vacuolar zinc transport systems of *Saccharomyces cerevisiae*. *J Biol Chem* **277**(42): 39187-39194

MacDiarmid CW, Milanick MA, Eide DJ (2003) Induction of the ZRC1 metal tolerance gene in zinc-limited yeast confers resistance to zinc shock. *J Biol Chem* **278**(17): 15065-15072

Maguire ME (2006) Magnesium transporters: properties, regulation and structure. *Front Biosci* **11**: 3149-3163

Maguire ME, Cowan JA (2002) Magnesium chemistry and biochemistry. *Biometals* **15**(3): 203-210

Mahan MJ, Slauch JM, Mekalanos JJ (1993) Selection of bacterial virulence genes that are specifically induced in host tissues. *Science* **259**(5095): 686-688

Mao DD, Tian LF, Li LG, Chen J, Deng PY, Li DP, Luan S (2008) AtMGT7: An Arabidopsis Gene Encoding a Low-Affinity Magnesium Transporter. *J Integr Plant Biol* **50**(12): 1530-1538

- Martinoia E, Maeshima M, Neuhaus HE (2007) Vacuolar transporters and their essential role in plant metabolism. *J Exp Bot* **58**(1): 83-102
- Maruyama T, Masuda N, Kakinuma Y, Igarashi K (1994) Polyamine-sensitive magnesium transport in *Saccharomyces cerevisiae*. *Biochim Biophys Acta* **1194**(2): 289-295
- Matsumoto H (2000) Cell biology of aluminum toxicity and tolerance in higher plants. *Int Rev Cytol* **200**: 1-46
- Milla PJ, Aggett PJ, Wolff OH, Harries JT (1979) Studies in primary hypomagnesaemia: evidence for defective carrier-mediated small intestinal transport of magnesium. *Gut* **20**(11): 1028-1033
- Millart H, Durlach V, Durlach J (1995) Red blood cell magnesium concentrations: analytical problems and significance. *Magnes Res* **8**(1): 65-76
- Miller SI (1991) PhoP/PhoQ: macrophage-specific modulators of *Salmonella* virulence? *Mol Microbiol* **5**(9): 2073-2078
- Miller SI, Kukral AM, Mekalanos JJ (1989) A two-component regulatory system (phoP phoQ) controls *Salmonella typhimurium* virulence. *Proc Natl Acad Sci U S A* **86**(13): 5054-5058
- Miller SI, Mekalanos JJ (1990) Constitutive expression of the phoP regulon attenuates *Salmonella* virulence and survival within macrophages. *J Bacteriol* **172**(5): 2485-2490
- Moncrief MB, Maguire ME (1998) Magnesium and the role of MgtC in growth of *Salmonella typhimurium*. *Infect Immun* **66**(8): 3802-3809
- Montell C (2003) The venerable inveterate invertebrate TRP channels. *Cell Calcium* **33**(5-6): 409-417
- Myers AM, Tzagoloff A, Kinney DM, Lusty CJ (1986) Yeast shuttle and integrative vectors with multiple cloning sites suitable for construction of lacZ fusions. *Gene* **45**(3): 299-310.
- Nadler MJ, Hermosura MC, Inabe K, Perraud AL, Zhu Q, Stokes AJ, Kurosaki T, Kinet JP, Penner R, Scharenberg AM, Fleig A (2001) LTRPC7 is a Mg²⁺-ATP-regulated divalent cation channel required for cell viability. *Nature* **411**(6837): 590-595
- Nelson N (1999) Metal ion transporters and homeostasis. *EMBO J* **18**(16): 4361-4371
- Nikko E, Andre B (2007) Evidence for a direct role of the Doa4 deubiquitinating enzyme in protein sorting into the MVB pathway. *Traffic* **8**(5): 566-581

- Nishikawa SI, Fewell SW, Kato Y, Brodsky JL, Endo T (2001) Molecular chaperones in the yeast endoplasmic reticulum maintain the solubility of proteins for retrotranslocation and degradation. *J Cell Biol* **153**(5): 1061-1070
- Nishimura K, Igarashi K, Kakinuma Y (1998) Proton gradient-driven nickel uptake by vacuolar membrane vesicles of *Saccharomyces cerevisiae*. *J Bacteriol* **180**(7): 1962-1964
- Nishimura K, Yasumura K, Igarashi K, Harashima S, Kakinuma Y (1999) Transcription of some PHO genes in *Saccharomyces cerevisiae* is regulated by spt7p. *Yeast* **15**(16): 1711-1717
- Okorokov LA, Kulakovskaya TV, Lichko LP, Polorotova EV (1985) H⁺/ion antiport as the principal mechanism of transport systems in the vacuolar membrane of the yeast *Saccharomyces carlsbergensis*. *FEBS Lett* **192**(2): 303-306
- Okorokov LA, Letrikevich SB, Lichko LP, Mel'nikova EV (1978) Vacuolar pool of magnesium in cells of the yeast *Saccharomyces cerevisiae*. *Biol Bull Acad Sci USSR* **5**(5): 638-640
- Okorokov LA, Lichko LP, Kholodenko VP, Kadomtseva VM, Petrikevich SB, Zaichkin EI, Karimova AM (1975) Free and bound magnesium in fungi and yeasts. *Folia Microbiol (Praha)* **20**(6): 460-466
- Okorokov LA, Lichko LP, Kulaev IS (1980) Vacuoles: main compartments of potassium, magnesium, and phosphate ions in *Saccharomyces carlsbergensis* cells. *J Bacteriol* **144**(2): 661-665
- Paidhungat M, Garrett S (1998) Cdcl and the vacuole coordinately regulate Mn²⁺ homeostasis in the yeast *Saccharomyces cerevisiae*. *Genetics* **148**: 1787-1798
- Palmer CP, Zhou XL, Lin J, Loukin SH, Kung C, Saimi Y (2001) A TRP homolog in *Saccharomyces cerevisiae* forms an intracellular Ca²⁺-permeable channel in the yeast vacuolar membrane. *Proc Natl Acad Sci USA* **98**(14): 7801-7805
- Park MH, Wong BB, Lusk JE (1976) Mutants in three genes affecting transport of magnesium in *Escherichia coli*: genetics and physiology. *J Bacteriol* **126**(3): 1096-1103
- Patil C, Walter P (2001) Intracellular signaling from the endoplasmic reticulum to the nucleus: the unfolded protein response in yeast and mammals. *Curr Opin Cell Biol* **13**(3): 349-355
- Payandeh J, Li C, Ramjeesingh M, Poduch E, Bear CE, Pai EF (2008) Probing structure-function relationships and gating mechanisms in the CorA Mg²⁺ transport system. *J Biol Chem* **283**(17): 11721-11733

- Payandeh J, Pai EF (2006) A structural basis for Mg²⁺ homeostasis and the CorA translocation cycle. *EMBO J* **25**(16): 3762-3773
- Pence NS, Larsen PB, Ebbs SD, Letham DL, Lasat MM, Garvin DF, Eide D, Kochian LV (2000) The molecular physiology of heavy metal transport in the Zn/Cd hyperaccumulator *Thlaspi caerulescens*. *Proc Natl Acad Sci U S A* **97**(9): 4956-4960
- Peng J, Schwartz D, Elias JE, Thoreen CC, Cheng D, Marsischky G, Roelofs J, Finley D, Gygi SP (2003) A proteomics approach to understanding protein ubiquitination. *Nat Biotechnol* **21**(8): 921-926
- Persson BL, Lagerstedt JO, Pratt JR, Pattison-Granberg J, Lundh K, Shokrollahzadeh S, Lundh F (2003) Regulation of phosphate acquisition in *Saccharomyces cerevisiae*. *Curr Genet* **43**(4): 225-244
- Perzov N, Nelson H, Nelson N (2000) Altered distribution of the yeast plasma membrane H⁺-ATPase as a feature of vacuolar H⁺-ATPase null mutants. *J Biol Chem* **275**(51): 40088-40095
- Petit-Jacques J, Sui JL, Logothetis DE (1999) Synergistic activation of G protein-gated inwardly rectifying potassium channels by the betagamma subunits of G proteins and Na⁽⁺⁾ and Mg⁽²⁺⁾ ions. *J Gen Physiol* **114**(5): 673-684
- Pianelli K, Mari S, Marques L, Lebrun M, Czernic P (2005) Nicotianamine over-accumulation confers resistance to nickel in *Arabidopsis thaliana*. *Transgenic Res* **14**(5): 739-748
- Piper RC, Cooper AA, Yang H, Stevens TH (1995) VPS27 controls vacuolar and endocytic traffic through a prevacuolar compartment in *Saccharomyces cerevisiae*. *J Cell Biol* **131**(3): 603-617
- Piskacek M, Zotova L, Zsurka G, Schweyen RJ (2008) Conditional knock-down of hMRS2 results in loss of mitochondrial Mg⁽²⁺⁾ uptake and cell death. *J Cell Mol Med*
- Pluthero FG (1993) Rapid purification of high-activity Taq DNA polymerase. *Nucleic Acids Res* **21**(20): 4850-4851
- Portnoy ME, Liu XF, Culotta VC (2000) *Saccharomyces cerevisiae* expresses three functionally distinct homologues of the nramp family of metal transporters. *Mol Cell Biol* **20**(21): 7893-7902
- Pozos TC, Sekler I, Cyert MS (1996) The product of *HUM1*, a novel yeast gene, is required for vacuolar Ca²⁺/H⁺ exchange and is related to mammalian Na⁺/Ca²⁺ exchangers. *Mol Cell Biol* **16**: 3730-3741
- Ptacek J, Devgan G, Michaud G, Zhu H, Zhu X, Fasolo J, Guo H, Jona G, Breitkreutz A,

Sopko R, McCartney RR, Schmidt MC, Rachidi N, Lee SJ, Mah AS, Meng L, Stark MJ, Stern DF, De Virgilio C, Tyers M, Andrews B, Gerstein M, Schweitzer B, Predki PF, Snyder M (2005) Global analysis of protein phosphorylation in yeast. *Nature* **438**(7068): 679-684

Quamme GA, de Rouffignac C (2000) Epithelial magnesium transport and regulation by the kidney. *Front Biosci* **5**: D694-711.

Rasmussen SW (1994) Sequence of a 28.6 kb region of yeast chromosome XI includes the FBA1 and TOA2 genes, an open reading frame (ORF) similar to a translationally controlled tumour protein, one ORF containing motifs also found in plant storage proteins and 13 ORFs with weak or no homology to known proteins. *Yeast* **10 Suppl A**: S63-68

Raths S, Rohrer J, Crausaz F, Riezman H (1993) *end3* and *end4*: two mutants defective in receptor-mediated and fluid phase endocytosis in *Saccharomyces cerevisiae*. *J Cell Biol* **120**: 55-65

Reinhart RA, Desbiens NA (1985) Hypomagnesemia in patients entering the ICU. *Crit Care Med* **13**(6): 506-507

Riazanova LV, Pavur KS, Petrov AN, Dorovkov MV, Riazanov AG (2001) [Novel type of signaling molecules: protein kinases covalently linked to ion channels]. *Mol Biol (Mosk)* **35**(2): 321-332

Ritchie G, Kerstan D, Dai LJ, Kang HS, Canaff L, Hendy GN, Quamme GA (2001) 1,25(OH)(2)D(3) stimulates Mg²⁺ uptake into MDCT cells: modulation by extracellular Ca²⁺ and Mg²⁺. *Am J Physiol Renal Physiol* **280**(5): F868-878

Roberg KJ, Rowley N, Kaiser CA (1997) Physiological regulation of membrane protein sorting late in the secretory pathway of *Saccharomyces cerevisiae*. *J Cell Biol* **137**(7): 1469-1482

Romani A, Dowell E, Scarpa A (1991) Cyclic AMP-induced Mg²⁺ release from rat liver hepatocytes, permeabilized hepatocytes, and isolated mitochondria. *J Biol Chem* **266**(36): 24376-24384

Romani A, Marfella C, Scarpa A (1993) Cell magnesium transport and homeostasis: role of intracellular compartments. *Miner Electrolyte Metab* **19**(4-5): 282-289

Romani A, Scarpa A (1992) Regulation of cell magnesium. *Arch Biochem Biophys* **298**(1): 1-12

Romani AM, Scarpa A (2000) Regulation of cellular magnesium. *Front Biosci* **5**: D720-734

Ross IS (1995) Reduced uptake of nickel by a nickel resistant strain of *Candida utilis*. *Microbios* **83**(337): 261-270

Rude RK (1993) Magnesium metabolism and deficiency. *Endocrinol Metab Clin North Am* **22**(2): 377-395

Rude RK, Oldham SB, Sharp CF, Jr., Singer FR (1978) Parathyroid hormone secretion in magnesium deficiency. *J Clin Endocrinol Metab* **47**(4): 800-806

Runnels LW, Yue L, Clapham DE (2001) TRP-PLIK, a bifunctional protein with kinase and ion channel activities. *Science* **291**(5506): 1043-1047

Rusinova R, Shen YM, Dolios G, Padovan J, Yang H, Kirchberger M, Wang R, Logothetis DE (2009) Mass spectrometric analysis reveals a functionally important PKA phosphorylation site in a Kir3 channel subunit. *Pflugers Arch*

Ryzen E, Wagers PW, Singer FR, Rude RK (1985) Magnesium deficiency in a medical ICU population. *Crit Care Med* **13**(1): 19-21

Sahni J, Nelson B, Scharenberg AM (2007) SLC41A2 encodes a plasma-membrane Mg²⁺ transporter. *Biochem J* **401**(2): 505-513

Salt DE (2004) Update on plant ionomics. *Plant Physiol* **136**(1): 2451-2456

Sambrook J, Fritsch, E.F. and Maniatis, T. (1989) *Molecular Cloning: A Laboratory Manual*: Cold Spring Harbor Laboratory Press, Cold Spring Harbor, N.Y.

Schiestl RH, Gietz RD (1989) High efficiency transformation of intact yeast cells using single stranded nucleic acids as a carrier. *Curr Genet* **16**: 339-346

Schindl R, Weghuber J, Romanin C, Schweyen RJ (2007) Mrs2p forms a high conductance Mg²⁺ selective channel in mitochondria. *Biophys J* **93**(11): 3872-3883

Schlingmann KP, Gudermann T (2005) A critical role of TRPM channel-kinase for human magnesium transport. *J Physiol* **566**(Pt 2): 301-308

Schlingmann KP, Waldegger S, Konrad M, Chubanov V, Gudermann T (2007) TRPM6 and TRPM7--Gatekeepers of human magnesium metabolism. *Biochim Biophys Acta* **1772**(8): 813-821

Schlingmann KP, Weber S, Peters M, Niemann Nejsum L, Vitzthum H, Klingel K, Kratz M, Haddad E, Ristoff E, Dinour D, Syrou M, Nielsen S, Sassen M, Waldegger S, Seyberth HW, Konrad M (2002) Hypomagnesemia with secondary hypocalcemia is caused by mutations in TRPM6, a new member of the TRPM gene family. *Nat Genet* **31**(2): 166-170

Schmitz C, Dorovkov MV, Zhao X, Davenport BJ, Ryazanov AG, Perraud AL (2005) The channel kinases TRPM6 and TRPM7 are functionally nonredundant. *J Biol Chem* **280**(45): 37763-37771

Schmitz C, Perraud AL, Fleig A, Scharenberg AM (2004) Dual-function ion channel/protein kinases: novel components of vertebrate magnesium regulatory mechanisms. *Pediatr Res* **55**(5): 734-737

Schmitz C, Perraud AL, Johnson CO, Inabe K, Smith MK, Penner R, Kurosaki T, Fleig A, Scharenberg AM (2003) Regulation of vertebrate cellular Mg²⁺ homeostasis by TRPM7. *Cell* **114**(2): 191-200

Schock I, Gregan J, Steinhauser S, Schweyen R, Brennicke A, Knoop V (2000) A member of a novel *Arabidopsis thaliana* gene family of candidate Mg²⁺ ion transporters complements a yeast mitochondrial group II intron-splicing mutant. *Plant J* **24**(4): 489-501.

Scott DA, Docampo R, Dvorak JA, Shi S, Leapman RD (1997) *In situ* compositional analysis of acidocalcisomes in *Trypanosoma cruzi*. *J Biol Chem* **272**(44): 28020-28029

Scott PM, Bilodeau PS, Zhdankina O, Winistorfer SC, Hauglund MJ, Allaman MM, Kearney WR, Robertson AD, Boman AL, Piper RC (2004) GGA proteins bind ubiquitin to facilitate sorting at the trans-Golgi network. *Nat Cell Biol* **6**(3): 252-259

Seelig MS, Rosanoff A (2003) *The Magnesium factor*: Avery a member of Penguin group (USA) Inc. New York.

Sheff MA, Thorn KS (2004) Optimized cassettes for fluorescent protein tagging in *Saccharomyces cerevisiae*. *Yeast* **21**(8): 661-670

Silva IR, Smyth TJ, Israel DW, Raper CD, Rufty TW (2001a) Magnesium ameliorates aluminum rhizotoxicity in soybean by increasing citric acid production and exudation by roots. *Plant Cell Physiol* **42**(5): 546-554

Silva IR, Smyth TJ, Israel DW, Raper CD, Rufty TW (2001b) Magnesium is more efficient than calcium in alleviating aluminum rhizotoxicity in soybean and its ameliorative effect is not explained by the Gouy-Chapman-Stern model. *Plant Cell Physiol* **42**(5): 538-545

Silva IR, Smyth TJ, Raper CD, Carter TE, Rufty TW (2001c) Differential aluminum tolerance in soybean: An evaluation of the role of organic acids. *Physiol Plant* **112**(2): 200-210

Silver S (1969) Active transport of magnesium in escherichia coli. *Proc Natl Acad Sci U S A* **62**(3): 764-771

- Simm C, Lahner B, Salt D, LeFurgey A, Ingram P, Yandell B, Eide DJ (2007) Saccharomyces cerevisiae vacuole in zinc storage and intracellular zinc distribution. *Eukaryot Cell* **6**(7): 1166-1177
- Smith RL, Gottlieb E, Kucharski LM, Maguire ME (1998) Functional similarity between archaeal and bacterial CorA magnesium transporters. *J Bacteriol* **180**(10): 2788-2791
- Smith RL, Maguire ME (1998) Microbial magnesium transport: unusual transporters searching for identity. *Mol Microbiol* **28**(2): 217-226
- Smith RL, Thompson LJ, Maguire ME (1995) Cloning and characterization of MgtE, a putative new class of Mg²⁺ transporter from *Bacillus firmus* OF4. *J Bacteriol* **177**(5): 1233-1238
- Snavely MD, Florer JB, Miller CG, Maguire ME (1989a) Magnesium transport in Salmonella typhimurium: 28Mg²⁺ transport by the CorA, MgtA, and MgtB systems. *J Bacteriol* **171**(9): 4761-4766
- Snavely MD, Florer JB, Miller CG, Maguire ME (1989b) Magnesium transport in Salmonella typhimurium: expression of cloned genes for three distinct Mg²⁺ transport systems. *J Bacteriol* **171**(9): 4752-4760
- Springael JY, Andre B (1998) Nitrogen-regulated ubiquitination of the Gap1 permease of Saccharomyces cerevisiae. *Mol Biol Cell* **9**(6): 1253-1263
- Springael JY, Nikko E, Andre B, Marini AM (2002) Yeast Npi3/Bro1 is involved in ubiquitin-dependent control of permease trafficking. *FEBS Lett* **517**(1-3): 103-109
- Sreedhara A, Cowan JA (2002) Structural and catalytic roles for divalent magnesium in nucleic acid biochemistry. *Biometals* **15**(3): 211-223
- Steel GJ, Fullerton DM, Tyson JR, Stirling CJ (2004) Coordinated activation of Hsp70 chaperones. *Science* **303**(5654): 98-101
- Sutton RA, Domrongkitchaiporn S (1993) Abnormal renal magnesium handling. *Miner Electrolyte Metab* **19**(4-5): 232-240
- Swaminathan S, Amerik AY, Hochstrasser M (1999) The Doa4 deubiquitinating enzyme is required for ubiquitin homeostasis in yeast. *Mol Biol Cell* **10**(8): 2583-2594
- Tagwerker C, Flick K, Cui M, Guerrero C, Dou Y, Auer B, Baldi P, Huang L, Kaiser P (2006) A tandem affinity tag for two-step purification under fully denaturing conditions: application in ubiquitin profiling and protein complex identification combined with in vivo cross-linking. *Mol Cell Proteomics* **5**(4): 737-748
- Takezawa R, Schmitz C, Demeuse P, Scharenberg AM, Penner R, Fleig A (2004)

- Receptor-mediated regulation of the TRPM7 channel through its endogenous protein kinase domain. *Proc Natl Acad Sci U S A* **101**(16): 6009-6014
- Tang CY, Bezanilla F, Papazian DM (2000) Extracellular Mg²⁺ modulates slow gating transitions and the opening of *Drosophila* ether-a-Go-Go potassium channels. *J Gen Physiol* **115**(3): 319-338
- Tang TS, Tu H, Wang Z, Bezprozvanny I (2003) Modulation of type 1 inositol (1,4,5)-trisphosphate receptor function by protein kinase a and protein phosphatase 1alpha. *J Neurosci* **23**(2): 403-415
- Tao T, Grulich PF, Kucharski LM, Smith RL, Maguire ME (1998) Magnesium transport in *Salmonella typhimurium*: biphasic magnesium and time dependence of the transcription of the mgtA and mgtCB loci. *Microbiology* **144** (Pt 3): 655-664
- Tao T, Snavely MD, Farr SG, Maguire ME (1995) Magnesium transport in *Salmonella typhimurium*: mgtA encodes a P-type ATPase and is regulated by Mg²⁺ in a manner similar to that of the mgtB P-type ATPase. *J Bacteriol* **177**(10): 2654-2662
- Tappero R, Peltier E, Grafe M, Heidel K, Ginder-Vogel M, Livi KJ, Rivers ML, Marcus MA, Chaney RL, Sparks DL (2007) Hyperaccumulator *Alyssum murale* relies on a different metal storage mechanism for cobalt than for nickel. *New Phytol* **175**(4): 641-654
- Tashiro M, Konishi M (1997) Na⁺ gradient-dependent Mg²⁺ transport in smooth muscle cells of guinea pig tenia cecum. *Biophys J* **73**(6): 3371-3384
- Tokunaga M, Kawamura A, Kohno K (1992) Purification and characterization of BiP/Kar2 protein from *Saccharomyces cerevisiae*. *J Biol Chem* **267**(25): 17553-17559
- Tong GM, Rude RK (2005) Magnesium deficiency in critical illness. *J Intensive Care Med* **20**(1): 3-17
- Townsend DE, Esenwine AJ, George J, 3rd, Bross D, Maguire ME, Smith RL (1995) Cloning of the mgtE Mg²⁺ transporter from *Providencia stuartii* and the distribution of mgtE in gram-negative and gram-positive bacteria. *J Bacteriol* **177**(18): 5350-5354
- Travers KJ, Patil CK, Wodicka L, Lockhart DJ, Weissman JS, Walter P (2000) Functional and genomic analyses reveal an essential coordination between the unfolded protein response and ER-associated degradation. *Cell* **101**(3): 249-258
- Uauy C, Distelfeld A, Fahima T, Blechl A, Dubcovsky J (2006) A NAC Gene regulating senescence improves grain protein, zinc, and iron content in wheat. *Science* **314**(5803): 1298-1301
- Vanderheyden V, Devogelaere B, Missiaen L, De Smedt H, Bultynck G, Parys JB (2008)

- Regulation of inositol 1,4,5-trisphosphate-induced Ca(2+) release by reversible phosphorylation and dephosphorylation. *Biochim Biophys Acta*
- Vescovi EG, Ayala YM, Di Cera E, Groisman EA (1997) Characterization of the bacterial sensor protein PhoQ. Evidence for distinct binding sites for Mg²⁺ and Ca²⁺. *J Biol Chem* **272**(3): 1440-1443.
- Vida TA, Emr SD (1995) A new vital stain for visualizing vacuolar membrane dynamics and endocytosis in yeast. *J Cell Biol* **128**(5): 779-792
- Voets T, Nilius B, Hoefs S, van der Kemp AW, Droogmans G, Bindels RJ, Hoenderop JG (2004) TRPM6 forms the Mg²⁺ influx channel involved in intestinal and renal Mg²⁺ absorption. *J Biol Chem* **279**(1): 19-25
- Wabakken T, Rian E, Kveine M, Aasheim HC (2003) The human solute carrier SLC41A1 belongs to a novel eukaryotic subfamily with homology to prokaryotic MgtE Mg²⁺ transporters. *Biochem Biophys Res Commun* **306**(3): 718-724
- Wachek M, Aichinger MC, Stadler JA, Schweyen RJ, Graschopf A (2006) Oligomerization of the Mg(2+)-transport proteins Alr1p and Alr2p in yeast plasma membrane. *FEBS J* **273**(18): 4236-4249
- Walder RY, Landau D, Meyer P, Shalev H, Tsolia M, Borochoowitz Z, Boettger MB, Beck GE, Englehardt RK, Carmi R, Sheffield VC (2002) Mutation of TRPM6 causes familial hypomagnesemia with secondary hypocalcemia. *Nat Genet* **31**(2): 171-174
- Wallach S (1988) Availability of body magnesium during magnesium deficiency. *Magnesium* **7**(5-6): 262-270
- Wang CY, Huang YQ, Shi JD, Marron MP, Ruan QG, Hawkins-Lee B, Ochoa B, She JX (1999a) Genetic homogeneity, high-resolution mapping, and mutation analysis of the urofacial (Ochoa) syndrome and exclusion of the glutamate oxaloacetate transaminase gene (GOT1) in the critical region as the disease gene. *Am J Med Genet* **84**(5): 454-459
- Wang CY, Shi JD, Huang YQ, Cruz PE, Ochoa B, Hawkins-Lee B, Davoodi-Semiromi A, She JX (1999b) Construction of a physical and transcript map for a 1-Mb genomic region containing the urofacial (Ochoa) syndrome gene on 10q23-q24 and localization of the disease gene within two overlapping BAC clones (<360 kb). *Genomics* **60**(1): 12-19
- Waters BM, Eide DJ (2002) Combinatorial control of yeast *FET4* gene expression by iron, zinc, and oxygen. *J Biol Chem* **277**(37): 33749-33757
- Weglicki WB, Mak IT, Stafford RE, Dickens BF, Cassidy MM, Phillips TM (1994) Neurogenic peptides and the cardiomyopathy of magnesium-deficiency: effects of substance P-receptor inhibition. *Mol Cell Biochem* **130**(2): 103-109

- Weglicki WB, Phillips TM (1992) Pathobiology of magnesium deficiency: a cytokine/neurogenic inflammation hypothesis. *Am J Physiol* **263**(3 Pt 2): R734-737
- Weglicki WB, Phillips TM, Freedman AM, Cassidy MM, Dickens BF (1992) Magnesium-deficiency elevates circulating levels of inflammatory cytokines and endothelin. *Mol Cell Biochem* **110**(2): 169-173
- Wei SK, Quigley JF, Hanlon SU, O'Rourke B, Haigney MC (2002) Cytosolic free magnesium modulates Na/Ca exchange currents in pig myocytes. *Cardiovasc Res* **53**(2): 334-340
- Wiesenberger G, Steinleitner K, Malli R, Graier WF, Vormann J, Schweyen RJ, Stadler JA (2007) Mg²⁺ deprivation elicits rapid Ca²⁺ uptake and activates Ca²⁺/calcineurin signaling in *Saccharomyces cerevisiae*. *Eukaryot Cell* **6**(4): 592-599
- Wiesenberger G, Waldherr M, Schweyen RJ (1992) The nuclear gene MRS2 is essential for the excision of group II introns from yeast mitochondrial transcripts in vivo. *J Biol Chem* **267**(10): 6963-6969
- Winzeler EA, Shoemaker DD, Astromoff A, Liang H, Anderson K, Andre B, Bangham R, Benito R, Boeke JD, Bussey H, Chu AM, Connelly C, Davis K, Dietrich F, Dow SW, El Bakkoury M, Foury F, Friend SH, Gentalen E, Giaever G, Hegemann JH, Jones T, Laub M, Liao H, Liebundguth N, Lockhart DJ, Lucau-Danila A, Lussier M, M'Rabet N, Menard P, Mittmann M, Pai C, Rebischung C, Revuelta JL, Riles L, Roberts CJ, Ross-MacDonald P, Scherens B, Snyder M, Sookhai-Mahadeo S, Storms RK, Veronneau S, Voet M, Volckaert G, Ward TR, Wysocki R, Yen GS, Yu K, Zimmermann K, Philippsen P, Johnston M, Davis RW (1999) Functional characterization of the *S. cerevisiae* genome by gene deletion and parallel analysis. *Science* **285**(5429): 901-906
- Wolf FI, Cittadini A (2003) Chemistry and biochemistry of magnesium. *Mol Aspects Med* **24**(1-3): 3-9
- Worlock AJ, Smith RL (2002) ZntB is a novel Zn²⁺ transporter in *Salmonella enterica* serovar *Typhimurium*. *J Bacteriol* **184**(16): 4369-4373
- Yang JL, You JF, Li YY, Wu P, Zheng SJ (2007) Magnesium enhances aluminum-induced citrate secretion in rice bean roots (*Vigna umbellata*) by restoring plasma membrane H⁺-ATPase activity. *Plant Cell Physiol* **48**(1): 66-73
- Zacharias DA, Violin JD, Newton AC, Tsien RY (2002) Partitioning of lipid-modified monomeric GFPs into membrane microdomains of live cells. *Science* **296**(5569): 913-916
- Zhang GH, Melvin JE (1992) Secretagogue-induced mobilization of an intracellular Mg²⁺ pool in rat sublingual mucous acini. *J Biol Chem* **267**(29): 20721-20727

Zhang GH, Melvin JE (1994) Intracellular Mg^{2+} movement during muscarinic stimulation. Mg^{2+} uptake by the intracellular Ca^{2+} store in rat sublingual mucous acini. *J Biol Chem* **269**(14): 10352-10356

Zhang GH, Melvin JE (1996) Na^+ -dependent release of Mg^{2+} from an intracellular pool in rat sublingual mucous acini. *J Biol Chem* **271**(46): 29067-29072

Zhang GH, Melvin JE (1997) Extracellular Mg^{2+} regulates the intracellular Na^+ concentration in rat sublingual acini. *FEBS Lett* **410**(2-3): 387-390

Zhao H, Butler E, Rodgers J, Spizzo T, Dueterhoeft S, Eide D (1998) Regulation of zinc homeostasis in yeast by binding of the ZAP1 transcriptional activator to zinc-responsive promoter elements. *J Biol Chem* **273**(44): 28713-28720

Zhao H, Eide DJ (1997) Zap1p, a metalloregulatory protein involved in zinc-responsive transcriptional regulation in *Saccharomyces cerevisiae*. *Mol Cell Biol* **17**(9): 5044-5052

Zhu Y, Davis A, Smith BJ, Curtis J, Handman E (2009) Leishmania major CorA-like magnesium transporters play a critical role in parasite development and virulence. *Int J Parasitol* **39**(6): 713-723

Zsurka G, Gregan J, Schweyen RJ (2001) The human mitochondrial Mrs2 protein functionally substitutes for its yeast homologue, a candidate magnesium transporter. *Genomics* **72**(2): 158-168.

Zubenko GS, Park FJ, Jones EW (1983) Mutations in *PEP4* locus of *Saccharomyces cerevisiae* block final step in maturation of two vacuolar hydrolases. *Proc Natl Acad Sci U S A* **80**(2): 510-514